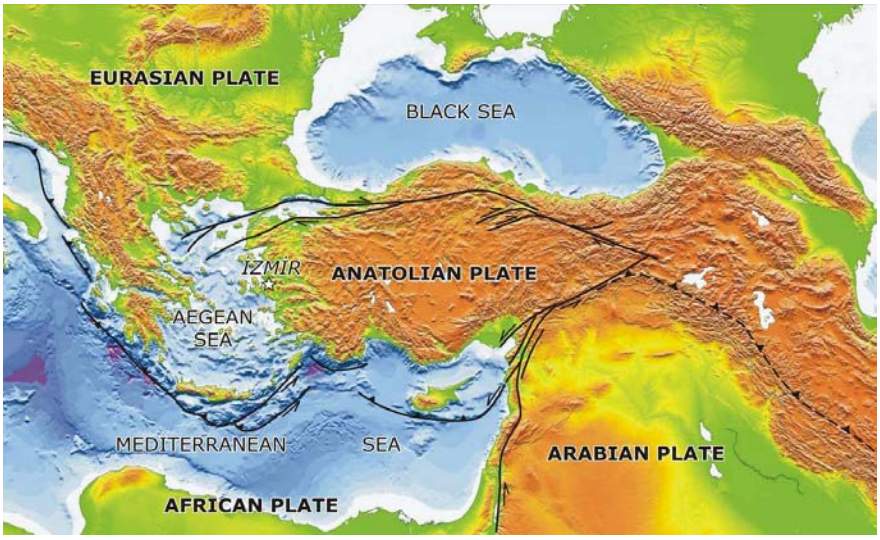

International Earth Science Colloquium on the Aegean Region

IESCA-2012

(1-5 October 2012, İzmir, Turkey)

NEOGENE BORATE DEPOSITS: Mineralogy, Petrology and Sedimentology;

A workshop with special emphasis on the Anatolian deposits

Cahit HELVACI, Federico ORTÍ, Javier GARCÍA-VEIGAS,
Laura ROSELL, Ibrahim GÜNDOĞAN

Universitat de Barcelona

DOKUZ EYLÜL ÜNİVERSİTESİ
İZMİR-1982

Cahit HELVACI, Federico ORTÍ, Javier GARCÍA-VEIGAS, Laura ROSELL, Ibrahim GÜNDOĞAN (2012).
NEOGENE BORATE DEPOSITS: Mineralogy, Petrology and Sedimentology;
A workshop with special emphasis on the Anatolian deposits.
International Earth Science Colloquium on the Aegean Region (IESCA-2012, İzmir, Turkey). 64pp.

Cahit Helvacı[(1)], Federico Ortí[(2)], *Javier García-Veigas[(3)], Laura Rosell[(2)], Ibrahim Gündoğan[(1)]

[(1)] Dokuz Eylül Üniversitesi; Mühendislik Fakültesi; Jeoloji Mühendisligi Bölümü; 35160 Buca, İzmir, Turkey

[(2)] Departament de Geoquímica, Petrologia i Prospecció Geològica; Facultat de Geologia; Universitat de Barcelona; Zona Universitària de Pedralbes; 08028 Barcelona, Spain

[(3)] CCiT, Universitat de Barcelona, Zona Universitària de Pedralbes, 08028 Barcelona, Spain

* Corresponding autor: Javier García Veigas (garcia_veigas@ub.edu)

This workshop was supported by projects CGL 2009-11096 of the Spanish Government and 2009 SGR 1451 of the Catalan Government.

INDEX

ABSTRACT

Borates constitute a group of mineral deposits of great economic interest. Although several genetic types have been identified (volcanic, hydrothermal, metamorphic and sedimentary), the most important type corresponds to those deposits formed in non-marine, evaporitic settings. Lacustrine basins related to volcanic terrains in which borates have precipitated are known in the stratigraphic record since the Oligocene, although those of Miocene age are most relevant. The borate minerals in all these basins were generated in saline lakes placed in volcanogenic (mainly pyroclastic) terrains with intense hydrothermal influence, under arid to semiarid conditions, and in some cases at low temperatures.

As in other evaporitic deposits, the origin, composition (chemical and mineralogical) and depositional environments of the borate deposits can be appropriately documented by means of petrologic and sedimentologic approaches (petrography, lithofacies analysis, cyclicity, facies belts, depositional sequences).

The purpose of this workshop is introducing the participants to the Petrology and Sedimentology of the Neogene Borate Deposits in western Anatolia (Turkey) and, to a lesser extent, in the Andean region (Puna, NW Argentina), although references to the deposits in western USA, and in other geological domains will be done.

The workshop is divided in four parts: The first part is an **Introduction** to the borate deposits and deals with general mineralogical and depositional aspects.

The second part summarizes the **Lithofacies** and **Petrography** of the most common borate minerals: ulexite, probertite, inyoite, meyerhofferite, colemanite, priceite, borax, hydroboracite and howlite, among others. Many of them are rock-forming minerals.

The third part presents examples of the depositional **Cycles** and **Successions** present in the Neogene and, to a lesser extent, the Holocene deposits involving borates, borates-sulfates, and borates-sulfates-chlorides.

The fourth part discusses aspects of some examples of **Neogene Borate Basins** in western Anatolia (Bigadiç, Kestelek, Kırka, Sultançayır, and Emet) and in La Puna region (NW Argentina). In the case of the Emet and the Kırka basins, the discussion is mainly based on accurate petrologic observations carried out by direct observation of borehole core samples under an Environmental Scanning Electron Microscope.

Workshop materials consist of: stratigraphic profiles; hand and borehole samples; thin sections; and different types of images (outcrops and quaries, hand and core samples, photomicrographs and SEM images).

Key words: borates, evaporites, lithofacies, petrology, depositional cycles and successions, diagenesis, Neogene, western Anatolia, NW Argentina

PART I: INTRODUCTION

1.1. Purpose

Borates constitute a group of deposits of great economic interest. Although there are several genetic types of borates (volcanic, hydrothermal, metamorphic, sedimentary), the most important type corresponds to those deposits formed in non-marine, evaporitic settings. Lacustrine basins in which borates have precipitated are known in the stratigraphic record since the Oligocene up to the Recent, although those of Miocene age are the most common and important.

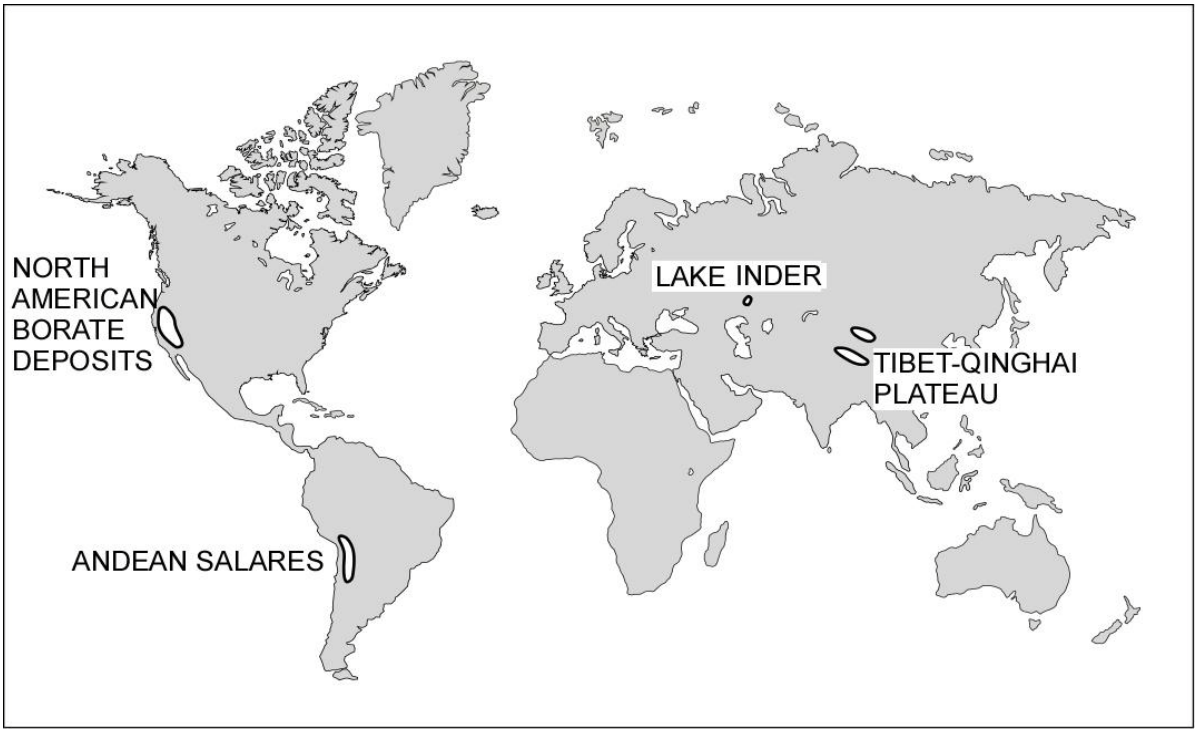

Figure 1.1. Main Holocene borate localities all over the world

The borate minerals in all these basins were generated in saline lakes placed in volcanogenic (mainly pyroclastic) terrains with intense hydrothermal influence, under arid to semiarid conditions, and in some cases at low temperatures. The most important areas of Holocene borate precipitation are shown in Fig. 1.1.

Minor borate occurences, however, are linked to ancient marine salt formations (Late Permian, Zechstein, Europe; Early Carboniferous, Mississippian Windsor Group, Canada; Early Permian Inder Lake region, Kazakhstan). These occurrences are mainly diagenetic borates dispersed in caprocks of salt domes, and were usually formed by the intrusion of boron-rich geothermal fluids.

In addition to a chemical or mineralogical approach to the description and classification of these lacustrine borate deposits, the composition and genesis can also be appropriately documented by means of petrologic and sedimentologic investigations. Because these deposits constitute a particular type of evaporites, a similar methodology can be applied to them: petrographic study, lithofacies analysis and interpretation of cyclicity, facies belts and depositional successions.

The purpose of this workshop is to introduce the participants to the Petrology and Sedimentology of the Neogene borates and borate-bearing deposits of lacustrine setting. Most of the examples will be taken preferentially from the western Anatolian deposits (Turkey) and, to a lesser extent, from the La Puna region (Central Andes, NW Argentina), although brief references to similar deposits in other regions will be made (California in western USA, Tibet-Qinghai Plateau in China).

1.2. Mineralogy

Boron is never found in the elemental form in nature. The name is derived from the Arabic ‘burak’ or the Persian ‘burah’ words meaning ‘white’. Boron is a minor element in the Earth with an average concentration of 15 ppm in the upper continental crust. It occurs in many metamorphic and acid plutonic rocks in the mineral tourmaline. In sediments, it is present as detrital tourmaline and as a minor element in illitic clays.

In natural waters, boron exists primarily as undissociated boric acid (H_3BO_3 or $B(OH)_3$).

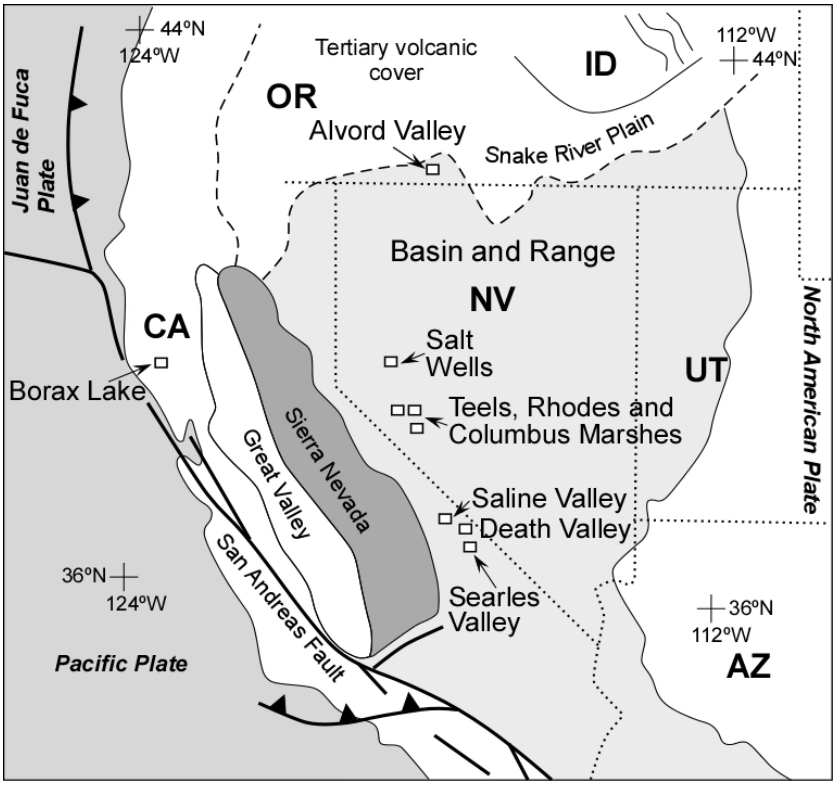

Figure 1.2. Borate localities in the Basin and Range Province (USA)

Also, boron interacts with water molecules to form the tetrahydroxyborate ion ($B(OH)_4^-$) and a number of polymeric borate ions (polyborates): diborate ($B_2O_5^{4-}$); triborate ($B_3O_7^{5-}$); tetraborate ($B_4O_9^{6-}$); etc. Concentration of boron in water ranges widely: it is from less than 7 ppm in freshwater, averaging 4.5 ppm in seawater, and from 0.3 to 100 ppm in groundwater. Hydrothermal water in some tectonically active regions related to volcanic processes can reach very high concentrations of boron. For instance, it is over 3500 ppm in the volcanic island of Santa Lucia (Lesser Antilles), where hot springs exhibit high temperatures (up to 80º C), low pH (down to pH 2), very high concentrations of sulfates (>6000 ppm) and contain a high anomalous microbial diversity (Stout *et al.*, 2009).

Boron combines with oxygen and other elements to form borates which contain the BO_3 (triangular) or BO_4 (tetrahedral) structural coordination units (Christ and Clark, 1977; Anovitz and Grew, 1996). These borate units may be polymerized similarly to the SiO_4 of the silicate mineral class. This results in more than 230 naturally occurring borate minerals identified until 1996 (Sureda, 1991; Garret, 1998) but the new analytical techniques allow the continuous identification of new borate minerals. Although borates can be formed with any cation, and form double salts with other anions, the most abundant minerals are formed with calcium, sodium or both elements.

Borates are strongly ionic compounds, soluble in hot water, and as the cations are generally alkalis or alkaline earth elements, most of them are transparent and colorless having a glassy luster. Owing to the anisotropy of the anion groups, most borates have a high optical anisotropy and exhibit interference colors of high orders (Jaffe, 1996). A connection can be established between the crystal structures of borate minerals and the conditions of pH and log of [H_2O] of their stability field: the proportion of tetrahedrally coordinated B to total boron in the structural unit increases with increasing pH (Schindler and Hawthorne, 2001).

Three different chemical formulation systems (structural, empirical, and oxide-like) are used in borate minerals making in many cases confusing their use and memorization. The main borate minerals present in evaporitic lacustrine deposits with the three formula types are listed in Table I-1: note that only the structural formula contains information about atomic organization although it is not so relevant from the genetic and sedimentologic points of view.

Neogene ore deposits with boron concentrations allowing industrial exploitation are restricted to four groups of major borates: Ca-borates (inyoite, meyerhofferite, colemanite and priceite), Na-Ca-borates (ulexite and probertite), Na-borates (borax, kernite) and Mg-Ca-borates (hydroboracite). Other borates occur as minor phases and do not require the presence of the major ones. According to all these, this workshop will be focused on the

lithological and petrological description of these four main groups.

1.3. Holocene environments

Borate minerals have precipitated during the Holocene in non-marine (endorheic, closed) basins from merely boratiferous brines or from more complex solutions. Borate minerals in these basins contain mainly Ca and Na, to a lesser extent Mg, and in some cases Sr and As also.

At present, a number of non-marine regions record significant precipitation of borate minerals in a number of evaporitic environments:

- the playas, marshes, and saline lakes of Great Valley, Sierra Nevada, and the Basin and Range provinces (western USA),
- the salares of the Central Andean Range (Argentina, Chile, Bolivia, Perú),
- the payas of Konya Karapınar region (central Turkey)
- the saline lakes of the Tibet-Qinghai Plateau
- Lake Inder (Kazakhstan, to the N of the Caspian Sea).

In these modern environments, either pure borate deposits devoid of significant amounts of other evaporite minerals, or borate deposits in complex parageneses with carbonates, sulfates or chloride may form from the concentrated solutions. The borate precipitation occurs in the following sites:

- in the vicinity to boratiferous, hydrothermal sources, where borates form cone or fan-shaped ('spring-apron') deposits
- underneath the dry surface of some saline playas and salars
- on the shore and, less commonly, on the floor of saline lakes.

1.3.1. Holocene borates in North America

Holocene borate deposits in the Western United Sates are scattered in alkaline lakes and playas from Southern Oregon throughout the states of California and Nevada (Fig. 1.2). All of them are related to the subduction process, started during the Cretaceous, of the Pacific Plate under the North American Plate and the associated plutonism and formation of a volcanic arc in the Sierra Nevada. The proto-Sierra Nevada remained tectonically stable since the Paleocene until the Neogene, when crustal extension caused extensive volcanism in both the Sierra Nevada and the Basin and Range Province. As the eruptions increased in frequency, the eastern edge of the modern Sierra Nevada Range began to rise along fractures and formed a block close to 650 km long and 110 km wide. Uplift of the eastern boundary of the Sierra Nevada continues today. A microplate with rigid behaviour (as a block) was formed in the junction zone of the Sierra Nevada and the Great Valley, which is bounded by the San Andres Fault on the west and the Eastern Sierra Fault on the east. Most Holocene borate deposits are located along the Sierra Fault System, in both the eastern side of the microplate and the west margin of the Basin and Range Province (Coolbaugh *et al.*, 2006a), although some of them are related to the western edge on the San Andres Fault (Borax Lake, California).

- *Borax Lake (California).* This lake, located in the San Andres transform Fault System, is a small alkaline lake which lies in a closed basin separated from the structural basin of the Clear Lake (Lake County, California) by a narrow ridge. With a maximum water depth of 1 m, the lake occupies in spring an area close to 1 km^2, which decreases up to 0.2 km^2 in summer, and occasionally disappears for several years. The area consists of a volcanic field containing lava and tuff deposits. A large magmatic chamber provides the geothermal field for the Geysers Steam Field, which was the largest geothermal power-generating system in the world. A number of thermal springs yielding highly boron-rich waters are located just northeast of Borax Lake. According to Garret (1998), the central portion of the lake mud surface is smooth, soft, and plastic with no crystals in its upper 30-40 cm, but at increasing depth, interstitially-grown idiomorphic borax crystals appear within the mud. During the summer of 1934, the lake became almost completely dry due to a prolonged dry period and evolved to a mud playa covered by a white efflorescent crust of halite crystals containing trona ($Na(CO_3)(HCO_3).2H_2O$), gaylussite ($Na_2Ca(CO_3)_2.5H_2O$) and glauberite ($Na_2Ca(SO_4)_2$). Borax was absent in the exposed surface although abundant idiomorphic crystals were found at a depth of 1.5 m.

- *Searles Lake (California).* Searles Valley is located at the northern edge of the Mojave Desert in the San Bernardino and Inyo Counties (California). In this valley, a number of sedimentary rock units of Tertiary and Quaternary ages and abundant mafic volcanic rocks of Miocene to Pliocene age crop out. The Searles (dry) Lake, in the center of the valley, is about 19 km long and 13 km in its widest point. This lake consists of an extensive mud flat around a salt flat that is periodically flooded by a 2-10 cm deep water body. The Quaternary record of the lake consists of 45 m of evaporites and mud sediments grouped in the Searles Lake Formation (Smith, 2009). Borax was harvested in the surface dried mud. Two non-outcropping saline bodies are composed of a great number of minerals accompanying halite. They can be grouped as Na-bearing carbonates (trona ($Na(CO_3)(HCO_3).2H_2O$); nahcolite ($Na(HCO_3)$), Ca-Na-bearing carbonates (gaylussite ($Na_2Ca(CO_3)_2.5H_2O$); pirssonite ($Na_2Ca(CO_3)_2.2H_2O$)), Na-bearing borates (borax; tincalconite), Na-bearing sulfates (thenardite (Na_2SO_4) and glaserite ($K_3Na(SO_4)_2$) and Na-bearing double or triple salts (sulfohalite ($Na_6(SO_4)_2FCl$); galeite ($Na_{15}(SO_4)F_4Cl$); hanksite ($KNa_{22}(SO_4)_9(CO_3)_2Cl$); burkeite ($Na_6(SO_4 2CO_3)$; tychite ($Na_6Mg_2(CO_3)_4(SO4)$);

schairerite ($Na_{21}(SO_4)_7F_6Cl$); northupite ($Na_3Mg(CO_3)_2Cl$). Up to 14 tuff beds containing vitric ash now altered to zeolites, K-feldpars, bentonite and smectite are interbedded with these evaporites (Hay and Guldman, 1987).

- Saline Valley (California). Saline Valley is a large (48 km long and 32 km wide), arid, dry valley sorrounded on the west by the Inyo Mountains (3050 m high) and on the east by the Panamint Range (1830 m). It is located 80 km southeast of the Bishop city, in the Inyo County (California), and takes part of the Mojave Desert and the Death Valley National Park. An extensive (42 km^2) dry playa covered by a 0.5 m thick salt crust occupies the center of the valley. Borax occurrences were discovered in 1874 prompting an extensive number of borate land locations up through the 1890. The mineralogy of the recent evaporite crust (Hardie, 1968) is mainly formed by halite mixed with muds and sands. The crust also contains minor amounts of thenardite, mirabilite ($Na_2SO_4.10H_2O$), glauberite, gypsum, calcite, dolomite and ulexite. Natural hot springs are found in the valley, which belong to a hydrothermal system originated by ascending meteoric water heated at an indeterminate depth. This water, supersaturated with respect to calcium carbonate, is the reservoir of the saline deposit.

- Death Valley (California). Death Valley is located in the Inyo County, southeastern California, on the western margin of the Basin and Range physiographic province. The valley is a pull-apart basin in which strike slip movement has been operating for more than 10 Myr along the Furnace Creek and the Death Valley Fault Zones. The valley currently houses three principal depressions, from north to south: the Cotton-Ball Basin, the Middle Basin, and the Badwater Basin. Inflow waters to Death Valley include streams that enter from the north (Salt Creek) and the south (Amargosa River). Several springs and seeps, associated with faults, discharge along the east and west margins. Seismic reflection profiles in Death Valley have identified a mid-crustal magma chamber, 15 km below the surface of the Badwater Basin which provides potential pathway for upward movement of hydrothermal waters (Lowenstein and Risacher, 2009). Badwater Basin constitutes the lowest point in North America, with an elevation of 86 m below the sea level. In this basin, the Eagle Borax Spring is one of the largest perennial sources located on the southwestern margin of the Death Valley salt pan. East to this spring, in direction to the central salt pan, the surface crust consists of halite and gypsum-cemented silt with ulexite, celestine, thenardite and probertite (Crowley, 1996). Other minor Mg- and K-bearing borates (aristarainite, hydroboracite, kaliborite, mcallisterite, rivadavite, and pinnoite) have been detected by spectroscopic thecniques.

- Salt Wells Marsh (Nevada). The Salt Wells Basin is a closed playa (15 km long, 5 km wide) located 20 km southeast of Fallon Village (Churchill County, Nevada). The basin is surrounded to the north by the volcanic rocks of the Stillwater Range (2680 m high), by the granites of the Sand Spring Range to the southwest and by the Cocoon Mountains to the southeast. The playa is divided into two subbasins (Eight Mile Flat and Four Mile Flat), which are covered by white salt crusts formed by ephemeral salt lakes. Cotton-ball ulexite was harvested from an area of 1.6 km^2 of the playa at Salt Wells during 1870 to transform it into borax (Garret, 1998). Coolbaugh *et al.* (2006b) report tincalconite and borax crusts with mirabilite and thenardite in a more widespread area. Borate occurrences are closely related to the areas of the playa being fed by ascending, thermal groundwater. The intense geothermal field in Salt Wells has allowed the construction of a power plant that taps a shallow geothermal reservoir with an estimated temperature of about 140ºC and up to 200ºC in the deeper part. Surface indicators of the geothermal activity related to the borate production include opalized sediments, siliceous sinter, argillitic alteration, and many ephemeral hot and warm springs (Coolbaugh *et al.*, 2006b).

- Teels, Rhodes, and Columbus marshes (Nevada). Teels and Rhodes marshes (Mineral County) and Columbus Marsh (Esmeralda County) are three borate-bearing playas located near the city of Columbus, southwestern Nevada. These playas were the world's leading sources of mined borate minerals during the 1870's and lasted for about a decade (Barker and Lefond, 1985). Teels Marsh is an ephemeral saline lake located in a block-faulted valley typical of the Basin and Range geomorphic province. The surrounding mountains consist of a granitic basement and Tertiary volcanic rocks. A tuffaceous deposit correlated to the age of recent volcanism generally occurs about 30 cm below the surface and varies in thickness from 1.3 to 5.1 m. Taylor and Surdam (1981) reported that interstitial waters associated with tuffaceous sediments are alkaline waters essentially of the Na-Cl-HCO_3-SO_4 type and exhibit a concentration gradient toward the playa center. Saline products at Teels Marsh consist of efflorescent crusts formed by a sandy mixture with halite and ulexite, and minor amounts of dolomite, calcite, trona, gypsum, gaylussite, burkeite ($Na_6(SO_4)_2.(CO_3)$), searlesite and mirabilite. In Rhodes and Columbus marshes ulexite occurs as nodules (cotton-ball) in wet, soft mud underlaying the playa surface (Bowser and Dickson, 1966). Field and satellite remote sensing spectroscopy allowed mapping the tincalconite surface distribution (borax in subsurface) on Teels, Rhodes and Columbus marshes (Kraft *et al.*, 2006).

- Fish Lake Marsh (Nevada). Fish Lake Valley is located in the Esmeralda County, Nevada. It is bounded to the west by the White Mountains (California), to the east by the Silver Peak Range, and to the north by the Volcanic Hills. Volcanic Hills are composed of Tertiary basalt flows and tuff deposits. An intense geothermal activity is present in the area (Littlefield and Calvin, 2010). At the northern edge, in contact

with the Volcanic Hills, there is a tuff-hosted mercury deposit with associated chalcedony, sulfur, gypsum and cinnabar. Near surface, groundwater sampling conducted recently by Lithium Corporation ("Lithco") has discovered lithium-enriched brines with anomalous boron (up to 2500 ppm) and potassium (up to 7200 ppm) concentrations. The northeastern corner of Fish Lake Valley is occupied by a small playa covered by a white saline crust containing borax and cotton-ball ulexite.

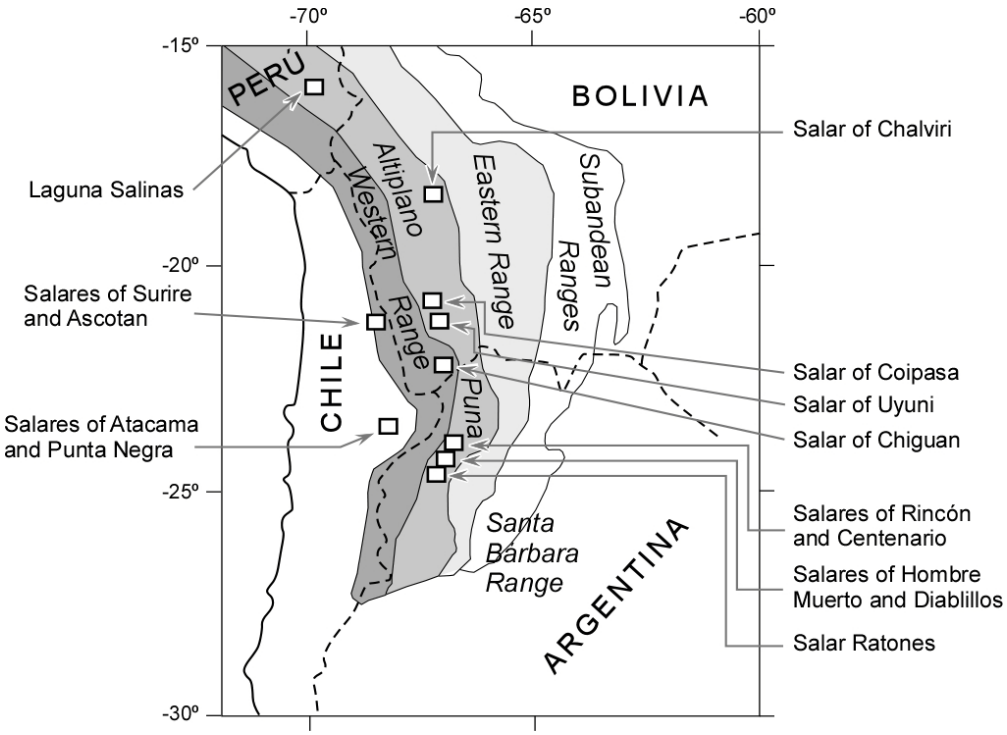

Figure 1.3. Borate localities in the Central Andean region (South America)

- Alvord Valley and Borax Lake (Oregon). Alvord Valley is a north-northeast-trending graben in the Basin and Range Province (Harney County, southeastern Oregon). The graben is bounded to the west by the tilted fault-block mountains of the Steens and Pueblo Range (2975 m high) and to the east by the Sheepshead and Trout Creeck mountains. The Alvord Basin consists of a large playa covering an area of about 250 km^2 in the north-central part of the valley. It includes the Alvord Desert in the north, the Alvord Lake in the central part, and the small Borax Lake (or Hot Lake) in the south. The Alvord Lake, of about 1 m deep, overflows the Alvord Desert during periods of heavy rainfall. In summer, the lake is quite small and develops a white, surficial alkaline crust. The saline crust surrounding this lake contains a mixture of ulexite and borax (Garret, 1998). The Alvord Basin is placed in a strong geothermal active area with hot springs: about 175 of these springs are distributed along a NE-SW trending normal fault. The discharging water is of the Na-HCO_3-SO_4-Cl type, and has T and pH values ranging from 24 to 95ºC and from 5.8 to 8.6, respectively (Colter *et al.*, 2004). Water in the Borax Lake has significant concentrations of boron (Koski and Wood, 2004).

1.3.2. Holocene borates in the Central Andean Range

The Altiplano-Puna Plateau with an average elevation above 3000 m, is the highest plateau in the world associated with abundant magmatism. It extends over an area of 1800 km long and 350-400 km wide of the Central Andean Range occupying parts of northern Chile and Argentina, western Bolivia and southern Perú. The Altiplano-Puna Plateau is bordered on the west by the present-day active volcanic arc of the Western Range, and in the east by the paleo-rift of the Eastern Range, the Santa Bárbara and Sierras Pampeanas system, and by the Subandean thrust belts. Both the western volcanic arc and the eastern volcanic centers have been active from Miocene times to present-day and are the origin of boron-rich fluids (Alonso, 1986). Combination of volcanic chains and faults fragments the Altiplano-Puna area in structural blocks which form endorheic depressions occupied by extensive salt pans or 'salares' surrounded by mud flats and alluvial systems (Fig. 1.3).

- *Argentinian salares*. A number of borate-bearing salares are distributed in the volcanic arc (Western Cordillera) and in the La Puna Plateau. In all of them, ulexite and borax ('tincal') have grown interstitially in salt-crusts and volcaniclastic muds. Ulexite occurs in two lithofacies: (1) isolated nodules usually flattened ('papas'), which can join together in a chicken-wire structure, and (2) massive beds ('barras') up to 2 m thick underlying the efflorescent salt-crust. According to Alonso (1999) and Helvacı and Alonso (2000), a marked transition from marginal travertine limestones to sulfates (gypsum), borates (ulexite, borax) and central chlorides (halite) is usually observed in the Argentinian salares of La Puna. Such a transition, however, is not so clearly observed in the salares of the Bolivia-Perú Altiplano. In the salares where the presence of sulfates (mirabilite, gypsum) is higher (Pocitos, Rincón and Río Grande), the distribution of borates is less important or absent, and those containing borates (Hombre Muerto, Rincón) exhibit lithium-rich brines. In some salares (Diablillos), borate deposits are more frequent than other detritial or evaporite materials. In some salares (Diablillos, Ratones, Centenario) a marked relation exist between borates and thermal springs, which are usually placed in travertine deposits along active faults (Alonso and Gutiérrez, 1984). In others (Hombre Muerto), boron is provided by streams and groundwater having leached pyroclastic materials of the surrounding volcanoes (Vinante and Alonso, 2006).

- *Bolivian salares*. Bolivia has a number of borate-bearing salares located in both the Western Andean Range (Chiguana, Empexa and Laguani) and the Altiplano (Chalviri) (Fig. 1.3). In all of them, the ulexite dispersed in salt crusts is exploited as a while. The Bolivian Salar of Uyuni, with an extension >10000 km^2, and an elevation of 3653 m, is the largest salt playa on the Earth together with the adjacent Salar of Coipasa. Although it is usually dried and covered by a thick salt crust, each year is flooded by a brine <1 m deep for 3-4 months in winter. In summer the brine falls to an interstitial position. Ulexite is harvested in the salt crust.

- *Chilean salares*. The Chilean salares of Atacama and Punta Negra are placed above 2300 m in the pre-Andean region, in the western side of the Western Range (Fig. 1.3). The Salar of Atacama', the largest salt flat in Chile (3000 km^2), is permanently free of superficial water. Although ulexite nodules are recognized in the salt crust, the salar is mainly a great reservoir of lithium, potassium and boric acid concentrated in underground brines. Halite crust with ulexite and minor hydroboracite, gypsum, thenardite, celestine, baritine and orpiment (As_2S_3) has been reported in other Andean salares, as those of Surire and Ascotán (Chong *et al.*, 2000).

- *Peruvian salares*. Laguna Salinas is a borate salar that lies at an altitude of about 4200 m, 64 km east of Arequipa village. The salar occupies an enclosed basin that is underlain by volcanic rocks. The area is flooded in winter and afterward it becomes completely dried forming an efflorescent salt crust of halite, thenardite and glauberite. Beneath the surface, a sandy mud bed up to 1 m thick with volcanic ash contains irregular nodules of ulexite and inyoite crystalline agregates.

1.3.3. Holocene borates in Karapınar-Konya region (central Turkey)

The basin located around the town of Karapınar (Konya) is surrounded by volcanoes which have been active in various phases from the Late Miocene to present. Currently active volcanism is evidenced by the discharge of thermal and mineral waters and magmatic gases. Potentially economic deposits of borate, chloride, sulfate and carbonate salts related to this volcanic activity are forming within the basin. Andesitic lavas of Late Miocene volcanism form Üzecik Mountains are located in the western part of the basin. Karacadağ, which is located in the eastern part of the basin, has a complex domal structure and completed its evolution in a few phases during the entire Pliocene. The lavas which form Karacadağ rise to an elevation of 1995 m are predominatly andesite, but locally trachyandesite, basaltic andesite and dacite are also present. All of them show a highly viscous flow character.

The southern part of the Karapınar Basin is delimited by lava flows and small volcanic cone and maar pyroclastics that formed as a result of several volcanic phases which began in the Early Quaternary and continued up until a few thousands years ago. Trachyandesitic and andesitic lava flows were formed during the first stage of volcanism in the Quaternary. Radiometric determinations done by the K/Ar method give ages between 1.1 and 1.2 Mys for these flows. Later, basaltic lavas, scoria and ash formed small volcanic cones and lava flows. Basaltic volcanic cones reach heights of 250 m. K/Ar radiometric age determinations give ages between 363.000 and 161.000 years for this stage of volcanism.

Later, maars (volcanic craters resulted from explosive eruptions) formed within the basin. Maar pyroclastics, formed successively as products of several different eruptions, are present as concentric rings around the maars. The maars of Meke Obruğu and Yılan Obruğu are small in size. As for the Mekegöl and Acıgöl maars, they are larger explosion craters measuring approximately 1.5 km in diameter. Later the maars were filled by waters forming maar lakes. A few thousand years ago, a scoria cone formed within the Meke maar lake during the last phase of basaltic volcanism.

There is evidence of active volcanic activity in the Karapınar Basin, such as the thermal and mineral waters and gases still emitted from the maars and along the major fault line in the eastern part of the basin. The gases contain predominantly CO_2 and have mantle-origin characteristics, based upon helium-and carbon-isotope ratios ($^3He/^4He = 159.10^{-6}$; $\delta^{12}C = -1.5‰$)

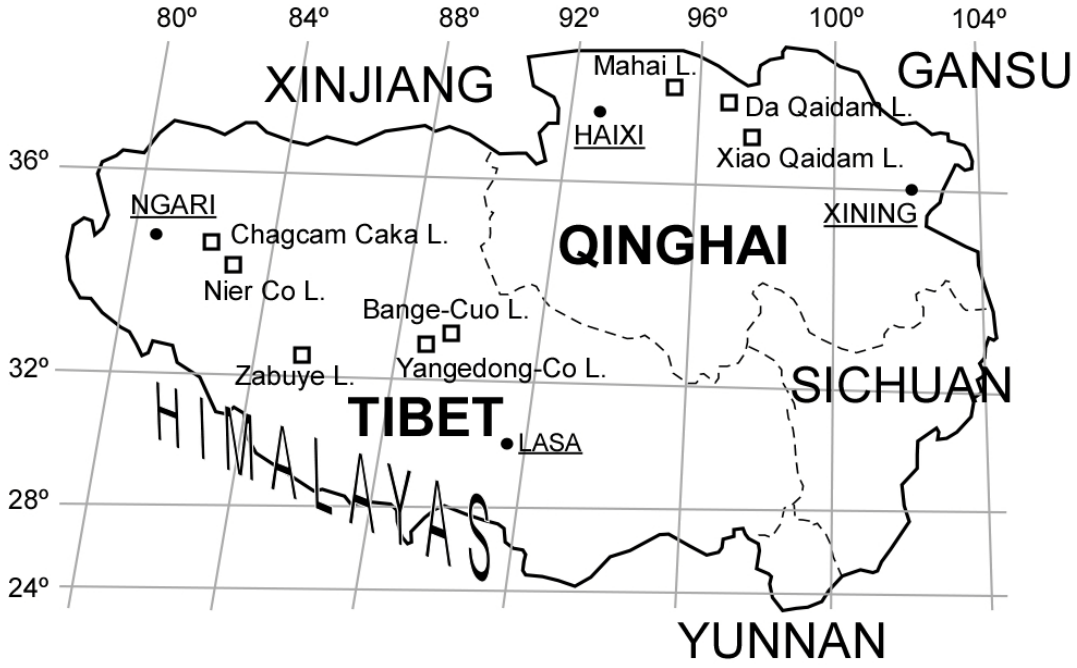

Figure .1.4. Borate localities in the Tibet-Qinghai Plateau (China)

Borate, chloride, sulfate and minor amounts of carbonate salts are actively forming in the basin. While NaCl is precipitating in the center of the basin, carbonate and CO_2 bearing waters are being discharged, and carbonates (probably trona) and Na sulfates have precipitated along the fault at the eastern edge of the basin. Ulexite, which is one of the common borate salts, seems to have formed earlier than the other salts and occurs as caulifflower or potato-shaped masses within unconsilidated sediment at depth of <1 m. Thenardite and glauberite are forming within the Acıgöl and Meke maar lakes.

The formation of borate and other salts in the Karapınar Basin is genetically related to the subalkaline volcanic rocks of this region. Na, B, Cl, SO_4 and CO_2 are carried into the basin by thermal and mineral waters related to this volcanism. Through detailed field, geochemical and drilling studies, it is probable that economically important salt deposits will be discovered (Helvacı and Ercan,1993).

1.3.4. Holocene borates in the Tibet-Qinghai Plateau (China)

The Tibet-Qinghai (Xizang-Qinghai) Plateau lies between the Himalayan Range to the south and the Kunlun Range to the north. It stretches about 1500 km north-to-south and 3500 km east-to-west. With an average elevation exceeding 4500 m and an area over 2.5 10^6 km^2 it is the highest, largest and flattest plateau in the world. It formed as a consequence of the collision between the continental crusts of the Indian and Eurasian plates 50 Myr ago. Over 70 saline lakes occur in the Tibet-Qinghai Plateau (Zheng Pianping, 1989), although borate minerals are only found in some lakes distributed in two areas: in the Qadam Basin of the Qinghai Province in the southern side of the Quilian Mountains, and in the Xizang (Tibet Province) in the northern side of the Himalayan Mountains (Fig. 1.4). Chemistry of borate-bearing lakes is strongly controlled by boron-rich hot springs related to an intense geothermal activity leaching acid magmatic rocks of the basement in these regions. Since the Würm glaciation more of these lakes remain as perennial and show a chemical differentiation. According to Zheng Mianping *et al.* (2005) borate precipitation has taken place during dry-cold climatic conditions.

- *Qinghai Province*. Da Qaidam Salt Lake, with an elevation of 4148 m and located in the north of the Qaidam Basin, is a typical halite-saturated lake enriched in lithium and boron. Two different borate occurrences have been differentiated. The principal orebody, located at the lake bottom, consists of halite, ulexite and pinnoite with minor gypsum, mirabilite, thenardite, glauberite, bloedite ($N_2Mg(SO_4)_2.2H_2O$) and epsomite ($MgSO_4$.

$7H_2O$). The second is exposed on the lake shores and consists of halite, ulexite, hydroboracite and gypsum with minor Mg-bearing borates (inderite, kurnakovite, mcallisterite and hungchaoite). Xiao Qaidam Salt Lake, with salinity over 279 g/L, is subsaturated in halite, although halite and mirabilite occur around the lake. Ulexite is mined in the surrounding sediments and also occurs with gypsum, mirabilite and pinnoite on the bottom muds (Sun Dapeng, 1990; Sun Dapend and Li Bingxiao, 1993).

-*Tibet (Xizang) Province*. Changcam Caka Salt Lake has the largest borate operation in the region. Two ore bodies are differentiated: in terraces around the margins of the modern lake and in the lake bottom. In both settings the ore consists of pinnoite and kurnakovite with minor ulexite, inderite and mirabilite. In the Nier Co Salt Lake, Mg-bearing borates (pinnoite and kurnakovite) mainly occur in several layers up to 4 m thick in the margins and on the bottom of the lake. In some of these layers mirabilite is present as a minor phase. Zabuye Salt Lake, with a salinity ranging between 36 and 44%, is supersaturated with respect to halite. Millions of metric tons of halite, apthitalite ($(KNa)_3Na(SO_4)_2$), trona and glauberite are deposited on the bottom of the lake. The lake is enriched in lithium and boron. Zabuyite, a lithium carbonate (Li_2CO_3), has been found for the first time and a mineral exploitation plant is conducted by mining lithium carbonate in solar ponds. Although no borate minerals have been found, isothermal evaporation experiments with the lake brine at 25ºC produced sylvite (KCl) and borax when 90% of water was removed (Nie *et al.,* 2009).

1.3.5. Holocene borates in Lake Inder (Kazakhstan)

Lake Inder, with a 36 m deep water mass, is a NaCl-saturated lake located north of the Caspian Sea and east of the Ural River. Despite no information is available about the occurrence and genesis of borate minerals in the Inder Lake region, some Mg-bearing borates were described for the first time (inderite, inderborite and kurnakovite). The main borate mineral consists of hydroboracite associated with minor inyoite, colemanite, szaibelyite (ascharite), ulexite and priceite. The lake receives drainage from the borate-bearing veins in caprocks of the domes of the Inder Salt, which are Lower Permian (Kungurian) in age. The boron source of Lake Inder as a sump accumulation of water leaching Permian, marine evaporites still remains controversial. Moreover, significant confusion is placed at that point because the same mineral assemblage is attributed to the modern lake and to the Permian salt domes (Garret, 1998; Kistler and Helvacı, 1994).

1.4. Mineralogical differences between Holocene and ancient lacustrine borate deposits

As mentioned above, only a reduced number of borate minerals, as borax and ulexite, are common precipitates in the Holocene occurrences. Other borates, as meyerhofferite, inyoite, probertite, howlite, hydroboracite, inderite and kurnakovite are less frequent, and some other borates, as colemanite, priceite and kernite are rare or almost absent (Alonso, 1986). The comparison between these occurrences and the distribution of the various borate minerals in the ancient (Neogene) deposits reveals some important differences (Fig. 1.5). Thus, in the Neogene deposits:

- colemanite is the most common Ca-borate;
- other Ca-bearing borates, as inyoite, priceite, probertite and howlite, are much more common than in the Holocene occurrences;
- kernite is mainly associated with borax at depth, suggesting the existence of a diagenetic cycle of mineral transformations (primary borax → replacive kernite at depth → secondary borax in exhumation);
- a number of Ca- and Na-bearing borates such as colemanite, priceite and borax can be replaced by secondary calcite close to the surface during exhumation; under these conditions related to groundwater circulation and weathering, calcite pseudomorphs after those precursor borates are commonly preserved.

According to all these differences, colemanite, ulexite, and borax (occasionally kernite) are the most common Ca- and Na-bearing rock-forming borates in the Neogene deposits and those of major petrologic relevance and economic interest as well.

1.5. Mineral zoning in the borate deposits: depositional *versus* diagenetic patterns

A number of Neogene borate deposits show a mineral zoning both in a lateral (from the margin to the center) and a vertical sense (from the base to the top). In some cases this zoning is symmetrical, while in others it is slightly asymmetrical. In general, this distribution can be assigned to a depositional control. Consequently, the mineral zones in this interpretation reflect the evolution of the brine composition in space and time.

In some cases, however, this zoning has been considered to be diagenetic based on the mineralogic differences recorded between the Holocene and the ancient (Neogene) deposits. Burial (thermal) diagenesis and reaction (with groundwater) diagenesis are the main types proposed in the literature to explain the borate zoning under non-depositional conditions (Smith and Medrano, 1996).

Burial diagenesis refers to dehydration and mineral transformation occurred in the deposits by increasing temperature during progressive burial. This interpretation could explain, in the Neogene deposits, the changes underwent by

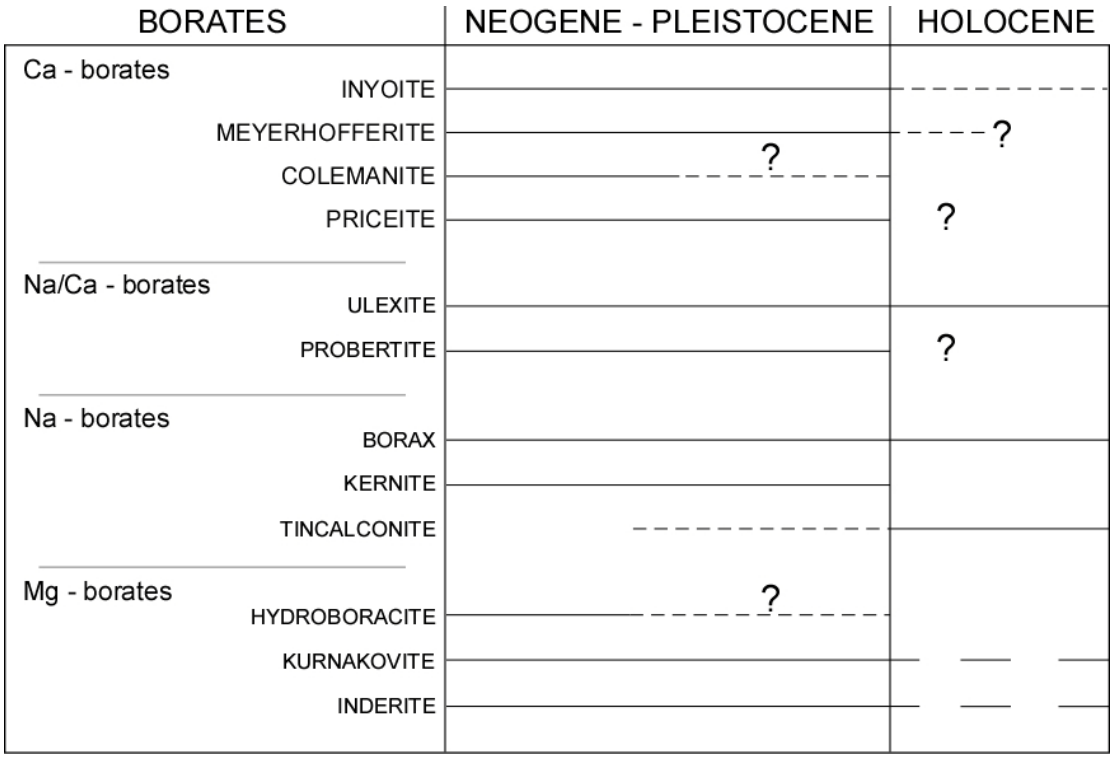

Fig. 1.5: Comparative distribution of some of the most common borates in recent and ancient deposits (based on Alonso, 1986, plate 30).

minerals in the hydration series of Ca-borates and Na-Ca-borates. For instance, the predominance in the Furnace Creek Fm (Death Valley, Miocene-Pliocene, California) of the less hydrated phases (colemanite, probertite) was related to the dehydration conversions of meyerhofferite-to-colemanite and of ulexite-to-probertite at burial depths of up to 1500 m (Smith and Medrano, 1996; Tanner, 2002).

Reaction diagenesis would occur when groundwater interacts with borate minerals forming these bodies (Smith, 1985). Thus, the presence in many Neogene deposits of a mineral zoning in association with a vein complex of various minerals (ulexite, colemanite, borax) cross-cutting the borate layers, was ascribed by Smith and Medrano (1996) to reaction diagenesis while the deposits were uplifted during the Neogene-Quaternary time.

A discussion on the possible interpretations of a mineral zoning in the Neogene deposits, i.e. depositional controls *vs*. diagenetic transformations, is out of the scope of this workshop (see comments in Helvacı and Ortí, 1998, 2004). Probably, many factors (geological setting, burial story of the region, sedimentologic and textural characteristics of the borate minerals, isotopic values, fluid inclusions composition, etc.) need to be taken into account for deciphering the prevailing mechanism causing the mineral zoning in a particular deposit.

Barker and Barker (1985) and Crowley (1996) applied the concept of chemical divides to explain the mineral sequences in the borate deposits. In particular, Crowley (1996) assumed the precipitation of rare Mg-borates present in some deposits as the end products of the evolution of the boratiferous brines. This is a sedimentologic alternative to previous interpretations that considered these minerals as late diagenetic and originated from reaction diagenesis (by groundwater action during exhumation). Such a depositional interpretation was assumed by Ortí and Alonso (2000) in the Argentinian hydroboracite deposits and by Helvacı and Ortí (2004) in the Turkish borax deposit.

As regards the assemblage of the Miocene Anatolian deposits, and on the basis of observations on (1) the regional context and (2) the lithofacies, petrography and depositional cycles in the borate units, Helvacı and Ortí (1998) emphasized that these deposits: (a) are mainly formed by high hydrated (borax, ulexite) and less hydrated (colemanite, probertite) minerals; (b) were never buried more than 300-500 m and so, a thermal diagenesis cannot be applied to them; (c) exhibit colemanite which can be largely interpreted as a mineralogically primary (*de novo*) precipitate that grew interstitially within the sedimentary matrix; and

(d) exhibit other Ca-bearing minerals, as meyerhofferite, priceite and howlite which can also be interpreted as interstitially grown forming mineralogically primary precipitates. All these observations clearly favour a depositional interpretation of the mineral zoning.

It seems likely that various mineralogical and textural transformations affecting the borate minerals in the Neogene deposits occurred from early diagenesis to initial or moderate burial diagenesis. Similarly, it is possible that some of the mineral associations found in the Ca- and Na-bearing borates are the result of total or partial reabsortion of former minerals in the boratiferous brines along the evaporative concentration process. In conclusion, as in other groups of evaporites, detailed studies of petrography, lithofacies and cyclicity can contribute greatly to understand the sedimentary environments and diagenetic transformations in borate deposits, in parallel with other research methods such as geochemical and isotopical determinations.

TABLE I-1: Borate mineral, formulation and chemical composition

	Structural formula	Empirical formula	Oxid like formula
Ca-borates			
Priceite	$Ca_2(B_5O_7(OH)_5).H_2O$	$Ca_4B_{10}O_{19}.7H_2O$	$4CaO\ 5B_2O_3\ 7H_2O$
Colemanite	$Ca(B_3O_4(OH)_3).H_20$	$Ca_2B_6O_{11}.5H_2O$	$2CaO\ 3B_2O_3\ 5H_2O$
Meyerhofferite	$Ca(B_3O_3(OH)_5).H_20$	$Ca_2B_6O_{11}.7H2O$	$2CaO\ 3B_2O_3\ 7H_2O$
Inyoite	$Ca(B_3O_3(OH)_5).4H_20$	$Ca_2B_6O_{11}.13H2O$	$2CaO\ 3B_2O_3\ 13H_2O$
Ca-Na-borates			
Probertite	$NaCa(B_5O_7(OH)_4).3H_2O$	$NaCaB_5O_9.5H_2O$	$Na_2O\ 2CaO\ 5B_2O_3\ 10H_2O$
Ulexite	$NaCa(B_5O_6(OH)_6).5H_2O$	$NaCaB_5O_9.8H_2O$	$Na_2O\ 2CaO\ 5B_2O_3\ 16H_2O$
Na-borates			
Kernite	$Na_2(B_4O_6(OH)_2).3H_2O$	$Na_2B_4O_7.4H_2O$	$Na_2O\ 2B_2O_3\ 4H_2O$
Tincalconite	$Na_2(B_4O_5(OH)_4).3H_20$	$Na_2B_4O_7.5H_2O$	$Na_2O\ 2B_2O_3\ 5H_2O$
Borax	$Na_2(B_4O_5(OH)_4).8H_20$	$Na_2B_4O_7.10H_2O$	$Na_2O\ 2B_2O_3\ 10H_2O$
Mg-borates			
Szaibelyite	$Mg(BO_2(OH))$	$Mg_2B_2O_5.2H_2O$	$2MgO\ B_2O_3\ 2H_2O$
Pinnoite	$Mg(B_2O(OH)_6)$	$MgB_2O_4.3H_2O$	$MgO\ B_2O_3\ 3H_2O$
Mcasllisterite	$Mg(B_6O_7(OH)_6)_2.9H_2O$	$Mg_2B_{12}O_{20}.15H_2O$	$2MgO\ 6B_2O_3\ 15H2O$
Hungchaoite	$Mg(B_4O_5(OH)_4).7H2O$	$MgB_4O_7.9H_2O$	$MgO\ 2B_2O_3\ 9\ H_2O$
Kurnakovite	$Mg(B_3O_3(OH)_5).5H_2O$	$Mg_2B_6O_{11}.15H_2O$	$2MgO\ 3B_2O_3\ 15H_2O$
Inderite	$Mg(B_3O_3(OH)_5).5H_2O$	$Mg_2B_6O_{11}.15H_2O$	$2MgO\ 3B_2O_3\ 15H_2O$
Mg-Na-borates			
Aristarainite	$Na_2Mg(B_6O_8(OH)_4)_2.4H_2O$	$Na_2MgB_{12}O_{20}.8H_2O$	$Na_2O\ MgO\ 6B_2O_3\ 8H_2O$
Rivadavite	$Na_6Mg(B_6O_7(OH)_6)_4.10H_2O$	$Na_6MgB_{24}O_{40}.22H_2O$	$3Na_2O\ MgO\ 12B_2O_3\ 22H_2O$
Mg-Ca-borates			
Hydroboracite	$CaMg(B_6O_8(OH)_6).3H_2O$	$CaMgB_6O_{11}.6H_2O$	$CaO\ MgO\ 3B_2O_3\ 3H_2O$
Inderborite	$CaMg(B_3O_3(OH)_5)_2.6H_2O$	$CaMgB_6O_{11}.11H_2O$	$CaO\ MgO\ 3B_2O_3\ 11H_2O$
Mg-K-borates			
Kaliborite	$KHMg_2(B_{12}O_{16}(OH)_{10}).4H_2O$	$K_2Mg_4B_{24}O_{41}.19H_2O$	$K_2O\ 4MgO\ 12B_2O_3\ 19H_2O$
Sr-borates			
Veatchite	$Sr_2(B_{11}O_{16}(OH)_5).H_2O$	$Sr_4B_{22}O_{37}.7H_2O$	$4SrO\ 11B_2O_3\ 7H_2O$
Tunellite	$Sr(B_6O_9(OH)_2).3H2O$	$SrB_6O_{10}.4.H_2O$	$SrO\ 3B_2O_3\ 4H_2O$
Borosilicates			
Bakerite	$Ca_4B_4(BO_4)(SiO_4)_3(OH)_3.H_2O$	$Ca_8B_{10}Si_6O_{35}.5H_2O$	$8CaO\ 5B_2O_3\ 6SiO_2\ 5H_2O$
Howlite	$Ca_2B_5SiO_9(OH)_5$	$Ca_2SiHB_5O_{12}.2H_2O$	$4CaO\ 5B_2O_3\ 2SiO_2\ 5H_2O$
Searlesite	$NaBSi_2O_5(OH)_2$	$NaBSi_2O_6.H_2O$	$Na_2O\ B_2O_3\ 4SiO_2\ 2H_2O$
Boroarseniates			
Cahnite	$Ca_2B(AsO_4)(OH)_4$	$Ca_2AsBO_6.2H_2O$	$4CaO\ B_2O_3\ As_2O_5\ 4H_2O$
Teruggite	$Ca_4MgAs_2B_{12}O_{22}(OH)_{12}.12H_2O$	$Ca_4MgAs_2B_{12}O_{28}.18H_2O$	$4CaO\ MgO\ 6B_2O_3\ As_2O_5\ 18H_2O$
Borophosphates			
Luneburgite	$Mg_3B_2(PO_4)_2(OH)_6.5H_2O$	$Mg_3P_2B_2O_{11}.8H_2O$	$3MgO\ P_2O_5\ B_2O_3\ 8H_2O$
Borosulfates			
Fontarnauite	$Na_2Sr(SO_4)(B_4O_6(OH)_2).3H_2O$	$Na_2SrSB_4O_{11}.4H_2O$	$Na_2O\ SrO\ SO_3\ 2B_2O_3\ 4H_2O$

PART II: LITHOFACIES AND PETROGRAPHY

Lithofacies. In this workshop we are using the word 'lithofacies' in the sense of macroscopic characteristics of the borate rocks, i.e., as a basic description informing on: a) the macroscopic structures/textures of both sedimentary and diagenetic interest, and b) the relationships between the borate and the host-sediment. Many terms of lithofacies, such as laminated, banded, nodular-banded, nodular, massive, enterolithic, brecciated, pseudo-morphic, and so on are the same than to those used in other evaporitic rocks.

As regards the sedimentologic interpretations of the borate lithofacies to be found in the literature, they commonly follow the interpretative patterns previously established for the Ca-sulfate lithofacies. Some aspects of the primary (depositional) origin of a particular borate mineral are: the perfect lamination or banding; the lateral stratigraphic continuity; and the alternation with one or several primary, non-borate minerals. Summing up, laminated and banded lithofacies are usually interpreted as subaqueous precipitates, while nodular, nodular-banded and enterolithic lithofacies tend to be interpreted as formed interstitially (within the sedimentary matrix) from underground positions of the water table (under subaerial, exposed conditions). This last point (the nodular lithofacies), however, should not be systematically applied to the borate lithofacies without a detailed sedimentological examination of the depositional cycles formed by the borates alone or in association with other evaporites (see below).

Crystalline fabrics. The petrographic observations refer mainly to the description and interpretation of the microscopic textures/structures forming the various lithofacies of borates. In many cases, these fabrics are formed by very small crystals. Not unfrequently, however, the fabrics are constituted by coarse-grained crystals attaining up to several centimeters in length.

Several petrographic features suggest a diagenetic (secondary) origin for some particular borate minerals: the geometry of grain boundaries; the presence of pseudomorphs of one mineral after a precursor one; and the presence of relics of a (precursor) mineral within the crystals of another. Of particular interest to decipher the diagenetic modifications in a borate paragenesis is the presence of pseudomorphs.

Primary, early diagenetic, secondary borates. According to both the modern and the ancient occurrences of borates, some of these minerals as borax, ulexite and inyoite are primary, free (subaqueous) precipitates: they form stratified deposits, where the crystals may exhibit fabrics indicating bottom growth conditions. The rest of borates, and also borax in some cases, precipitate interstitially within a preexistent host-sediment or matrix (clay, tuff) under synsedimentary/early diagenetic conditions. This is usually a displacive growth, but the matrix can result embedded and cemented also. Finally, borates can be secondary also: in some cases they replace other preexistent/precursor minerals.

Studied material. This workshop is focused on the lithofacies and petrographic features of the most common borate minerals forming the Neogene Anatolian (Turkey) deposits. These deposits were originated in non-marine, evaporitic settings during the Miocene, and are distributed in five mining districts: Bigadiç (colemanite, ulexite), Emet (colemanite, probertite), Kestelek (colemanite, probertite), Kırka (borax, probertite), and Sultançayır (priceite, howlite). At present, the latter explotation is not active. A number of studies have been devoted to the mineralogy, stratigraphy and genesis of all these deposits (Helvacı and Firman, 1976; Ataman and Baysal, 1978; Helvacı, 1977, 1978, 1994, 1995; Kistler and Helvacı, 1994; Mordogan and Helvacı, 1994; Palmer and Helvacı, 1995; Palmer and Helvacı, 1997; Helvacı and Ortí, 1998, 2004; Ortí *et al.*, 1998; García-Veigas *et al.*, 2011; among many others).

Additionally, some references will be done to the Neogene borate deposits in La Puna region (Central Andes, NW Argentina), from which hand samples and petrographic material is also available.

On the basis of the Neogene borate occurrences in Western Anatonia and Central Andean region, the study of lithofacies and petrography can be separated in two groups: the rock-foming borates and the accessory borates. Only their most significant characteristics are cited in this text, but additional information is given separately in Table II-1. The optical and crystallographic characteristics of most of the borate minerals studied in this workshop are summarized in the Appendix.

2.1. Rock-forming Na-Ca borates

2.1.1. Ulexite

Lithofacies. Ulexite is characterized by a white, sometimes silky luster, and a very fine grained texture. Main lithofacies are the following:

- *Nodular, and nodular-banded*. Ulexite nodules display a variety of morphologies, from almost spherical to cauliflower-like (cotton-ball), flattened, irregular or with interpenetrating boundaries. The size of these nodules ranges between <1 cm (micronodules) and up to 30-40 cm (Fig. 2.1A).
- *Vertically elongated (columnar, tooth-shape).* Some ulexite layers are formed by very narrow (usually <1 cm in diameter) nodules elongated vertically up to some tens of centimeters (Fig. 2.1B).
- *Laminated*. In this lithofacies, laminae (<1 cm thick) of ulexite may alternate with carbonate and lutitic laminae. The inner structure of these

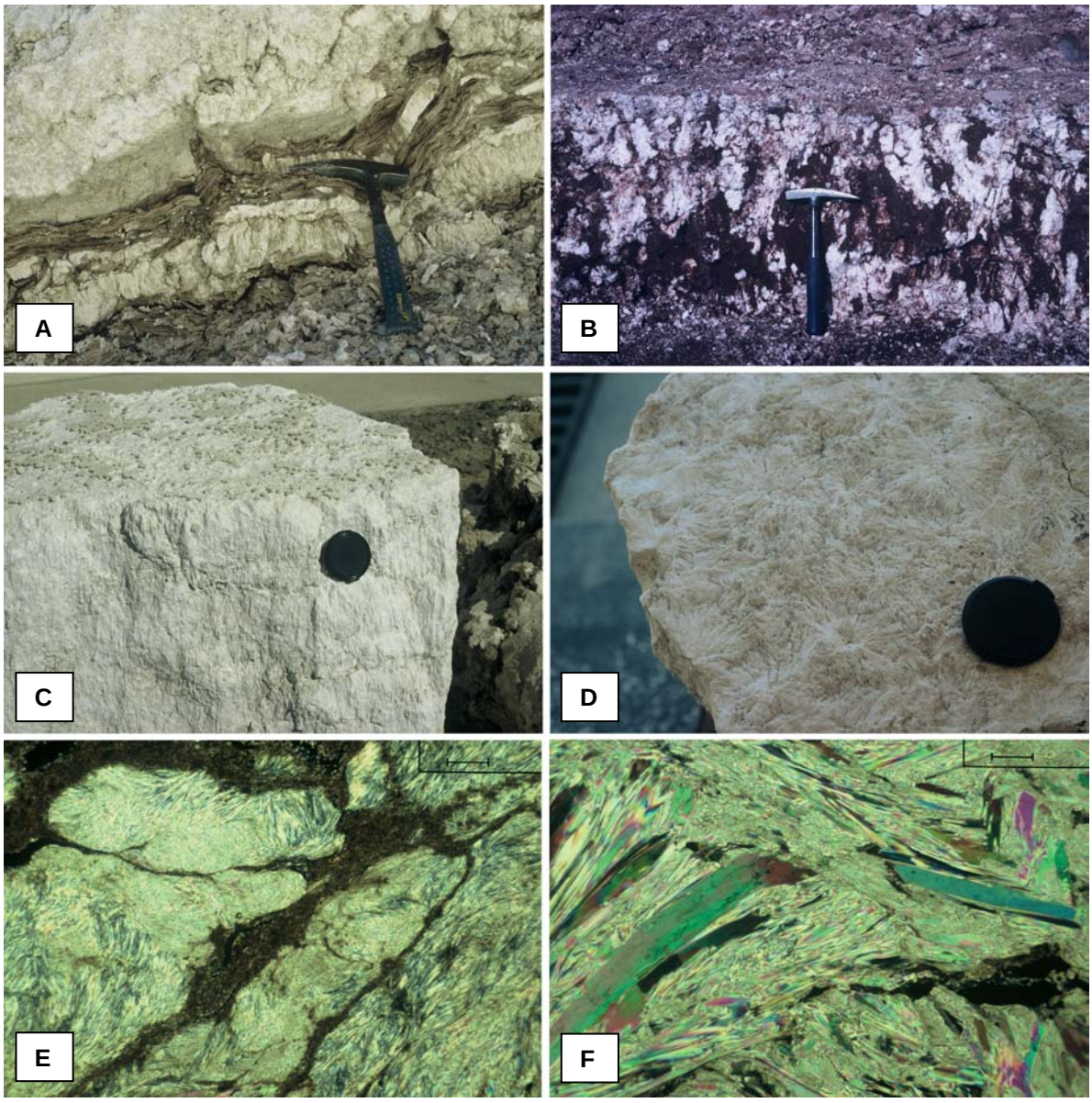

Figure 2.1. ULEXITE
A) Various lithofacies (nodular-banded, columnar, fibrous veins) of ulexite (white, fibrous material) alternating with laminated claystones (dark material) (Kurtpınarı deposit, Bigadiç district, Miocene, Anatolia).
B) View of a vertical trench sectioning the floor of a Holocene salar. The nodules of ulexite ('papas'; fine-grained, white material) have grown in a dark, clayey matrix. The columnar arrangement of the nodules suggests a control by capillary action (Mina Maggi, Salar Centenario, NW Argentina).
C) Banded to massive lithofacies of ulexite. Small crystals at the top corresponds to tunellite. Lens cap: 6 cm in diameter (Bigadiç district, Miocene, Anatolia).
D) Top view of a layer formed by banded to massive lithofacies of ulexite, showing the radiating crystalline fabric. Lens cap: 6 cm in diameter (Bigadiç district, Miocene, Anatolia).
E) Photomicrograph of ulexite micronodules wich are surrounded by a dark, clayey matrix. Note the variable size and interlocking character of the micronodules. Bar: 0.32 mm. Crossed nicols.
F) Photomicrograph of fibrous fabric in a micronodular lithofacies of ulexite. Deformation, bending and breakage of the fibers are common and probably occurred during the growth and mutual interaction of the micronodules. Scale bar: 0.32 mm. Crossed nicols.

ulexite laminae tends to be micronodular and more unfrequently massive.

- *Banded, and banded-massive*. Bands (1 - 10 cm thick) and layers (>10 cm thick) of ulexite are common (Fig. 2.1C). These bands are formed by fibrous, massive to poorly-defined nodular masses of fibrous ulexite, which commonly display radiating fabrics (Fig. 2.1D).

- *Fibrous (satin-spar) veins*. These veins (<1 - 20 mm thick) are very common in the borate units. They can be parallel to bedding (Fig. 2.1A) or crosscut (and cement) all sedimentary materials, both the borate minerals and the matrix, in whatever direction.

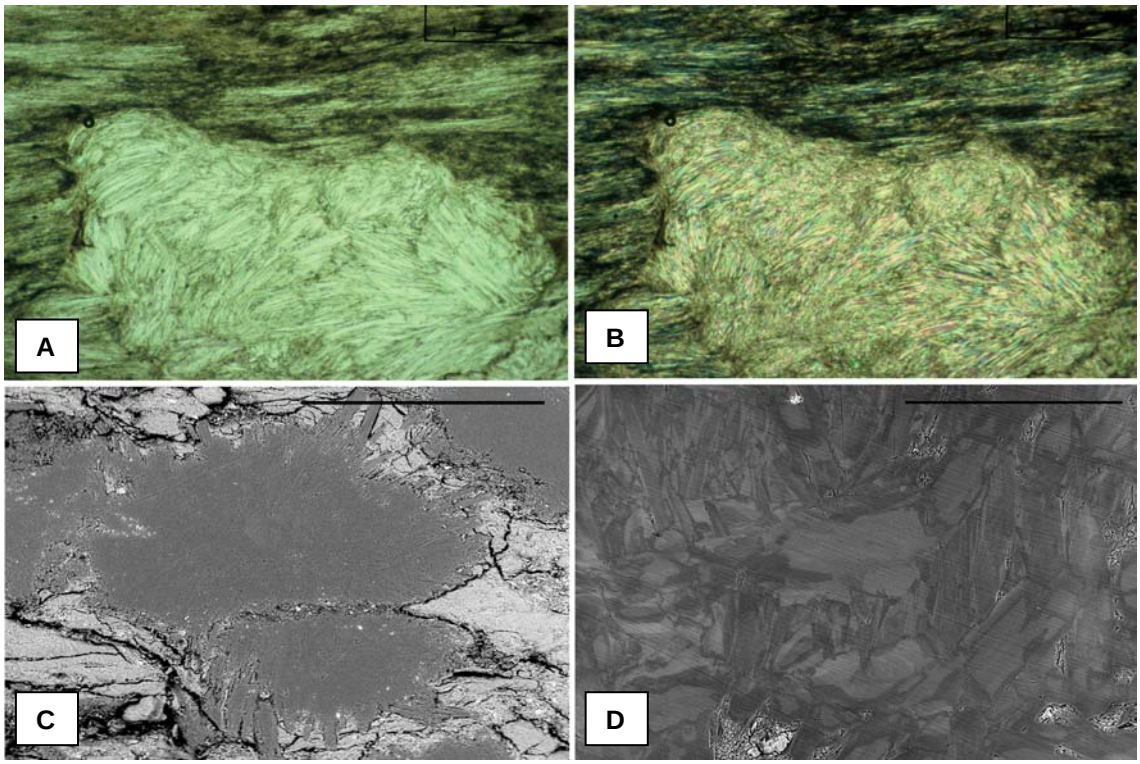

Figure 2.2. PROBERTITE
A) and B) Photomicrographs of a probertite micronodule within laminated lithofacies of the same mineral. Note the small groups of subparallel fibers of probertite forming the micronodule. Scale bar: 0.32 mm (A: normal light; B: crossed nicols), (Kestelek district, Miocene, Anatolia).
C) SEM-BSE image of a micronodule of probertite growing insterstitially in a clayey matrix. Scale bar: 1 mm (Kırka district, Miocene, Anatolia).
D) SEM-BSE image of probertite crystals showing a strontium chemical zonation. Scale bar: 0.5 mm (Kırka district, Miocene, Anatolia).

Crystalline fabrics. Ulexite displays two major crystalline fabrics:
- *Parallel fibers*.The most common fabric is made up of small groups of almost parallel to each other fibers or needles. These fibrous groups exhibit micronodular or fusiform shapes in which the fibers display tangencial to fascicular fabrics, as well as bending and breakage features (Fig. 2.1E,F).
- *Radiating fibers*. Less common is a large, fibrous-radiating fabric. This fabric forms large nodules or massive lithofacies in which the fibers reach up to 5 mm in length (Fig. 2.1D).

2.1.2. Probertite

Lithofacies. The major lithofacies of probertite are nodular and laminated:
- *Nodular*. Probertite usually occurs as grey, and dirty yellow, or dirty white clusters and nodules, which are composed of fibrous crystals ranging from 5 to 50 mm in length. These fibers are oriented parallel to one another or may display radiating fabrics (Fig. 2.2.A,B,C).
- *Lenses and massive beds*. Probertite occasionally forms 20 to 30 cm thick lenses in the ulexite beds, though massive layers up to 1 m thick are encountered in some ulexite beds.
- *Laminated*. In the exploratory boreholes of the Emet district (García-Veigas *et al.*, 2011), probertite forms laminae with variable thickness (from one to some millimeters thick, besides other unusual lithofacies known in this mineral (banded, banded-nodular, nodular, brecciated) (Fig. 2.2.A,B)

Crystalline fabrics. The crystalline fabrics of probertite are formed by fibrous crystals also of variable sizes, from extremely fine to millimetric arranged in micronodules and micro-bundles (Fig. 2.2A,B).

2.2. Rock-forming Ca-borates

2.2.1. Inyoite

Inyoite occurs rarely as discrete, transparent prismatic to *tabular crystals*, and also as crystal groups and intergrown crystalline masses. Some of these euhedral crystals are up to 2.5 cm in length, but most are microscopic. Locally, inyoite occurs as clear, coarse-grained, euhedral aggregates (Fig. 2.3A,B).

Replacive inyoite. In the occurrences with other minerals such as meyerhofferite, colemanite, ulexite and hydroboracite, replacive inyoite is found scattered within them (Fig. 2.3C,D).

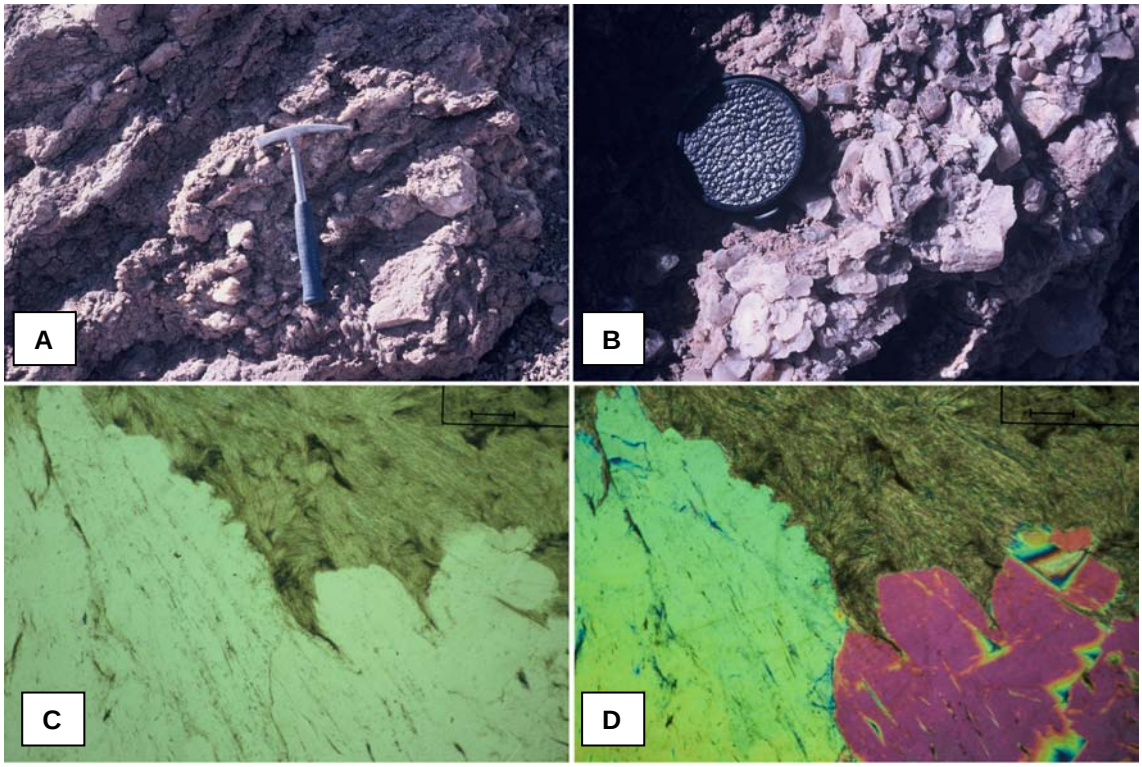

Figure 2.3. INYOITE
A) Masses and layers of primary inyoite alternating with lutite horizons (Monte Azul deposit, Miocene, NW Argentina).
B) Close view of one of the inyoite layers in A. Note the transparent, prismatic to tabular habit of the crystals. Lens cap: 6 cm in diameter (Monte Azul deposit, Miocene, NW Argentina).
C) and D) Photomicrographs of fibrous masses of ulexite (fine-grained, brownish material) being replaced by transparent, coarse-crystalline inyoite. Bar: 0.32 mm (C: normal light; D: crossed nicols) (Acep deposit, Bigadiç district, Miocene, Anatolia).

2.2.2. Meyerhofferite

Lithofacies. The main lithofacies of meyerhofferite are the following:
- *Nodular.* Meyerhofferite occurs as nodules up to 15 cm in diameter, which are composed of coarse-crystalline radiating crystals (Fig. 2.4A). These nodules have grown interstitially within a sedimentary matrix. Small vugs in the center of the nodules (Fig. 2.4B) may contain acicular crystals of the same mineral.
- *Crystalline masses*. Yellow-white, coarse-crystalline meyerhofferite usually occurs as a net-texture made up of transparent crystals, regularly oriented in two systems which cross to about 90º.

Crystalline fabrics. Under the microscope, meyerhofferite shows a tabular to prismatic habit (Fig. 2.4C,D). The sections normal to the prisms usually show two cleavage systems which cross almost perpendicularly. In these sections, the optical extinction forms a very low angle with the cleavage (Fig. 2.4.E,F).

2.2.3. Colemanite

Lithofacies. The main lithofacies of colemanite are the following:
- *Nodular, and nodular-banded*. Colemanite nodules have variable sizes between <1 cm and >50 cm (meganodules), and display different shapes from spherical to ovoid, hemispheroidal, flattened, discoidal, lenticular, flaser-shaped, cauliflower-like, elongated, and irregular (Fig. 2.5 A,B). Each nodule is a single structure or can be composite, and it occurs isolated or grouped in open or in closely packed patterns deforming and trapping the matrix. Some nodules display growth-bands that are arranged concentrically (zoned growth) (Fig. 2.5C,D). This zoning may involve: a) a coarse-crystalline colemanite core with a blocky, cementing fabric; b) an intermediate zone of radiating fabric; and c) an outer zone with a dendritic fabric. The crystalline core may project through the intermediate zone by means of septaria-like radiating bands. Locally, the center of the nodules may be empty or may have a vuggy texture, where a drusy coat made up of euhedral, coarse-sized crystals of colemanite surrounds the central hollow.
- *Fibrous-banded lithofacies*. The fibrous growth of colemanite in bands and thin layers is a common feature (Fig. 2.5E).
- *Isolated crystals*. Euhedral crystals of colemanite occur interstitially within the

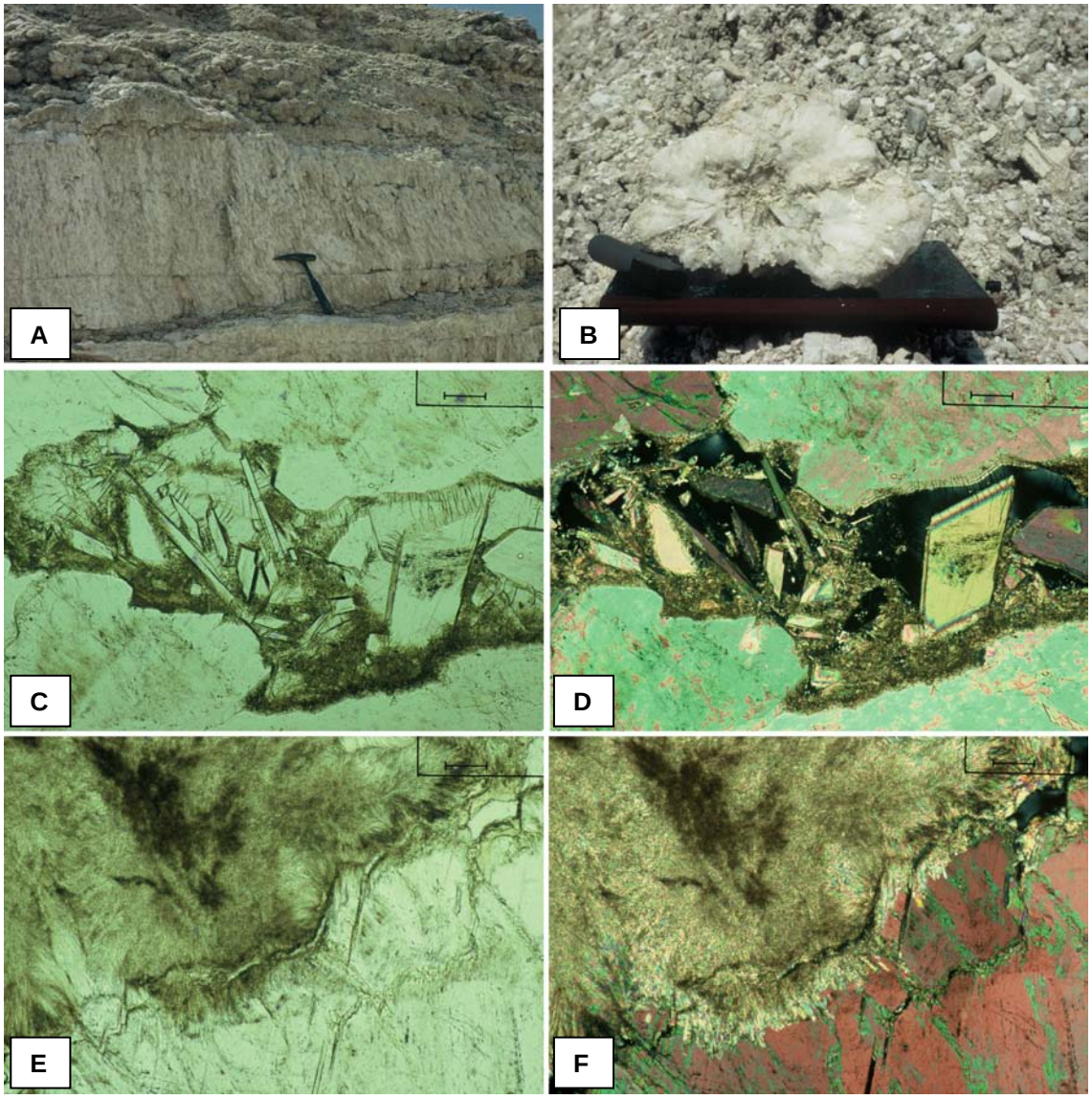

Figure 2.4. MEYERHOFFERITE
A) Depositional cycle of claystone-ulexite-meyerhofferite, where nodular meyerhofferite overlies a layer of columnar ulexite. Hammer for scale (Simav deposit, Bigadiç district, Miocene, Anatolia).
B) Close view of one nodule of meyerhofferite. Note the white color and coarse size of the meyerhofferite crystals, their roughly radial arrangement, and the central hollow. Length of the nodule: 16 cm.
C) and D) Photomicrographs of a meyerhofferite nodule. The clayey matrix includes fine-grained, euhedral crystals of meyerhofferite. This matrix is located in the boundary between large crystals of meyerhofferite. The fine-grained crystals, which constitute a first generation of interstially-grown meyerhofferite, are trapped by the progressive development of a coarse-grained, second generation forming the nodule. The two generations are mineralogically primary. Scale bar: 0.32 mm (C: normal light; D: crossed nicols).
E) and F) Photomicrographs of a contact boundary between fibrous ulexite (fine-grained, brownish material in the upper part) and transparent, coarse-crystalline meyerhofferite. Fibrous ulexite replaces meyerhofferite. Scale bar: 0.64 mm (E: normal light; F: crossed nicols).

sediment matrix, either isolated and unoriented or grouped in small, irregular aggregates.

- *Massive, vuggy-brecciated lithofacies*. Some colemanite layers exhibit a brecciated texture with vugs, drusy cavities and septaria structures, as well as coarse-crystalline masses. Vugs and cavities are commonly coated by coarse euhedral, transparent crystals of the same mineral.

- *Fibrous (satin-spar) veins*. These are veins (<2 mm to >10 cm thick) that are parallel or crosscut the host sediment and the borate units.

Crystalline fabrics. The crystals forming the nodules have several centimeters in length, and are arranged in subgroups with the same optical orientation. Colemanite crystals can also be small in size, either isolated (Fig. 2.5F) or grouped (Fig. 2.5G,H).

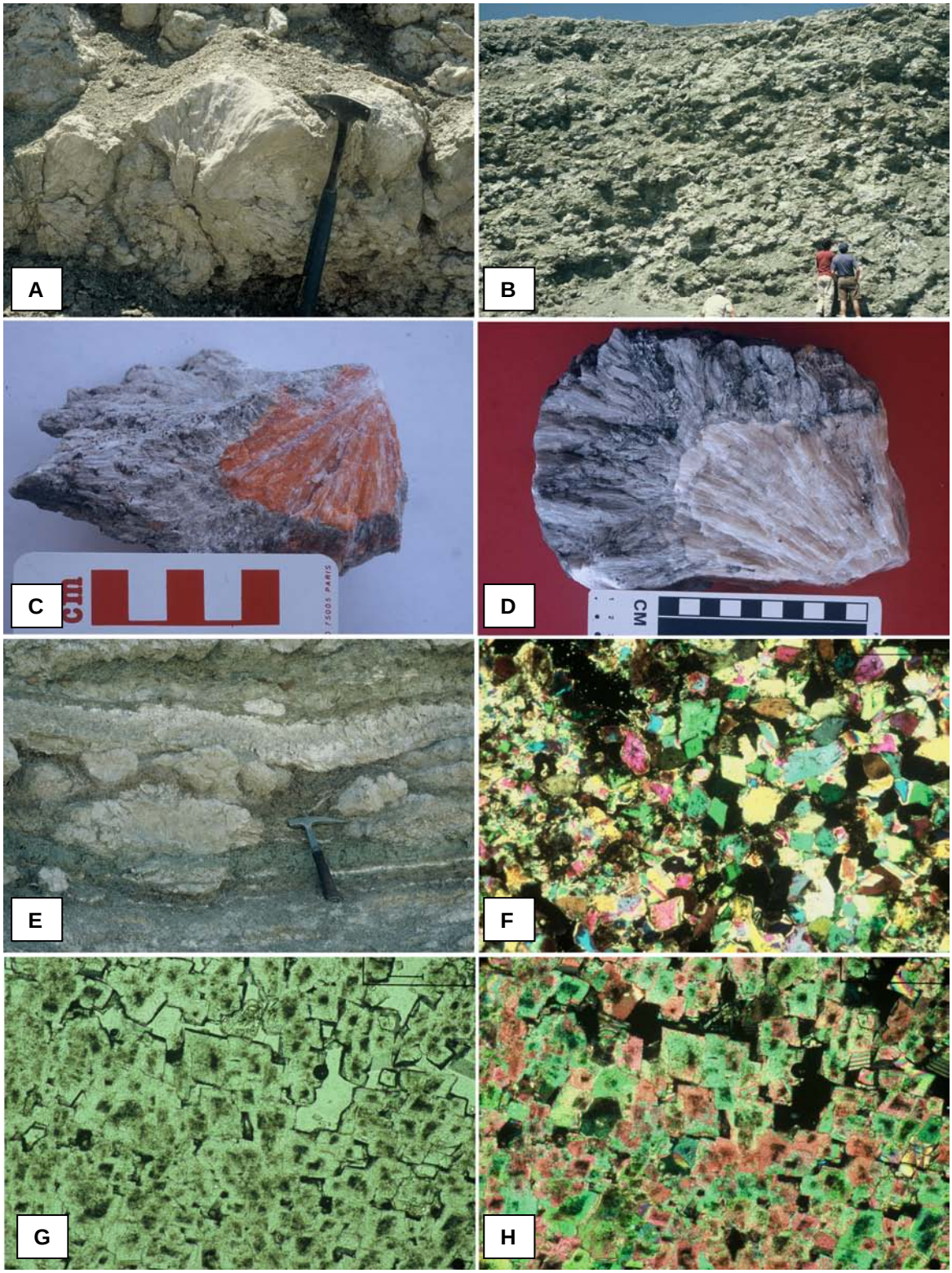

Figure 2.5. COLEMANITE
A) Large nodule of colemanite in a nodular-banded lithofacies of this mineral. Note the radiating fabric of the crystals forming the nodule (Kapıkaya deposit, Bigadiç distric, Miocene, Anatolia).
B) View of a colemanite exploitation front. Note the interlocking fabric of the nodules. Diameters of the nodules range between 10 and 80 cm (Espey deposit, Emet district, Miocene, Anatolia).
C) Close view of a fragment of a colemanite nodule in which the radiating crystals in the central part are totally impregnated by realgar (reddish material). Scale in centimeters (Emet district, Miocene, Anatolia).
D) Close view of a fragment of a colemanite nodule. The central part is formed by radiating crystals of colemanite (light brown), whereas in the external part, a branching-to-dendritic fabric trapping sedimentary matrix prevails (dark grey). Note the zoned pattern (lamination) in the boundary between the two parts. Scale in centimeters (Emet district, Miocene, Anatolia).
E) Colemanite lithofacies grading from isolated nodules to fibrous-banded layers. The colemanite growth is always displacive. Host sediment is grey lutite and tuff horizons (Emet district, Miocene, Anatolia).

F) Photomicrograph of a fine-grained mosaic fabric of colemanite forming the center of a nodule. Note the euhedral (rhombohedral) sections. Some crystals show zoned growth and syntaxial overgrowths. The overgrowths tend to be subhedral and to display undulose extinction. Scale bar: 0.32 mm, crossed nicols (Kireçlik mine, Bigadiç district, Miocene, Anatolia).
G) and H) Photomicrographs of the central part of a colemanite nodule. The fabric is formed by a mosaic of euhedral to subhedral crystals with almost the same optical orientation. Some porosity is present. Scale bar: 0.32 mm (G: normal light; H: crossed nicols) (Bigadiç district, Miocene, Anatolia).

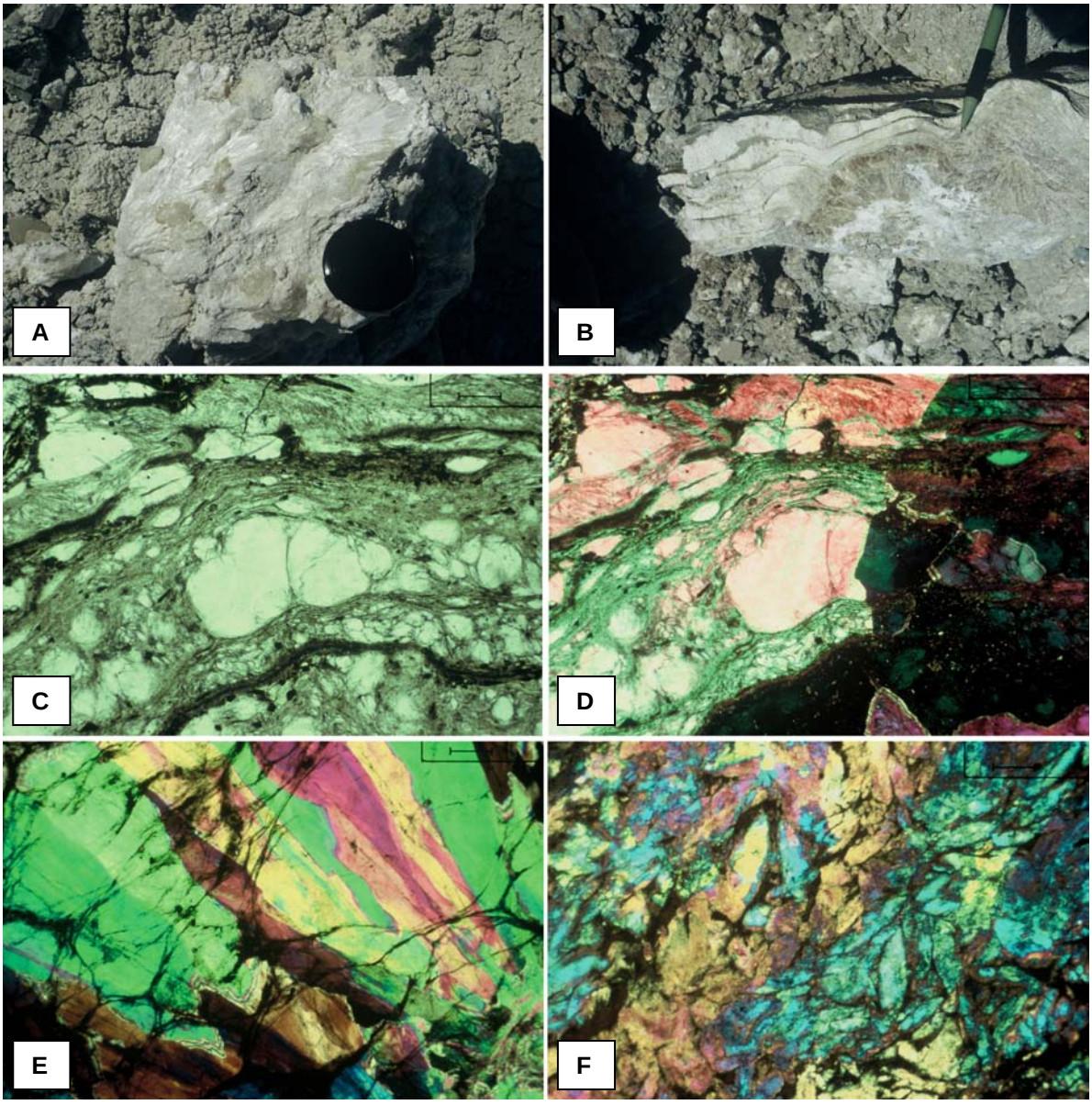

Figure 2.6. REPLACIVE COLEMANITE
A) Close view of a fragment of ulexite mass (white, fibrous material) containing centimeter-sized crystals (porphyroblasts) of replacive, secondary colemanite. Lens cap: 6 cm (Acep deposit, Bigadiç district, Miocene, Anatolia).
B) Close view of a block of secondary colemanite (brownish material) replacing a banded lithofacies of fine-grained ulexite (white material). Note that the radiating colemanite crystals preserve both banding and deformation in the ulexite lithofacies (banding can be seen throughout the colemanite masses). Pencil for scale (Acep deposit, Bigadiç district, Miocene, Anatolia).
C) and D) Photomicrographs of replacive colemanite. In normal light (C), the laminated sedimentary matrix and abundant micronodules of (precursor) ulexite can be seen. In crossed nicols (D), two large, anhedral crystals of colemanite (light area on the left and dark area on the right) replace the ulexite and cement poikilitically the matrix. Note that colemanite preserves both the lamination and the micronodular lithofacies of ulexite. Scale bar: 0.32 mm (Emet deposit, Miocene, Anatolia).
E) Photomicrograph of replacive colemanite with radiating fabric. The micronodular lithofacies of the precursor ulexite has been preserved. Scale bar: 0.32 mm, crossed nicols (Bigadiç district, Miocene, Anatolia).
F) Photomicrograph of a portion of a colemanite nodule. Large, anhedral crystals of colemanite have replaced and preserved pseudomorphs of a precursor mineral (lenticular gypsum?). Scale bar: 0.32 mm, crossed nicols (Emet deposit, Miocene, Anatolia).

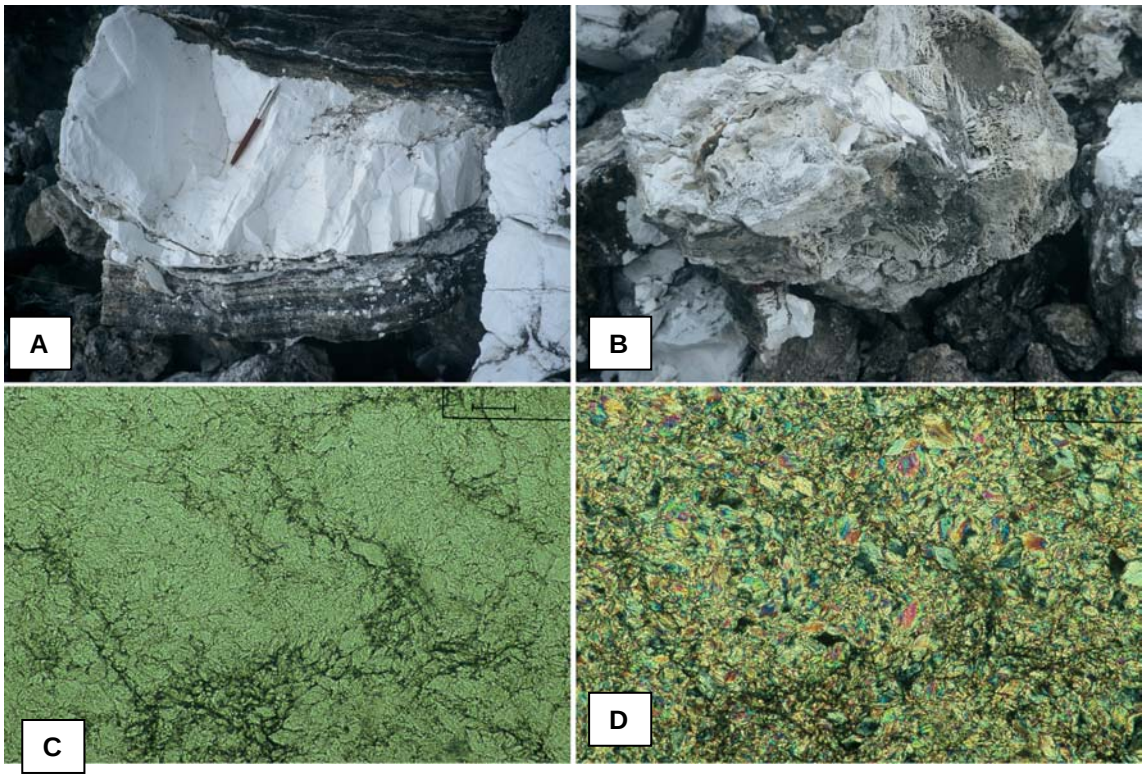

Figure 2.7. PRICEITE
A) Banded lithofacies of priceite (white material) intercalated between laminated secondary gypsum (grey material). The priceite mass displaces the laminae of secondary gypsum (Sultançayır deposit, Miocene, Anatolia).
B) Mass of priceite being transformed into secondary calcite. Remains of priceite (fine-grained, massive, white material) can be seen. Calcite displays a porous net-texture. Fallen block in a front quarry; length of the block: 75 cm (Sultançayır deposit, Miocene, Anatolia).
C) and D) Photomicrographs of priceite fabric. Note the rhombohedral sections of the tiny priceite crystals. Some clayey matrix (dark material) is scattered between the dense mass of priceite. Scale bar: 0.32 mm (C: normal light; D: crossed nicols) (Kireçlik mine, Bigadiç distric, Miocene, Anatolia).

Replacive colemanite. Euhedral crystals (porphyroblasts) of colemanite (Fig. 2.6A) as well as discoidal nodules, radial aggregates, bands and irregular masses of this mineral can replace other borates and are found embedded in their lithofacies (Fig. 2.6B). Fibrous ulexite is the borate which most commonly is replaced by colemanite. Frequently the geometry of the ulexite micronodules is preserved within the colemanite fabric (Fig. 2.6C,D,E). Colemanite pseudomorphs after other minerals can be easily identified (gypsum, in Fig. 2.6F)

2.2.4. Priceite

Priceite (*pandermite)* is mainly found as fine-crystalline, milky-white material. It frequently exhibits a hard, hornlike structure with a concoidal fracture, but on exposure to the atmosphere it desintegrates into a kaolin-like mass.

Lithofacies. The main priceite lithofacies are the following:

- *Discontinuous bands, lenticular layers, and stratiform masses*. These occurrences have a thickness up to several tens of centimeters (Fig. 2.7A).
- *Nodular.* Nodules and masses displaying a poorly-defined nodular morphology reach sizes comprised between <1 cm and >1 m in diameter.
- *Veins*. Veins, as well as irregular masses and dykes, are present locally filling discontinuities or crosscutting the host sediment.
- *Laminated*. Laminae and thin bands (few centimeters in thickness) are made up of extremely fine priceite crystals. These laminae can display micro-convoluted structures.

Crystalline fabrics. Under the microscope, priceite is commonly composed of tiny (<20 μm), equant, unoriented rhombohedrons which form a homogeneous crystalline fabric devoid of sedimentary matrix. These crystals may display an internal fibrous appearance and undulose extinction (Figs. 2.7C, D). Prismatic crystals, either unoriented or arranged in parallel to each other are also present.

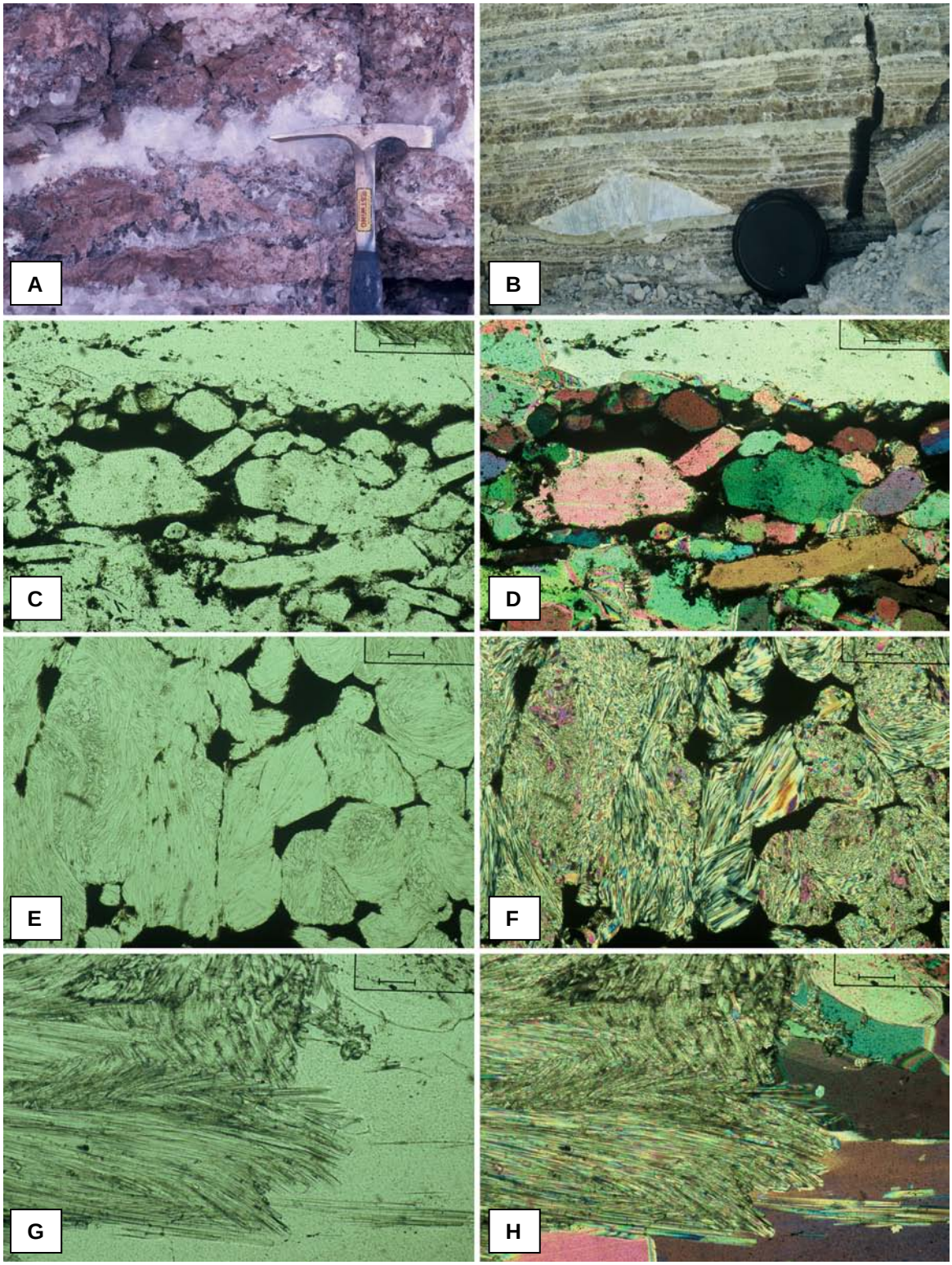

Figure 2.8. BORAX
A) Banded lithofacies of borax ('tincal'; white to transparent material) alternating with clay/tuff matrix (brownish material). Note the coarse size (up to 2 cm) of some borax crystals. (Tincalayu deposit, Upper Miocene, NW Argentina).
B) Laminated lithofacies of borax (brown material) alternating with dolomitic, marly laminae (white laminae). Palisade fabric (bottom-nucleated, upward-directed, competitively grown crystals) can be seen in some borax laminae. In the lower part, a discoidal nodule of fibrous ulexite is present. The growth of this nodule is early diagenetic, being coeval with the sedimentation of the borax laminae. Under the microscope, the replacive nature of this ulexite nodule can be seen in next photographs E-F. Lens cap: 6 cm (Kırka deposit, Miocene, Anatolia).

C) and D) Photomicrographs of a borax laminae. In the central lower part, the borax crystals are oriented parallel to bedding and are embedded in matrix (dark material). In the upper part, a large borax crystal is present, which shows pressure-solution features in its contact with the small borax crystals underneath. Scale bar: 0.32 mm. (C: normal light; D) crossed nicols) (Kırka deposit, Miocene, Anatolia).
E) and F) Photomicrographs of pseudomorphs of fibrous ulexite after (precursor) borax. Note the various orientations and fascicular arrangements, the variable size, and the deformation features of ulexite fibers within the pseudomorphs. The photomicrograph corresponds to a zone close to the contact between the ulexite nodule and the borax laminae in B. Scale bar: 0.32 mm. (E: normal light; F: crossed nicols).
G) and H) Photomicrographs of ulexite fibers replacing borax crystals, in the contact zone between an ulexite nodule and a borax lamina. Scale bar: 0.32 mm. (G: normal light; H: crossed nicols) (Kırka deposit, Miocene, Anatolia).

2.3. Rock-forming Na-borates

2.3.1. Borax

Lithofacies. The main borax lithofacies are the following:
- *Laminated and banded lithofacies*. They consist of alternations of planar laminae (<1 cm thick) and bands (1 cm to a few dm thick) of borax, with laminae of sedimentary matrix (Fig. 2.8A,B). Borax crystals are transparent to brownish, and can show a zoning formed by solid inclusions of the matrix. These crystals are euhedral to subhedral, with sizes oscillating between <1 mm and up to 1 cm (Fig. 2.8C,D).
- *Interstitial macrocrystals*. This lithofacies consists of layers (between 20 and 50 cm thick) rich in marly and clayey matrix, in which displacive, coarse crystals of borax (up to several cm) are present. These crystals are euhedral and transparent, and they are often devoid of internal zoning.
- *Massive crystalline*. This lithofacies is formed by massive, matrix-free, subhedral to anhedral, transparent crystals of borax, which form layers up to several meters thick. Crystalline sizes range between 1 and 2 cm. No particular orientation of these crystals is observed.

Crystalline fabrics. In the borax laminae of the Kırka deposit (Anatolia), two crystal fabrics may be distinguished:
- *Palisade fabric*. It is formed by matrix-poor, brown-colored crystals up to 1-2 cm high, which are arranged in a subvertical fabric. These crystals exhibit a planar base and an euhedral apex; dissolution surfaces can be observed at the top of the crystals locally.
- *Unoriented fabric*. In this fabric, the crystals are euhedral to anhedral in shape, and are surrounded by sediment matrix resulting in a clastic appearance. Locally, some tendency to normal grading is observed. In some laminae, prismatic to tabular crystals are arranged parallel to the lamination suggesting a cummulate character. In the Kırka deposit, borax crystals of the two types of fabrics can be replaced by ulexite (Fig. 2.8E,H).

2.4. Rock-forming Ca-Mg-borates

2.4.1. Hydroboracite

Lithofacies. Hydroboracite usually occurs as nodules and small masses with a conical appearance. These occurrences are formed by radiating needle-shaped crystals, with sizes comprised between 0.5 and 5 cm. Hydroboracite associates mainly with colemanite and ulexite.

In the Neogene deposits in NW Argentina, hydroboracite is fine-grained, displays a number of lithofacies, and forms thick deposits of economic interest (Ortí and Alonso, 2000) (Fig. 2.9A,B).

Crystalline fabrics. Under the microscope, the needle-shaped crystals have a fibrous texture resembling ulexite. Groups of these crystals show flow-like arrangements (Fig. 2.9C, D).

Replacive hydroboracite. Hydroboracite can occur also as indivual porphyroblastic crystals replacing any preexistent borate mineral in some deposits.

2.5. Accessory borates

2.5.1. Howlite

Lithofacies. This Ca-bearing mineral occurs as white, compact *nodules* (<1 cm up to 10 cm in diameter), which are dense and structureless resembling unglazed porcelain. These nodular masses may be embedded in clay laminae accompanying the colemanite layers. In the Sultançayır deposit (Anatolia), these nodules displace/replace both the gypsum beds and the priceite lithofacies (Fig. 2.10A). Howlite accompanies priceite, colemanite and gypsum, and can alter to calcite.

Crystalline fabrics. Under the microscope, the crystalline fabric of howlite is homogeneous and fine-grained. It is formed by prisms up to 0.15 mm in length that may be unoriented (decussate fabric) or arranged in small groups of a parallel tendency (Fig. 2.10C,D). Micronodular structures and poorly-defined spherulites can be observed.

2.5.2. Bakerite

Bakerite is visible only under the microscope, forming crystalline aggregates (from <30 μm to 0.2 mm in size), which display high relief and

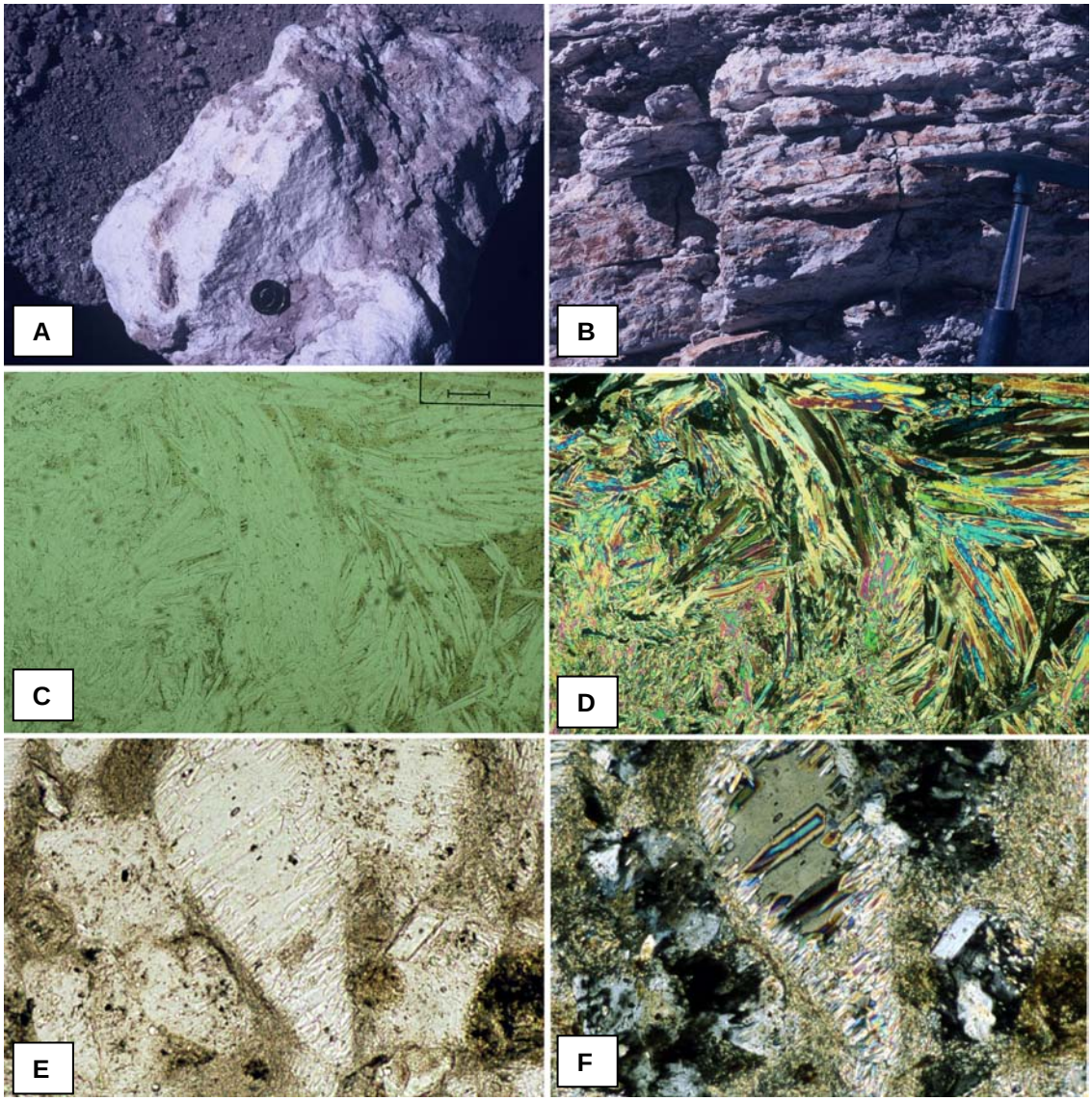

Figure 2.9. HYDROBORACITE
A) Fine-grained, irregular to nodular mass of hydroboracite (white material) with accompanying matrix (brownish material). Diameter of the coin: 3 cm (Monte Amarillo Mb,Sijes Fm, Upper Miocene, NW Argentina).
B) Hydroboracite. Same locality as in A.
C) and D) Photomicrographs of a portion of a hydroboracite nodule. Fibrous-to-prismatic, fine-grained crystals of hydroboracite. Note that the prisms display variable orientations and some deformation features (bending, breakage). Some clayey matrix (brownish material) is present between the prisms. Scale bar: 0.32 mm (C: normal light; D: crossed nicols) (Kırka deposit, Miocene, Anatolia).
E) and F) Photomicrographs of gypsum crystals being replaced by hydroboracite fibers. Note that the fibers are arranged parallel to the cleavage planes of the gypsum crystals. Length of the crystal in the center: 0.28 mm (E: normal light; F: crossed nicols) (Monte Amarillo Mb, Sijes Fm, Upper Miocene, NW Argentina).

variable shapes, from ovoid to perfectly spherulitic (Fig. 2.10B). Poorly-defined radial fabrics are present in these aggregates. Also, unoriented, microcrystalline masses of bakerite are recorded. This mineral replaces both priceite and gypsum, and is replaced by howlite.

2.5.3. Tincalconite

An alteration product of borax is tincalconite. This mineral does not form independent crystals, but occurs as a thin film made up of microscopic, fibrous crystals. These films develop on the borax crystals when they are in contact with dry atmosphere.

2.5.4. Kurnakovite

Kurnakovite is found in the Kırka deposit (Anatolia), where it forms a discontinuous layer at the top of the main borate body. This layer is formed by colorless, grey or pink, elongated (1 to 20 cm long) euhedral crystals (Fig. 2.11D) and also by crystalline aggregates (İnan *et al.*, 1973; Helvacı and Ortí, 2004). These crystals coexist with ulexite, inderite and tunellite, and less frequently with borax also.

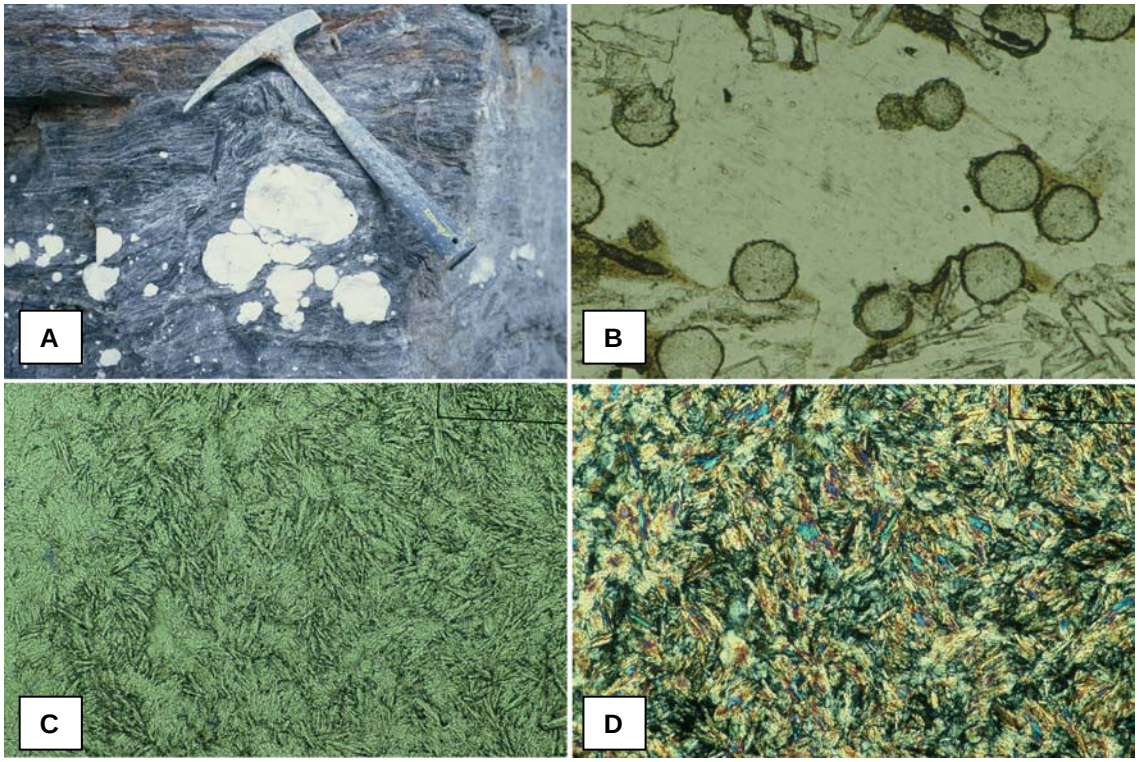

Figure 2.10. HOWLITE, BAKERITE
A) Howlite nodules (white material) displacing laminated (secondary) gypsum (Sultançayır deposit, Miocene, Anatolia). B) Photomicrograph of spherulites of bakerite cemented by a single poikilitic crystal of secondary gypsum (central part of the photograph). Surrounding this poikilitic crystal many laths (prisms) of anhydrite are still preserved. Average diameter of the spherulites: 0.26 mm. Crossed nicols (Sultançayır deposit, Miocene, Anatolia).
C) and B) Photomicrographs of a portion of howlite nodule. Note the prevalent, decussate fabric of the prisms. Scale bar: 0.16 mm (C: normal light; D: crossed nicols) (Kurtpınari deposit, Bigadiç district, Miocene, Anatolia).

2.5.5. Tunellite

Tunellite commonly occurs as individual, thin, flattened or *tabular crystals* (1 to 5 cm long). Pure tunellite crystals are colorless and transparent, and have perfect cleavages parallel to crystal surfaces (resembling muscovite).

Alternativelly, tunellite occurs as small, white, flattened *nodules* with radiating structures which have grown within the interbedded clays. Some of these nodules may exhibit internal porosity. Tunellite is associated with ulexite, probertite, colemanite and hydroboracite.

Crystalline fabrics. Under the microscope, the tunellite nodules are formed by crystalline fabrics exhibiting equant to prismatic sections (Fig. 2.11A,B,C). Prisms show straight extinction and are arranged in fan-shape and radial aggregates. Pores and small vugs are located in the core of some of these aggregates.

2.5.6. Veatchite-A

Veatchite-A occurs rarely in the Emet deposit, where it appears as a white mineral often with clay inclusions, with nodules from 2 to 6 cm in diameter made up of needle-shaped crystals. Locally, very small nodules are grouped together and show mammilary appearance. Veatchite-A associates mainly with colemanite. Field and textural evidence show that veatchite-A replaces colemanite (Helvacı, 1984).

Crystalline fabrics. Veatchite-A occurs as felted masses of very small crystals.

2.6. Facies and petrography of borates and sulfates: a brief comparison

Although lacustrine borates are much less common than sulfates or chlorides, some morphologic and genetic relations exist between all these evaporitic groups. This is particularly valid for sulfates, with which borates exhibit marked similarities in lithofacies, crystalline fabrics, depositional conditions, sedimentary environments, and diagenetic processes including various types of chemical cements. Some of the sedimentological or diagenetic interpretations time ago well established for sulfates, can be applied for a number of borate occurrences. For instance: (1) the sabkha setting of nodular/enterolithic anhydrite for the playa/salar setting of nodular/enterolithic ulexite, and (2) the diagenetic cycle of Ca-sulfates (primary gypsum – replacive anhydrite – secondary gypsum) for the burial-exhumation cycle of Na-borates (primary borax – kernite – secondary borax).

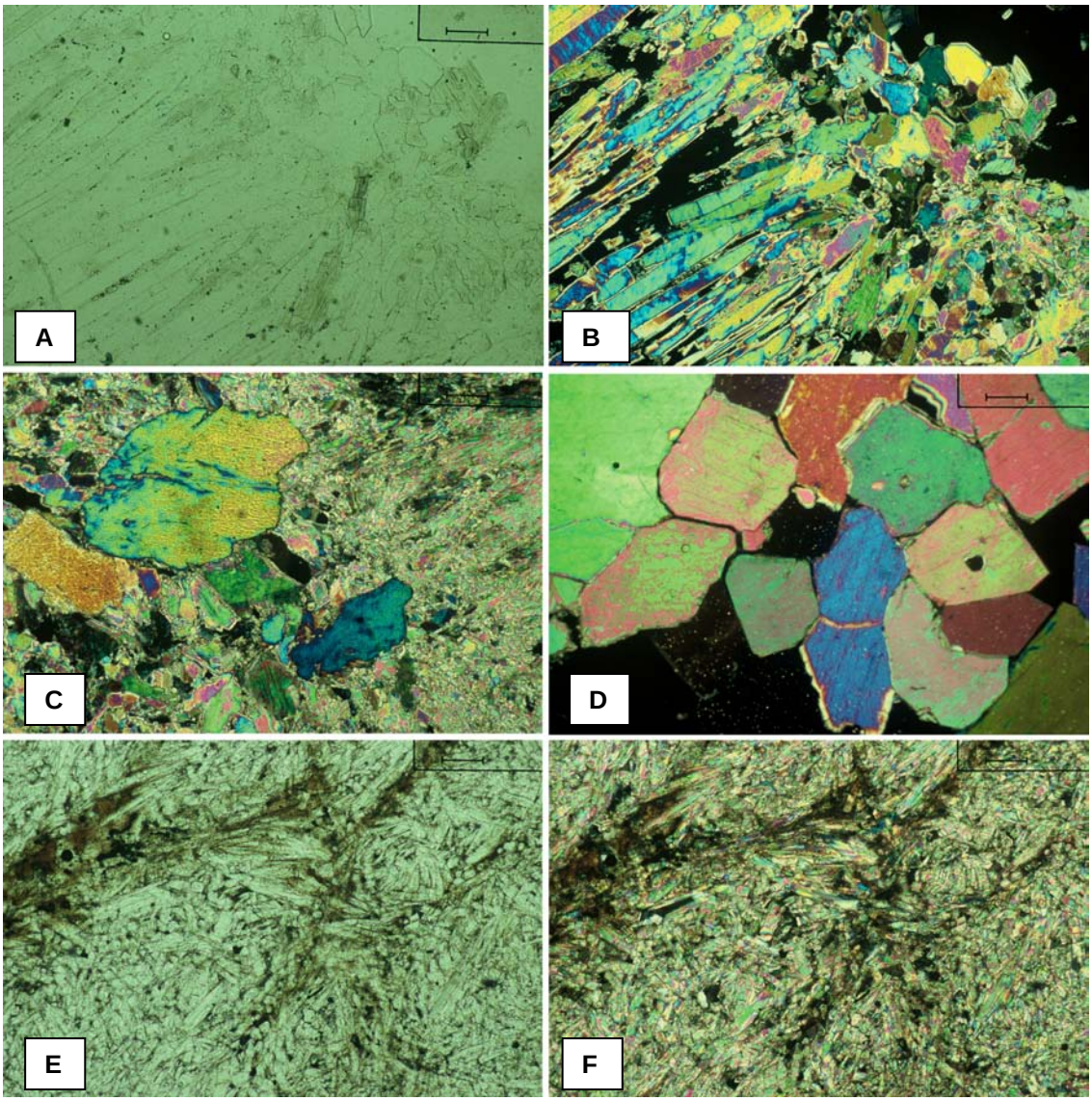

Figure 2.11. TUNELLITE, KURNAKOVITE, TERUGGITE
A) and B) Photomicrographs of a portion of a tunellite nodule. Note the prismatic to equant habits of tunellite, as well as the porosity (dark areas in B). Scale bar: 0.32 mm (A: normal light; B: crossed nicols) (Kırka deposit, Miocene, Anatolia).
C) Photomicrograph of a portion of a tunellite nodule. Fine-grained, fibrous texture of tunellite replaces coarse crystals of colemanite (upper left part). Scale bar: 0.32 mm. Crossed nicols (Kırka deposit, Miocene, Anatolia).
D) Photomicrograph of interlocking mosaic (equant to subhedral) fabric of kurnakovite. Scale bar: 0.64 mm. Crossed nicols (Kırka deposit, Miocene, Anatolia).
E) and F) Photomicrographs of a portion of a composite nodule of teruggite. Note the decussate, prismatic masses of teruggite, which contain some clayey matrix (brownish material). Scale bar: 0.32 mm (E: normal light; F: crossed nicols) (Emet deposit, Miocene, Anatolia).

In the Neogene deposits, however, it is worth emphasizing some textural or diagenetic differences which can be found between these two mineral groups:

Monomineralic deposits. Several borates may form large deposits of economic interest which are practically monomineralic or in which the presence of other borates is unimportant. This is the case of colemanite, ulexite, borax, priceite, probertite and hydroboracite (see Part IV of this workshop). However, the ability of forming large, practically monomineralic deposits of economic interest in the long list of evaporitic sulfates is limited to gypsum/anhydrite and glauberite.

Fibrous crystalline fabrics. Several borates exhibit fibrous textures both to the macro- and the micro-scale as primary, depositional features, a fact that is not at all common in sulfates. The question is that many of the borate microfiber (<10 μm in length) occurrences seem

to be free, subaqueous precipitates. Ulexite, probertite and priceite, among other borates, may form very thin depositional laminae totally integrated by microfibers (Fig. 2.12A,B) either as decussate or oriented individuals, or as groups arranged in tiny bundless or micronodules. On the one hand, in these thin laminae any non-borate sedimentary matrix can be totally absent, strongly suggesting that microfibers are in fact subaqueous precipitates. On the other hand, microfibers never display palisade fabrics or cumulate textures in these laminae, suggesting that they nucleated directy in the sediment-water interphase, or slightly below it, and that they grew indistinctly fom the 'free' brine or the interstitital borate-saturated solution.

Nodular growth. Few sulfate minerals, mainly anhydrite and gypsum, and glauberite to a lesser extent, exhibit nodular lithofacies. In the borate group, however, the nodular growth is extremely common in many minerals. Only in borax and kernite, nodular lithofacies have not been described. The borate occurrence as nodules is mostly valid for those borates which have an accessory character in a particular deposit. This fact could result from a low growth rate of many borates in the precipitating environments.

Subaqueous/burial growth of borate nodules. On the basis of lithofacies description and the characterization of individual depositional cycles made in this workshop (see Part III), some nodular lithofacies in borates could have been formed interstitially below the sediment-water interface (under a free water body) and to variable depths. Such an interpretation has not been formerly well documented for nodular sulfates. Moreover, the extensive development of large nodules (up to >80cm in diameter) in some borate minerals, as colemanite in the Emet district (Anatolia, see Part IV), suggests that, after its interstitial nucleation close to the surface, the nodules continued growing from shallow to moderate burial depth.

Pseudomorphs and other evidence of diagenetic transformations. The identification of pseudomorphs is one of the best petrographic tools to document these types of transformations. For sulfates this is particularly useful in the diagenetic cycle of Ca-sulfates, in which several types of pseudomorphs are formed. In the case of borates, these transformations are extremely difficult to be characterized between fibrous borates, for instance in the relations between ulexite and probertite. The characterization is more easily recognized in the case of the replacement of a non-fibrous by a fibrous borate, for instance when ulexite replaces borax (Fig. 2.8E,F). In contrast, the total replacement of a fibrous by a non-fibrous borate mineral only can be documented by the preservation in the replacive fabric of (1) the original lithofacies (micronodules, lamination, etc.) (Fig 2.6C,D), or (2) fiber relics of the precursor borate. In other cases, the difficulty derives from the fact that the attribution to a particular borate mineral of the habitus preserved in the pseudomorph is ambiguous. Commonly, however, the replacement of sulfate crystals by a borate mineral can be more easily documented given that the sulfate habitus is better known (Fig. 2.6F).

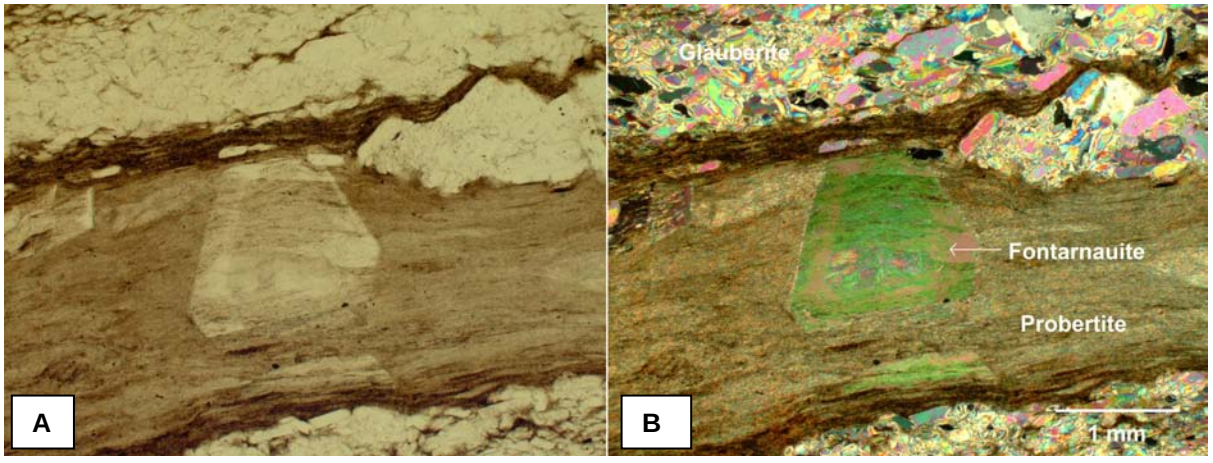

Figure 2.12. FONTARNAUITE
A) and B) Fontarnauite crystal replacing a fine-grained probertite lamina between two glauberite laminae (A: normal light; B: crossed nicols) (Emet district, Miocene, Anatolia)

TABLE II-1: Additional observations of borate lithofacies and crystalline fabrics; *some interpretative aspects.*

ULEXITE

- Nodular and nodular-banded. Nodules may occur isolated within the host sediment (matrix), or in close associations forming layers (nodular-banded lithofacies). They may be single, but frequently they are composite (multinodular).

These two lithofacies have grown displacively within the matrix, and can be interpreted as formed interstitially during periods of underground position of the water level in the sedimentary environment

- Vertically-elongated (columnar, tooth-shaped). This lithofacies forms strong, resistent layers in which the length of the individual fibers can attain up to 1 cm, and the matrix can be absent. Nodules seem to grow upward competitively.

The columnar lithofacies has an uncertain interpretation: its formation could be an original (competitive) growth mode; it could also be favored by preexistent plant-root structures on an exposed lake floor; and it could be related to persistent capillary action too.

- Laminated. In the micronodules forming the laminae, fiber fabrics vary from randomly oriented to normal to bedding.

This lithofacies corresponds to subaqueous, lake-bottom deposition during shallow lake stages. Some ulexite bands and thin laminae associated with carbonate varves and laminated claystone could represent deeper precipitates.

- Banded, massive-banded. In these lithofacies the proportion of matrix is usually very low.
- Fibrous (satin-spar veins). Fibers attain several cm in length.

The fibrous veins are cementing (diagenetic) precipitates.

- Replacive ulexite. Locally, some (secondary) ulexite replaces other minerals as borax (Fig. 2.8G,H) and meyerhofferite) (Fig. 2.4E,F).

PROBERTITE

- Nodular. Micronodules integrated by microfiber groups of probertite can be distinguished surrounding the large fibers that form the nodules. Clay partings may fill the space between some fiber groups.

Nodular probertite has formed interstitially, in general as a mineralogically primary mineral.

- Laminated. *In both the finely laminated and banded lithofacies, probertite is a primary mineral, which has precipitated subaqueously.*
- Associations. Probertite is mainly associated with ulexite, colemanite and hydroboracite
- Replacive probertite. *In the parageneses formed by probertite and various ulexite lithofacies, a replacement of ulexite by probertite can be observed locally. This suggests that probertite precipitated at a more advanced concentration stage than ulexite, a possibility that agrees with the theoretical requirement of higher temperature and lower water activity for probertite instead of ulexite precipitation. In this case, following to the ulexite, probertite is indicative of drier, more arid conditions in the boratiferous lakes.*

INYOITE

Modern deposits of primary inyoite have been described by Muessig (1958) in a saline pan in Perú, and by Helvacı and Alonso (1994) in Lagunita Playa (NW Argentina). İnan et al. (1973) cited in the Kırka deposit the local finding of discrete crystals and masses of inyoite at the top of the colemanite layers, which were interpreted as a primary occurrence of inyoite. Also, some colemanite pseudomorphs after possible inyoite have been described (Helvacı and Ortí, 1998). Despite the former observations, inyoite lithofacies clearly indicating a primary origin have not been firmely documented in the Anatolia deposits. In some inyoite occurrences with ulexite, the latter mineral is clearly replaced by inyoite (Fig. 2.3C, D), as proved by the presence of both fiber relicts and pseudomorphic micronodules of (precursor) ulexite, which are retained in the inyoite crystals. In the ulexite-inyoite occurrence of the Pleistocene Blanca Lila Formation (NW Argentina), Vandervoort (1997) interpreted a displacive (diagenetic) lithofacies of inyoite as precipitated from boron-rich brines which percolated downward throughout the sedimentary section during or following the deposition of the overlying ulexite beds.

COLEMANITE

- Nodular and nodular-banded. The nodules are composed of elongated, straight to slightly curved, fibrous or bladed crystals that radiate from the core outward as stellate clusters. Large nodules are locally flattened suggesting some dissolution by compaction, pressure-solution or mechanical readjustment. In all these nodules, colemanite is transparent to dirty, and white to grey, but locally displays dark tonalities ('black colemanite' was cited in the Argentinian deposits as a Mn- and/or Fe-rich variety by González-Barry and Alonso, 1987). Nodules may display other structures and fabrics, in particular when the crystalline size is small. Thus, a sucrosic-mosaic fabric formed by rhombohedral sections of tiny crystals with almost the same optical orientation is observed in some nodules. In other cases, equant, rhombohedral crystals display zoned cores which evolve outwards to anhedral and fibrous fabrics. In some deposits, nodular colemanite is reddish to orange due to the presence of replacive realgar. Locally, colemanite can also be impregnated or replaced by native sulfur.

Nodular and nodular-banded (as well as fibrous-banded and individual crystals) lithofacies have characteristics of displacive and/or poikilitically cementing precipitates which have nucleated from interstitial solutions within an unconsolidated matrix. The presence of curved crystals and some mechanical readjustment suggest that the growth was concurrent with compaction. Generally the nodules do not display pseudomorphs or relics of any precursor phase. The septaria-like radiating bands and associated vuggy texture in some nodules suggest nucleation of colemanite in a very soft, fluid-rich matrix, which later underwent progressive fracturation (Helvacı and Ortí, 1998). All these features are compatible with interstitial growths under synsedimentary conditions and with continuated growth later on. Thus, many nodules can be interpreted as (1) having initiated the growth displacively both in playas beneath the sediment-air interface and in shallow to ephemeral lakes beneath the sediment-water interface, and (2) having continuated the growth during initial-to-moderate burial. However, other smaller, flaser-shaped nodules that displace the fine laminae of matrix are clearly associated with deeper lacustrine settings. Presumably they have also grown interstitially, close to the water-sediment interface, under a relatively deep water body. In all these cases, in which colemanite is not associated with other borates, a number of features (perfect cyclicity, lithofacies characteristics, petrographic observations) suggest that nodular colemanite is a mineralogically primary mineral.

- Fibrous-banded. This lithofacies is made up of fibrous crystals, which can be arranged perpendicularly to the bands on both sides of a stratification joint or a central parting.
- Isolated crystals. Such crystals, which are centimeter-sized, may display internal banding as well as anhedral to fibrous, syntaxial overgrowths, which are embedded in the surrounding matrix

- Massive, vuggy-brecciated. *This lithofacies seems to represent mainly a reprecipitation product after partial dissolution of colemanite lithofacies.This could be particularly valid in those deposits in which other borates -or evidence of their previous existence- are absent.*

- Fibrous (satin-spar) veins. *These veins are secondary, cementing features formed by the circulation of fluids throughout the borate formation along fractures and cavities. Differential compaction, deformation by tectonism, or decompression during uplift of the deposit created the necessary net of fractures.*

- Replacive colemanite. The replacive crystals of (secondary) colemanite usually retain relics of ulexite fibers and preserve micronodular shapes of this precursor mineral.

PRICEITE

- Discontinuous bands, lenticular layers, and stratiform masses. The bands commonly evolve to isolated patches with irregular morphology, which are embedded in a host rock. These lithofacies are weathered to calcite near the surface.

No pseudomorphs or relics of precursor borates are observed in all these lithofacies suggesting a (mineralogically) primary origin for priceite. In the Sultançayır deposit, the local presence of fine lamination indicates that priceite was a (free) subaqueous precipitate.

BORAX

- Laminated lithofacies. In the laminae, it is frequent to notice an upward transition from palisade to unoriented fabrics. The borax laminae may intercalate some ulexite nodules, which have planar bases and convexe top surfaces: the borax laminae thin out and adapt to the top surfaces of the nodules.

In the Kırka deposit, the laminated lithofacies indicates a subaqueous, probably shallow precipitation. The palisade fabric suggests a competitive bottom growth, whereas the matrix-rich crystals with unoriented fabric suggest more variable precipitation conditions, perhaps including some reworking. However, diagnostic structures of tractive transport are absent. The normal gradding seems to have a chemical origin.

- Other lithofacies. *The massive, crystalline lithofacies could represent a precipitation occurred in a matrix-free, deeper setting. In contrast, the interstitially-grown, macrocrystalline lithofacies can be interpreted as formed at moments of subaerial exposure (in accordance with present-day occurrences of this lithofacies in the salars of the Andean region).*

HYDROBORACITE

No relics or pseudomorphs of other precursor borates can be recognized in the fibrous hydroboracite fabrics. Although commonly the nodules are interstitially-grown and primary mineralogically, hydroboracite also may replace colemanite to the macroscopic scale and other borates to the microscopic scale. In these cases, it is clearly diagenetic. In the Argentinian deposits, however, this mineral is a primary, subaqueous, free precipitate.

MEYERHOFFERITE

- Nodular. In the Simav deposit, nodules of meyerhofferite form layes in alternation with ulexite beds; small partings of matrix can be found trapped between the large radiating cystals of the nodules. These partings contain small calcite crystals, and tiny crystals of idiomorphic meyerhofferite. The latter crystals contain zones formed by small particles and may display an arqueated morphology as an original (not deformational) feature.

No evidence of a (mineralogically) secondary origin of these nodules can be deduced given that no relics or pseudomorphs of a precursor phase are present in the radiating crystals. On the contrary, this lithofacies seems to represent a primary precipitate of meyerhofferite which was formed under synsedimentary conditions.

- Associations. Meyerhofferite is mainly associated with colemanite, inyoite, hydroboracite and ulexite.

HOWLITE

- Nodular. *In the Sultançayır deposit, where howlite replaces both former sulfates (gypsum) and borates (priceite), sedimentological evidence indicates that howlite was an early diagenetic product that precipitated both as mineralogically primary (de novo) nodules and as replacive nodules on priceite (Ortí et al., 1998). Deformational features in the prismatic crystals forming the nodules resulted from mechanical compaction.*

- Crystalline fabrics. *Accompanying the small prisms, also equant to rectangular sections of large howlite crystals are seen; commonly these large prisms are bent and broken. Around some nodules, also fine microcrystalline quartz -resembling chert- and opal can be seen in thin, discontinuous films. In these nodules, a partial alteration to calcite is recorded, suggesting that the silica films are by-products of the howlite alteration.*

KURNAKOVITE

In the Kırka deposit, kurnakovite can be considered as a mineralogically primary mineral, derived from final brines enriched in sodium and magnesium (Helvacı and Ortí, 2004).

TUNELLITE

Tunellite is commonly a mineralogically primary borate. However, remnants of colemanite crystals can be observed within the tunellite lithofacies locally; this fact indicates that tunellite can also be a replacive (secondary) precipitate. In association with others borates, tunellite appears to have replaced all of them.

KERNITE

Kernite crystals are found in the underground works of the Kırka deposit, in the deeper part of the sodium borate body

TERUGGITE

- Nodular. Teruggite occurs as very pure white, powdery nodules of 2 to 10 cm in diameter. Occasionally, spherulites of teruggite are associated with colemanite. Some tiny, euhedral crystals can be present in the nodules.

- Crystalline fabrics. The crystals forming these nodules are very small and show prismatic habits elongated in the c axis, with pseudohexagonal sections. These crystals tend to be needle-like, and frequently are broken (Fig. 2.11E, F).

CAHNITE

Cahnite is white and light brown with a notably glassy lustre. It occurs only rarely in the Emet deposit (Anatolia), both as very small spherulites within the powdery nodules of teruggite, and as a coating on euhedral colemanite crystals present in vugs of colemanite nodules. The spherulites of cahnite rarely exceed 2 mm in diameter. Usually they occur singly, but occasionally two or three of them coalesce together.

- Crystalline fabric. The cahnite spherulites contain needle-shaped and fibrous crystals which often show a radial fabric.

PART III: CYCLES AND SUCCESSIONS

3.1. Depositional cycles and successions

The sedimentary distribution of the Holocene Ca- and Na-bearing borates in the shallow lakes and playas is mainly controlled by the mineral solubility, which is usually lower for Ca-borates and higher for Na-borates (colemanite: 0.8 g/L; ulexite 7.6 g/L; borax: 47 g/L), and by the lateral gradient of salinity. These two factors contribute to the existence in these deposits of 'facies belts', which roughly consist in the precipitation of Ca-borates on the marginal zones of the lacustrine systems, and Na-borates in the central zones (Alonso, 1986; Helvacı, 1995).

In the Neogene deposits, besides the existence of these facies belts, the presence of vertical repetitions (cyclicity) can be clearly observed. Individual cycles have variable thicknesses, from less than one meter to several meters or tens of meters.

Borate successions, with thicknesses from tens to hundreds of meters, refer to the whole stratigraphic section forming the borate units. These successions can be composed by the repetitions of individual borate cycles, or by irregular alternations of borate layers and non-borate host rocks.

The cyclicity shown by the most common borate deposits can be exemplified by some of the Neogene deposits of Anatolia (Turkey) as well as by modern and Neogene deposits of the Andean Region (NW Argentina) and West USA (California). The borate minerals forming these deposits can be grouped in three major chemical (cationic) types: Ca-(Na), Ca-Na, and Na-(Ca). In those deposits involving sulfates and chlorides also, more complex chemical types need to be considered.

In general, the individual cycles selected for examples (Table III-1) can be intepreted as shallowing and with increasing salinity upward. Sedimentological interpretations of these cycles will be done in Part IV. Detailed information on these cycles as well as on the borate successions selected for examples is show in Table III-1.

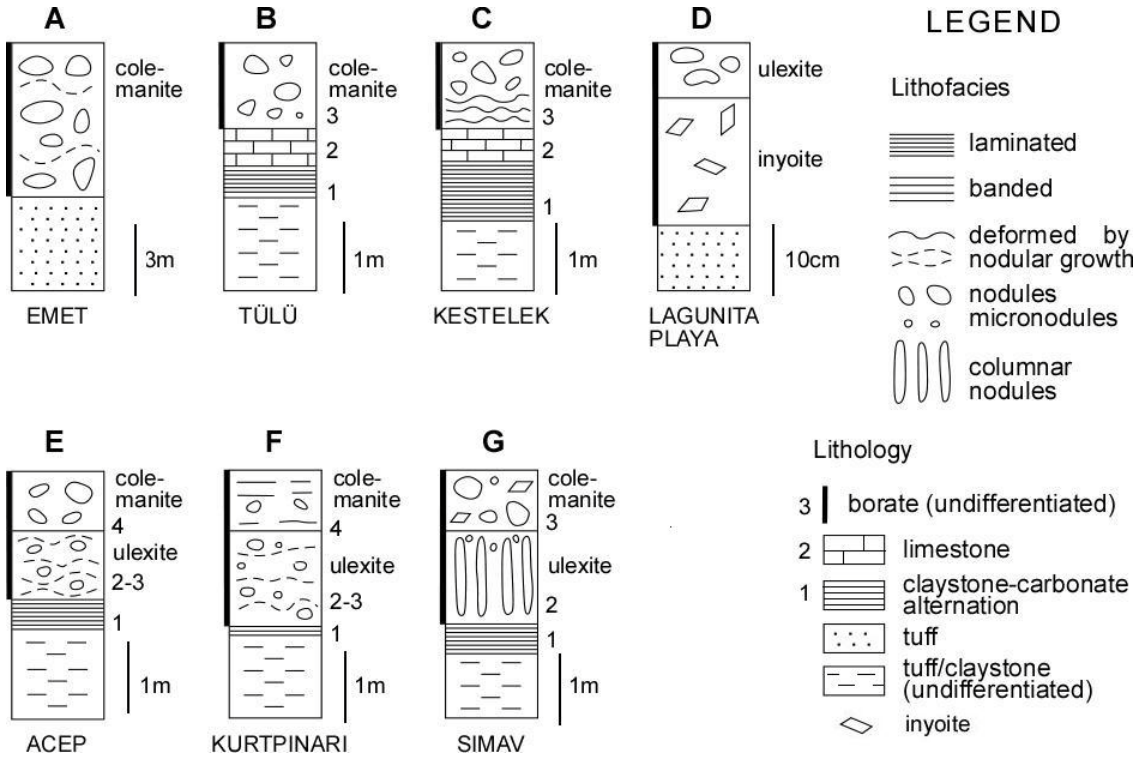

Figure 3.1. Examples of individual cycles of borates. A: marginal part of the Emet discrict; B: Tülü deposit, Bigadiç district; C: Kestelek district; D: Lagunita Playa (NW Argentina); E: Acep deposit, Bigadiç district; F: Kurtpınarı deposit, Bigadiç district; G: Simav deposit, Bigadiç district. All examples based on Helvacı and Ortí (1998), except D (Helvacı and Alonso, 1994)

3.2. Examples of individual cycles

Chemical types: Ca-(Na)-borate and Ca-Na-borate (Fig. 3.1)

Colemanite (Fig. 3.1A):
Emet deposit (Anatolia)

Colemanite (Fig. 3.1B):
Tülü open pit mine (Bigadiç district, Anatolia)

Colemanite (Fig. 3.1C)
Kestelek district (Anatolia)

Ulexite, inyoite (Fig. 3.1D)
Lagunita Playa (NW Argentina)

Ulexite, colemanite (Fig. 3.1E,F):
Acep and Kurtpınarı deposits (Bigadiç district; Anatolia).

Ulexite, meyerhofferite (Fig. 3.1G)
Simav deposit (Bigadiç district, Anatolia)

3.3. Examples of successions with only borates.

Chemical types: Na-Ca-borate and Na-(Ca) borate (Fig. 3.2A-D)

Colemanite – ulexite – probertite – ulexite - colemanite (Fig.3.2A).
Furnace Creek Fm (California)

Ulexite – borax (+kernite) – ulexite - colemanite (Fig. 3.2B)
Boron deposit (California)

Colemanite – ulexite – borax – ulexite - colemanite (Fig. 3.2 C)
Kırka deposit (Anatolia)

Colemanite – inyoite – ulexite – borax - (ul-iny-ul-bor) – ulexite – inyoite (Fig. 3.2D)
Loma Blanca deposit (NW Argentina)

?- inyoite-ulexite-borax
Tincalayu deposit (NW Argentina)

From these examples, the following complete succession of borate intervals can be deduced: Ca-borates → Ca-Na-borates → Na-borates → Ca-Na-borates → Ca borates.

This idealized succession can be found complete and symmetrical, as in the Kırka deposit, or assymmetrical with several intervals missing (colemanite? ulexite? in the Tincalayu deposit) or with one interval absent (colemanite? in the Boron deposit). Very often, the missing interval is located at the base of the succession, where ulexite occupies the place of the Ca-borates. The absence of the Ca-borate interval in some deposits could be the result of:
- the great ability of ulexite to precipitate, even under metastable conditions,
- the early consumption of Ca by calcite/dolomite or gypsum precipitation in the case of higher contribution of carbonate/bicarbonate- or sulfate-rich waters.

Thus, many papers accept the existence of the following general successions, which reflects the most common mineralogic distribution in the borate deposits of the Na-(Ca)-borate chemical type: colemanite – ulexite – borax – ulexite – colemanite (Bowser and Dickson, 1966; İnan et al, 1973; Alonso, 1991; Kistler and Helvacı, 1994; Helvacı, 1995; Helvacı and Ortí, 2004, among others).

Also, repetition of intervals in the succession can be recorded in some particular deposits, as in Loma Blanca (Miocene, Argentina). In this deposit, borax (+kernite) occupies the central position in the succession and prevails volumetrically, being subordinated the rest of borates (ulexite, inyoite, colemanite).

All of the aforementioned successions have a depositional (chemical) origin and are organized according to the solubility of the borate minerals. In the ideal evaporative evolution, a boratiferous brine progressively increases in salinity and alkalinity in order to equilibrate the higher boron concentration. As a result of the different solubility products, the early precipitation of Ca-borates changes the cationic character from Ca- to Na-rich allowing first the ulexite and further the borax precipitation (Palmer and Helvacı, 1995).

In detail, the interpretation of the various mineral successions present in the Neogene deposits requieres caution, in particular as regards the Ca-borates, whose origin has been a subject of debate in the literature. This is the case for: (a) colemanite, which is considered by many authors to be only a secondary mineral coming from the transformation of precursor phases (inyoite, meyerhofeite, ulexite); and (b) inyoite, which in some cases has been interpreted as formed following the ulexite precipitation; thus, in the Blanca Lila Formation inyoite has been considered an early diagenetic mineral precipitated from interstitial solutions underneath the ulexite interval but subsequently to it (Vandervoort, 1997).

3.4. Examples of borate successions with associated sulfates and chlorides

Besides the aforementioned cases in which the precipitating solutions are dominated by borate, some examples are known where borate is accompanied by other anions resulting in evaporitic deposits of more complex parageneses. Apparently, however, examples of genetic relations between borates, sulfates and chlorides are more common in the Holocene than in the ancient deposits.

In the today's salars of La Puna region (NW Argentina), two opposite facies belts have been documented from the margin to the center:
- borate - sulfate - chloride (halite) in the Salar of Rincón (Igarzábal, 1991)
- sulfate - borate - chloride (halite) in the Salar of Hombre Muerto (Alonso, 1991).

In the Miocene Sijes Formation of the same region, Ortí and Alonso (2000) described a lateral facies change involving sulfates in the margin (gypsum) and borates in the center (hydroboracite) (see Part IV).

In the Neogene formations of Anatolia, a similar facies belt, i.e. sulfate in the margin (gypsum) and borate in the center (priceite) was documented by Ortí *et al.* (1988) (see Part IV). In the marginal part of the Emet borate distict, Helvacı and Firman (1976) interpreted the

following facies belt, from the margin to the center: carbonate - sulfate (gypsum) - borate (colemanite). In the central part of the same district, however, the following facies belts was deduced (García-Veigas *et al.*, 2011) from the margin to the center on the basis of new borehole information: carbonate (dolomite) – borate (colemanite and probertite) - sulfate (glauberite) - chloride (halite).

Apparently, borate minerals can precipitate in a wide range of salinities and chemical types of waters. In the parageneses in which both borates and sulfates are involved, in some cases borates occupy the center of the lake systems while in others occupy the margins. In the parageneses where NaCl is also present, halite always occupies the most central part. Recent borehole information in the Anatolian districts (Emet, Kırka) indicates that borate associations with other evaporitic groups can be more varied and complex than thought up to now (García-Veigas *et al*., 2011)

In the examples of successions which follow, the chemical types correspond to: Ca-borate-sulfate, Ca-Mg-borate-sulfate and Ca-Na-(K)-borate-sulfate-chloride.

Gypsum-priceite-gypsum (Fig. 3.2E)
Sultançayır deposit (Anatolia)

Inyoite-ulexite-gypsum (Fig. 3.2F)
Blanca Lilla Fm (NW Argentina)

Colemanite - gypsum – hydroboracite - gypsum (Fig. 3.2G)
Monte Amarillo Mb, Sijes Fm (NW Argentina)

Colemanite – probertite – glauberite – halite – glauberite – probertite – colemanite (Fig. 3.2H)
Emet Basin, central part (Anatolia)

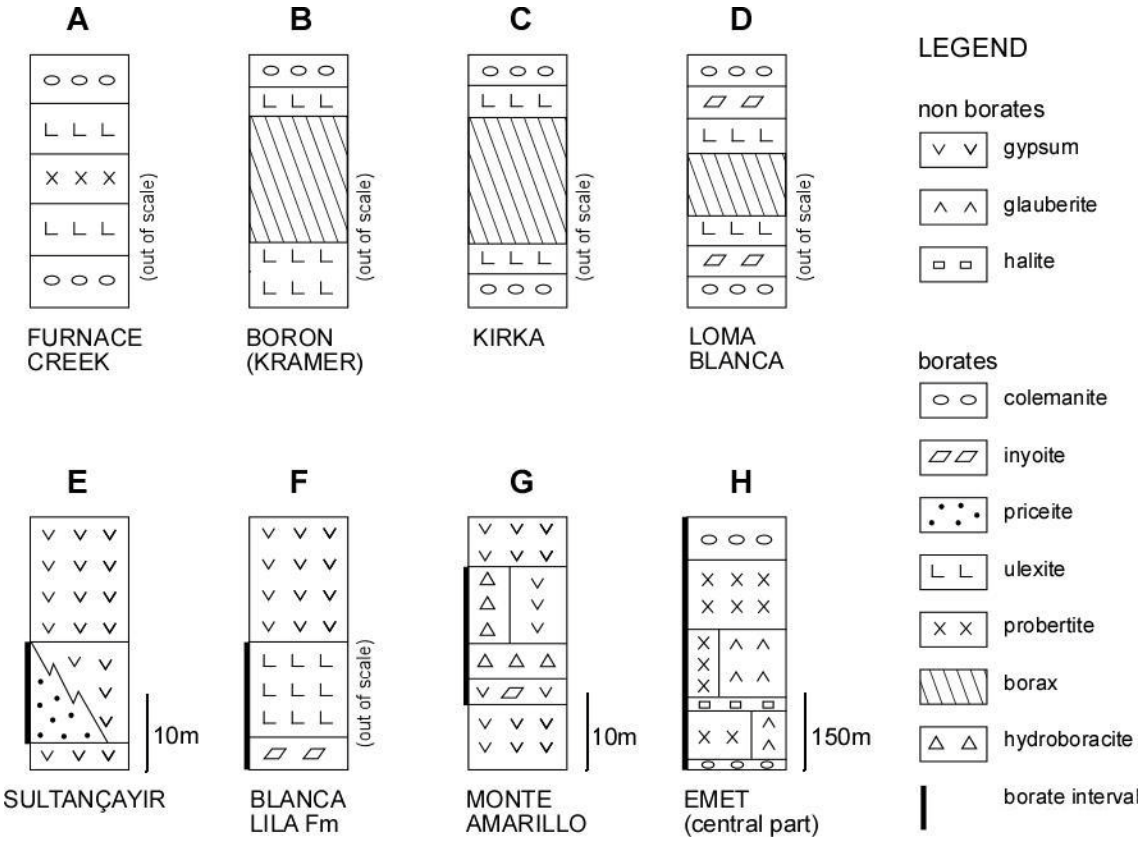

Fig. 3.2. Examples of borate successions with only borates (A-D), and borate sucessions with sulfates/chlorides (E-H). A: Furnace Creek Fm; B: Boron (Kramer) deposit; C: Kırka deposit; D: Loma Blanca deposit; E: Sultançayır district; F: Blanca Lila Fm; G: Monte Amarillo Mb; H: Emet district, central part. Based on: A: McAllister (1970); B: Bowser (1965); C: Helvacı and Ortí (2004); D: Alonso et al. (1988); E: Ortí et al. (1998); F: Vandervoort (1997); G: Ortí and Alonso (2000); H: García-Veigas et al. (2011).Schemas out of scale: A, B, C, D and F.

TABLE III-1: Individual cycles and successions in lacustrine borate deposits

COLEMANITE cycles	Depositional intervals	Figure	Reference
Emet deposit (Anatolia, Miocene)	(1) claystone/tuff layer (2) nodular/meganodular colemanite	Fig. 3.1A	Helvacı and Ortí, 1998 (Fig.7A)
Tülü open pit mine, Bigadiç district (Anatolia, Miocene).	(1) alternations of carbonate varves and finely-laminated dark claystone (2) laminated, pelletal mudstone (and some nodules of colemanite) (3) nodular colemanite bed with minor intercalations of laminated mudstone	Fig. 3.1B	Helvacı and Ortí, 1998 (Fig. 4A)
Kestelet deposit (Anatolia, Miocene)	(1) finely-laminated dark claystone and carbonate varves (some preserved as original aragonite) (2) laminated carbonate (with some lenticular and flaser-shaped nodules of colemanite) (3) nodular colemanite bed	Fig. 3.1C	Helvacı and Ortí, 1998 (Fig. 7B)
ULEXITE-INYOITE cycle			
Lagunita Playa (NW Argentina, Miocene)		Fig. 3.1D	Helvacı and Alonso, 1994 (Fig. 3)
ULEXITE-COLEMANITE cycles			
Acep and Kurtpınarı deposits, Bigadiç district (Anatolia, Miocene)	(1) alternations of laminated claystones and carbonate varves (2) nodular to columnar ulexite (3) ulexite (thin bands, nodular-banded, columnar) with minor colemanite (4) alternations of nodular ulexite with nodular and vuggy colemanite.	Fig. 3.1E,F	Helvacı and Ortí, 1998 (Fig. 4B)
ULEXITE–MEYERHOFFERITE cycle			
Simav deposit, Bigadiç distric (Anatolia, Miocene)	(1) laminated to massive claystone (2) columnar ulexite (3) nodular meyerhofferite with minor inyoite	Fig. 3.1G	Helvacı and Ortí, 1998
COLEMANITE–ULEXITE-PROBERTITE succession			
Furnance Creeck Formation, Death Valley (California, Miocene-Pliocene)	colemanite → ulexite → probertite → ulexite → colemanite	Fig. 3.2A	Mc Allister, 1970
COLEMANITE/INYOITE-ULEXITE–BORAX successions			
Kramer deposit (Boron, California, Miocene)	ulexite → borax (+ kernite) → ulexite → colemanite	Fig. 3.2B	Bowser and Dickson, 1966 Kistler and Helvacı, 1994 (Fig. 4)
Kırka deposit (Anatolia, Miocene)	colemanite → ulexite → borax → ulexite → colemanite	Fig. 3.2C	Kelvacı and Ortí, 2004 (Fig. 4)
Loma Blanca deposit (NE Argentina, Miocene)	colemanite → inyoite → ulexite → borax → ulexite → inyoite	Fig. 3.2D	Alonso *et al*., 1988 (Fig. 3)
Tincalayu deposit (NE Argentina, Miocene)	inyoite → ulexite → bórax		Alonso, 1986 Alonso, 1991
BORATE and SULFATE successions			
Sultançayır deposit (Anatolia, Miocene)	gypsum → priceite (pandermite) → gypsum	Fig. 3.2E	Ortí *et al*., 1998 (Fig. 4)
Blanca Lilla Fm. (Argentina, Pleistocene)	inyoite → ulexite → gypsum	Fig. 3.2F	Vandervoort, 1997
Monte Amarillo Mb., Sijes Fm. (Argentina, Miocene)	gypsum → inyoite/colemanite→ hydroboracite → gypsum	Fig. 3.2G	Ortí and Alonso, 2000 (Figs. 10 and 11)
BORATE, SULFATE and CHLORIDE successions			
Doğanlar boreholes, Emet district, central part (Anatolia, Miocene)	colemanite → probertite → glauberite → halite → probertite → colemanite	Fig.3.2H	García-Veigas *et al*., 2011

PART IV: EXAMPLES OF NEOGENE BORATE BASINS

This last part of the workshop deals with particular petrologic and sedimentologic aspects of selected Neogene borate deposits in western Anatonia (Turkey) and La Puna region (NW Argentina) avoiding comprehensive descriptions and interpretations of the basins. In the Kestelek Basin (Anatolia), mainly colemanite is present. In the Bigadiç Basin (Anatolia), both colemanite and ulexite are exploited in several localities. In the Kırka Basin (Anatolia) borax is actively benefied, and a thick probertite deposit has been recently prospected in the subsurface. In the Sultançayır Basin (Anatolia), Ca-borates (mainly priceite) are interbedded within a thick gypsum succession. In the Emet Basin (Anatolia), a clear distinction can be established between a marginal succession with only borates (mainly colemanite) and a central succession in which a complex paragenesis involving borates (mainly probertite), sulfates (mainly glauberite) and chlorides (halite) is known to exist in the subsurface. In the Neogene Pastos Grandes Basin (La Puna, in NW Argentina), the association of hydroboracite and gypsum contains the largest hydroboracite resources known up to now.

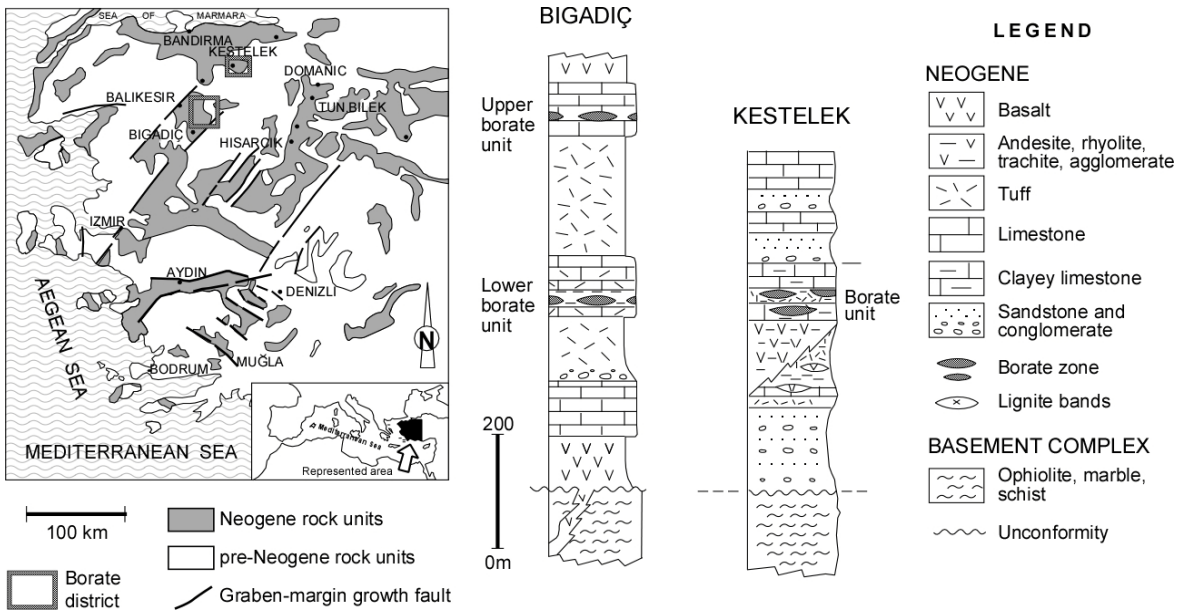

Figure 4.1. Stratigraphic succession in the Bigadiç and Kestelek Neogene borate basins of western Anatolia (Turkey) (modified form Helvacı and Ortí, 1998; Fig. 1)

4.1. Bigadiç Basin

In the Bigadiç Basin, the Paleozoic basement is overlain by a thick Neogene succession (Fig. 4-1). The borate deposits form two units (lower and upper borates) separated by thick tuff units. Colemanite and ulexite are the dominant minerals in the two borate units. Minor borates are: howlite, probertite and hydroboracite in the lower borate unit; and inyoite, meyerhofferite, priceite, hydroboracite, howlite and tunellite in the upper borate unit. The Bigadiç Basin has a number of mining localities such as Tülü, Acep, Simav, Kurtpınarı and Kireçlik (Helvacı, 1995).

Individual cycle: interpretation. In the Part III, some individual cycles in these localities in the Bigadiç Basin were cited (Tülü, Acep, Kurtpınarı and Simav). As an example of them, the cycle in the Tülü deposit (Fig. 3.1B) can be selected for a sedimentological interpretation.

Succession in the Tülü deposit is about 65 m thick and is dominated by colemanite layers in alternation with claystone-carbonate beds. The individual cycle in the Tülü deposit involves these depositional stages (Fig. 4.2):

- Stage I: Deep lake (perennial; from few meters to tens of meters). This stage is characterized by the sedimentation of dark, finely-laminated claystone in rhythmic alternations with carbonate varves; these alternations might reflect seasonal climatic changes. Probably the water mass was stratified, the lower mass being anoxic and hypersaline.

Stage II: shallow lake (<1 m to a few meters). This stage represents a drop in the water level, which resulted in the sedimentation of laminae of pelletal carbonate mudstone in a stratified water mass with only minor episodes of subaerial exposure. Some colemanite small

nodules could develop within the carbonate laminae or within the top sediments of the preceeding stage;

Stage III: Shallow-ephemeral lake to playa-lake. In this stage, the underground position of the water table and the associated brine

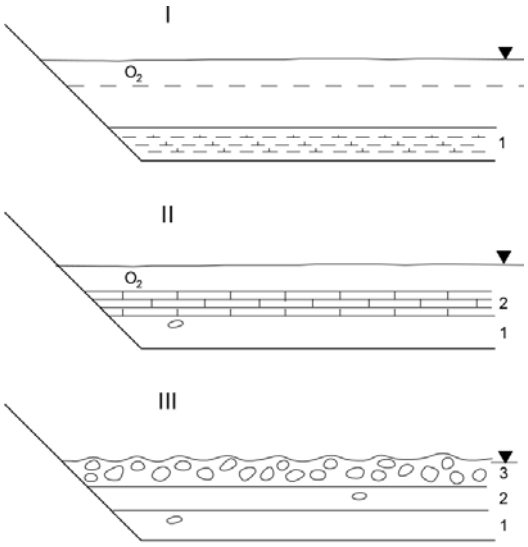

Figure 4.2. Evolutive stages of the individual cycle in the Tülü borate deposit. Bigadiç district. Anatolia. 1: alternations of carbonate varves and finely-laminated dark claystone; 2: laminated, pelletal mudstone (and some nodules of colemanite); 3: nodular colemanite bed with minor intercalations of laminated mudstone (modified from Helvacı and Ortí, 1998; Fig. 5)

evolution resulted in the interstitial growth of large nodules, thin layers, and individual crystals of displacive colemanite.

This individual cycle displays a shallowing upwards trend. Colemanite is a mineralogically primary mineral and pseudomorphs of any precursor borate mineral were not found. In other colemanite layers of the Tülü succession, however, some ulexite pseudomorphs can be found (Fig. 4.3). This suggests that, in this particular case, the ulexite growth could locally predate that of colemanite.

Replacement of ulexite by colemanite. In contrast to the Tülü deposit, in the Acep deposit some colemanite cycles display features indicating a replacement of precursor ulexite: radial aggregates of colemanite contain remnants of ulexite nodules and micronodules (Fig. 4.4). In the Kurtpınarı deposit, some precursor ulexite micronodules within the replacive colemanite can be also distinguished (Fig. 4.5).

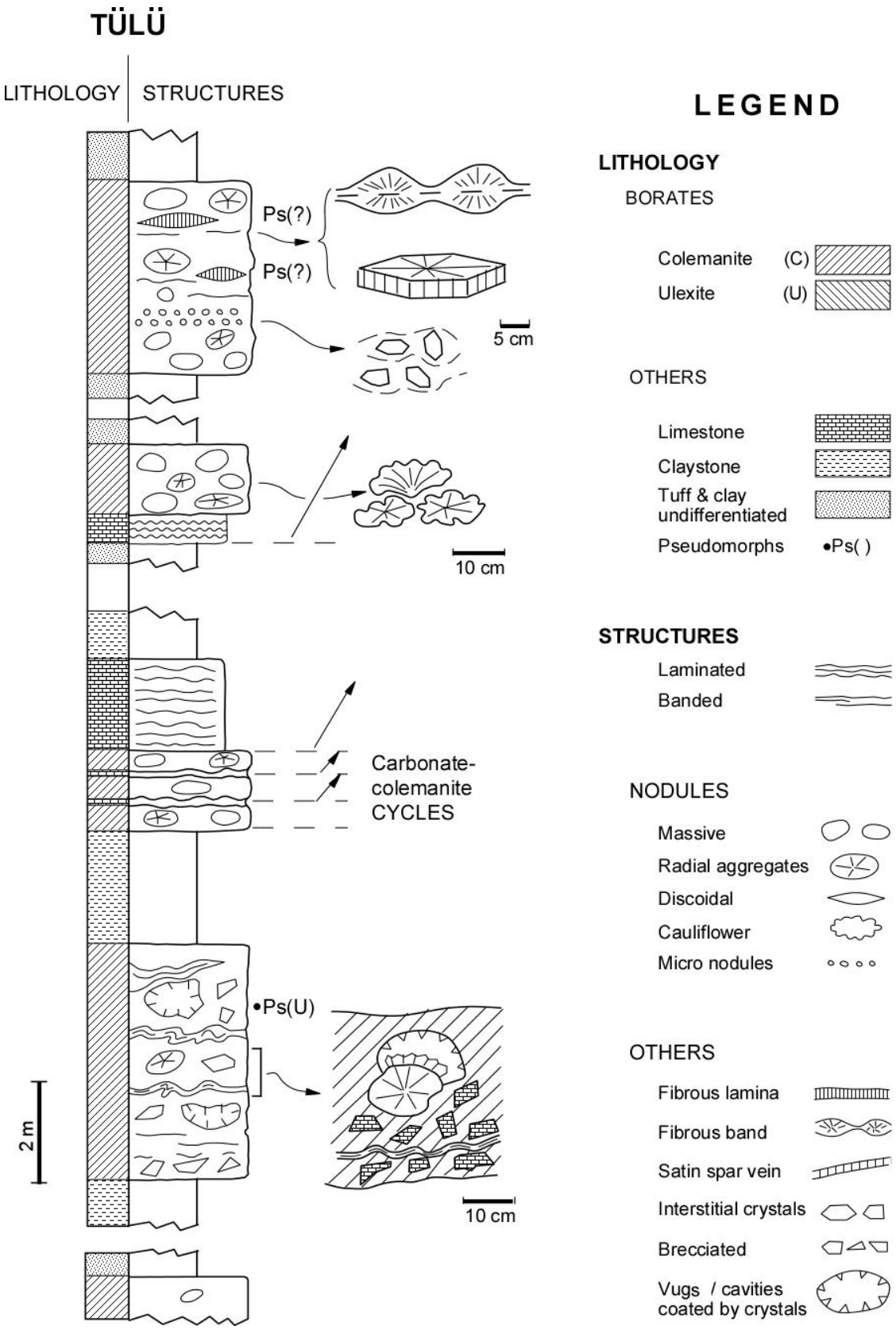

Figure. 4.3. Partial stratigraphic succession in the Tülü borate deposit, Bigadiç district, Anatolia. Some individual cycles are shown as well as colemanite layers with particular lithofacies. In these layers it is indicated the petrographic presence of some pseudomorphs after ulexite micronodules, Ps(U), within the colemanite (modified from Helvacı and Ortí, 1998; Fig. 4A).

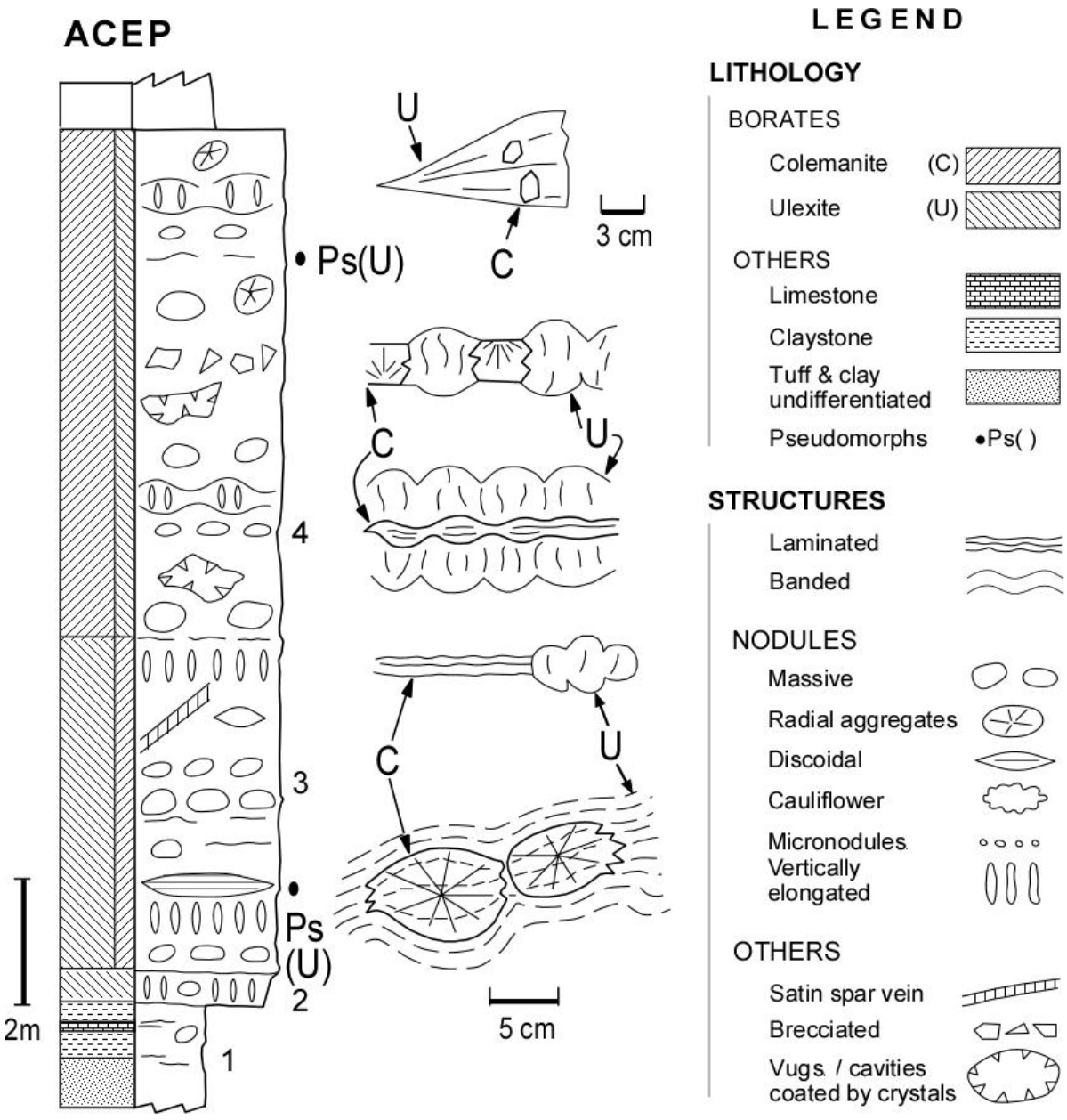

Figure 4.4. Individual cycle in the Acep borate deposit, Bigadiç district, Anatolia. On the right of the cycle, macroscopic details of colemanite (C) replacement on ulexite (U) are shown. Ps(U) refers to the petrographic presence of some pseudomorphs after ulexite micronodules within the colemanite (modified from Helvacı and Ortí, 1998; Fig. 4B).

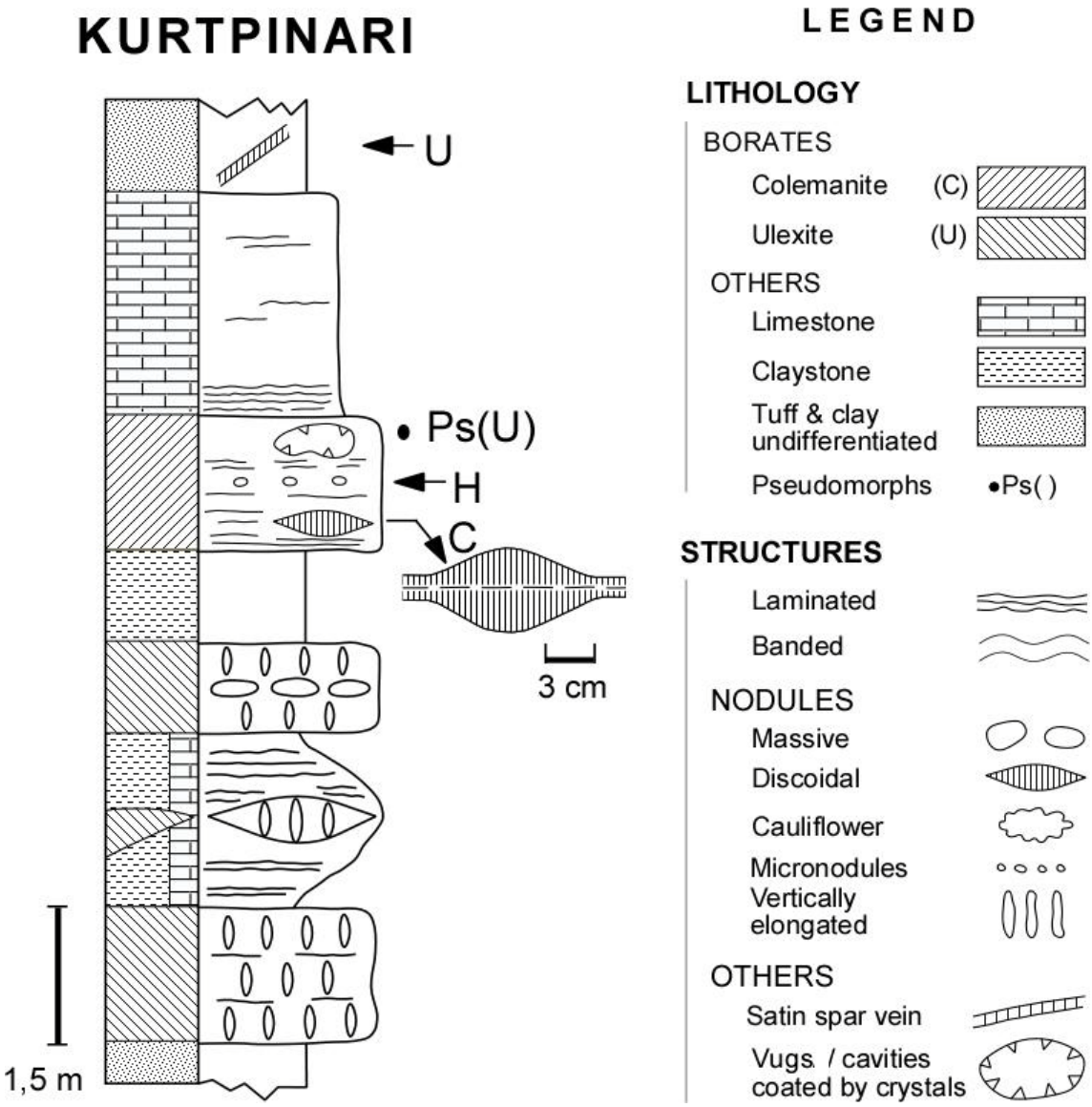

Figure. 4.5. Partial stratigraphic succession in the Kurtpınarı borate deposit (Bigadiç district, Anatolia), showing an irregular alternation of ulexite, colemanite and carbonate beds. Ps(U) refers to the petrographic presence of some pseudomorphs after ulexite micronodules within the colemanite.

4.2. Kestelek Basin

In the Kestelek deposit (western Anatolia), a Miocene succession rests unconformably on a Paleozoic and Mesozoic basement complex (Helvacı, 1994) (Fig. 4.1). In this succession, a borate unit is intercalated with clay, marl, limestone, tuffaceous limestone and tuff. Colemanite, ulexite and probertite predominate, with rare hydroboracite. A part of the borate succession in this deposit is represented in Fig. 4.6, in which some individual cycles are included. Interval (1) in these cycles is formed by finely-laminated dark claystone and carbonate varves.

Subaqueous colemanite nodules. The great thickness of interval (1) in the individual cycles indicates a deep-lake stage at the beginning of the cycle. The lenticular and hemilenticular nodules of colemanite included in these cycles can form relatively thin layers. The presence of this type of layers (interval 3) at the top of the cycles sugges that these nodules were formed interstitially under synsedimentary conditions below the sediment-water interface. Likely the depth of the water body was moderate.

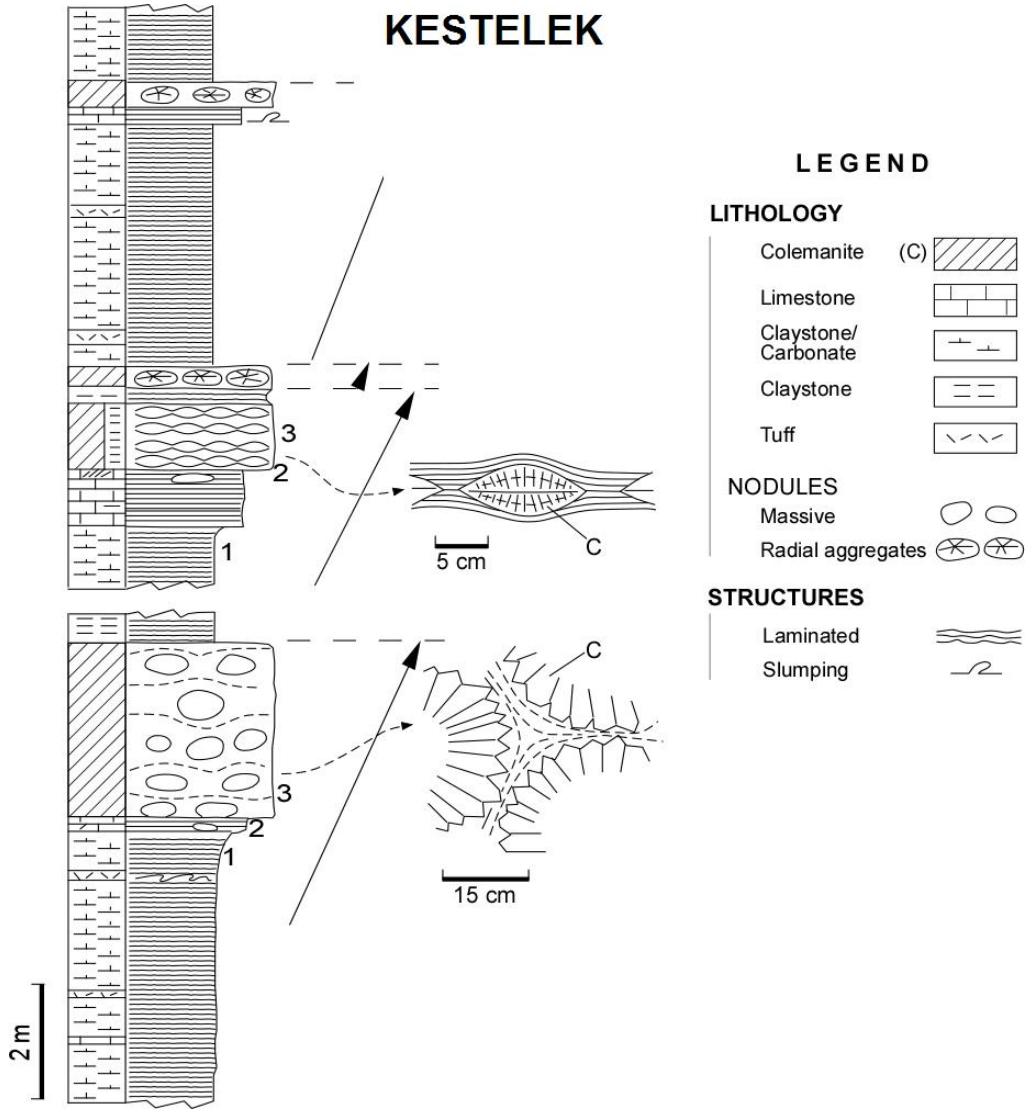

Figure 4.6. Partial stratigraphic succession in the Kestelek open pit borate mine, Anatolia, showing individual cycles and details of colemanite nodules. Cycle intervals: (1) finely-laminated dark claystone and carbonate varves (some preserved as original aragonite); (2) laminated carbonate (with some lenticular and flaser-shaped nodules of colemanite); (3) nodular colemanite bed (modified from Helvacı and Ortí, 1998; Fig. 7B).

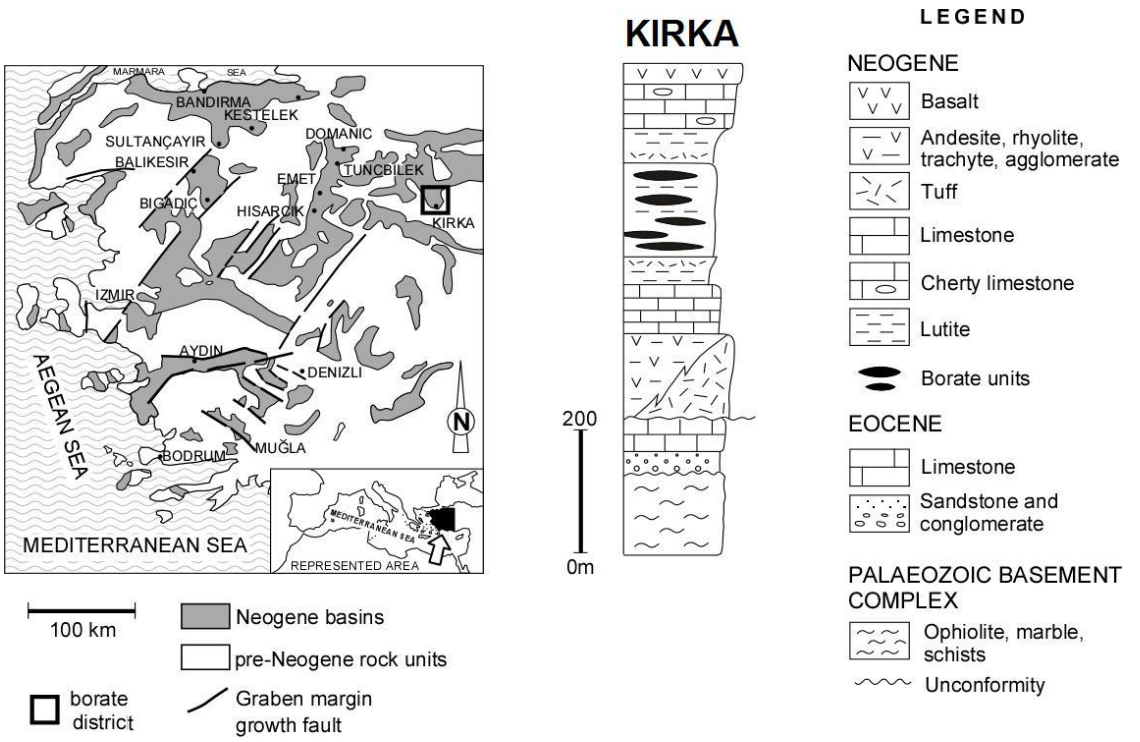

Figure 4.7. Stratigraphic succession of the Kırka borate district in Anatolia (modified from Helvacı and Ortí, 2004; Fig. 1)

4.3. Kırka Basin

The Kırka Basin contains a non-marine, volcano-sedimentary succession higher than 400 m thick of Miocene age, which rests unconformably on a Paleozoic metamorphic basement, a Mesozoic ophiolitic complex and an Eocene sedimentary cover. The succession is composed of the following units from base to top: volcanic rocks and tuffs (80 m), lower limestone (80 m), lower clay horizon with interbedded marls and tuffs (40 m), borate unit (>70 m), upper claystone with tuff, marl and coal bands (60 m), upper limestone (>50 m), and basalt (>30 m) (Fig. 4.7).

4.3.1. Central part of the basin

In the central part of the basin, a borate unit up to 145 m thick locally crops out. The major borates forming this unit are borax, ulexite and colemanite, which are the ore minerals. Other Ca-, Na-, Mg- and Sr-borates are present in subordinated amounts (İnan *et al.*, 1973; Helvacı, 1978, 1983; Çolak, 1995). Dolomite is the main carbonate, with minor amounts of magnesite and calcite. Strontianite is also present. This borate unit contains the only borax ore body in Turkey, with a B_2O_3 content of 20-25%.

The borate deposit was formed in a lacustrine setting. The boron in this deposit is assumed to have been derived from the hydrothermal activity associated with intense contemporaneous volcanism in the region during the Miocene and with the leaching of country rocks (Kistler and Helvacı, 1994). It is estimated that the borate unit underwent limited burial (300-400 m).

Borate succession. The succession in the borate unit consists of the following layers or intervals, in ascending order (Fig. 4.8): colemanite; ulexite; laminated borax (A); interstitial macrocrystalline borax (B); crystalline massive borax (C); laminated borax, with lenticular nodules of ulexite (D); fibrous, columnar ulexite, with Mg-bearing borates (inderite, kurnakovite) (E); nodular to massive colemanite (F). This succession is practically symmetrical.

Borax lithofacies: interpretation. Borax crystals in the various lithofacies range in size beween 0.1 and 10 mm. The predominant lithofacies (laminated, banded, massive crystalline) indicate free precipitation on the lake floor. In the middle of the succession, however, a interstitial macrocrystalline borax lithofacies could be interpreted as formed during an exposure episode. Under this point of view, the borax sedimentation reflects an evolution from a predominantly subaqueous setting at variable depths (perennial lake stage) in the lower part, to an interstititat setting (playa-lake stage), and again to a subaqueous setting in the upper part. The evaporative concentration of the boratiferous solutions in the lake together with the periodic changes in temperature of the water mass, are considered to be the main controls on the borax crystallization. Within the borax laminae of interval (D), flattened nodules of ulexite are developed. The growth of these nodules was coeval with the accumulation of the

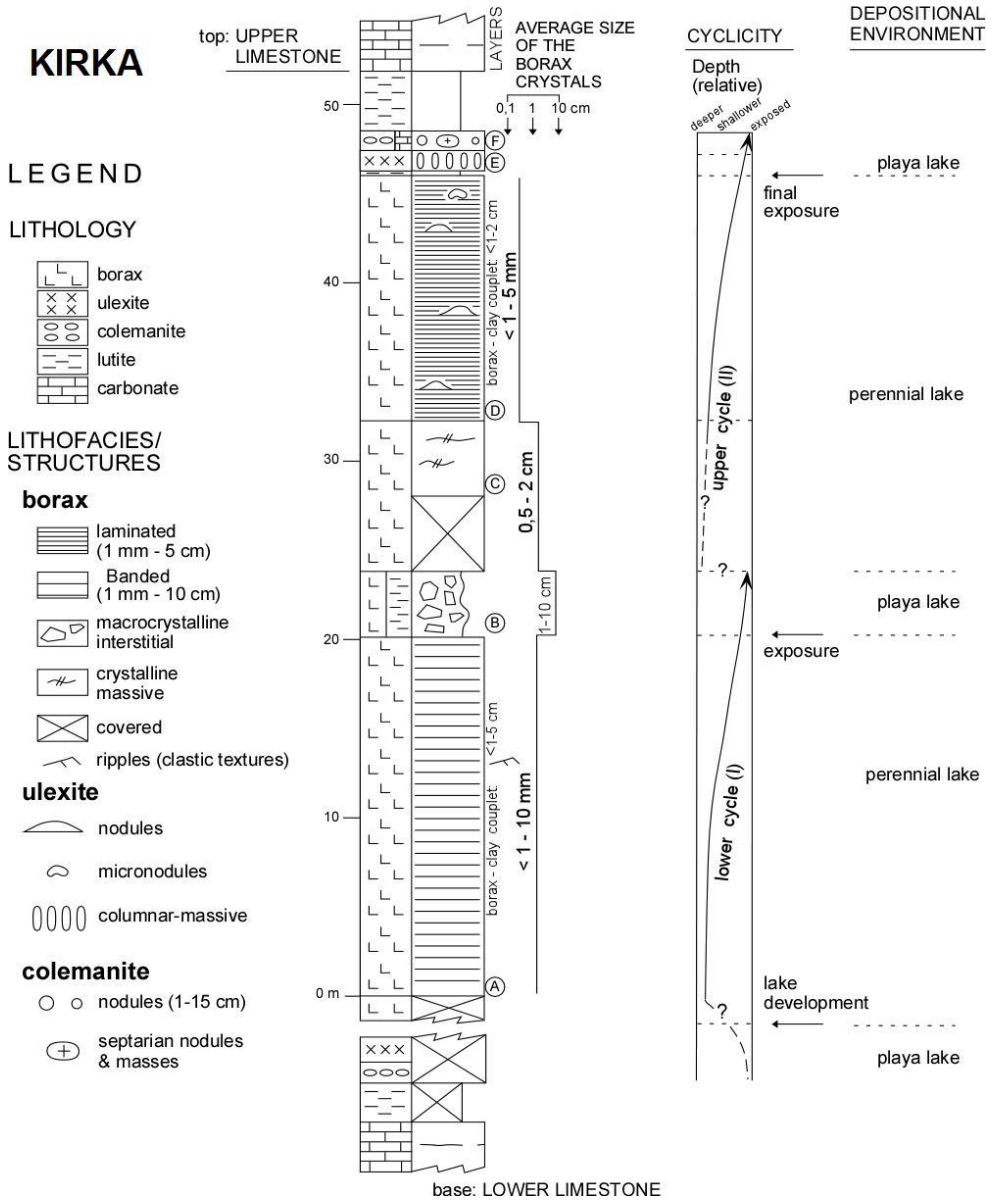

Figure 4.8. Stratigraphic succession in the central part of the Kırka borate deposit (modified from Helvacı and Ortí, 2004, fig. 4).

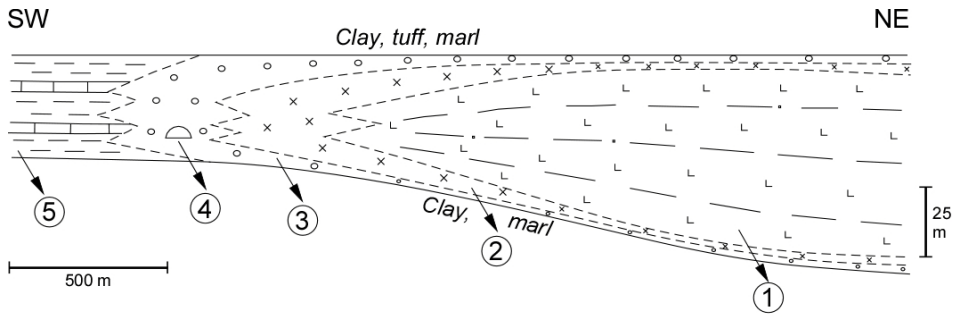

Figure 4.9. Interpretative scheme of the lateral facies distribution in the central part of the Kırka borate deposit (modified from Helvacı and Ortí, 2004, fig. 2). 1: central body of laminated borax; 2: nodular and massive ulexite; 3: nodular and massive colemanite; 4: colemanite mine (inactive); 5: marginal lutites and carbonates.

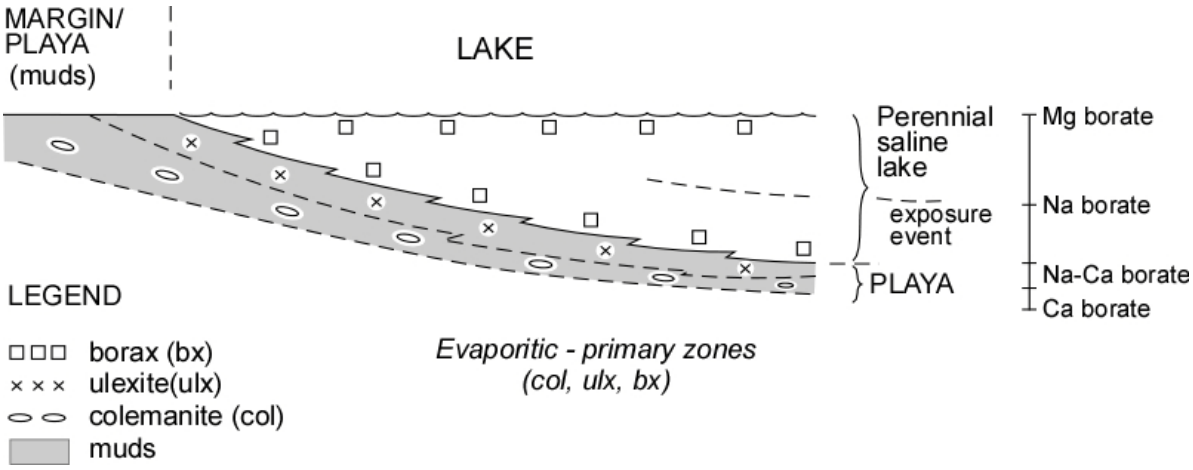

Figure 4.10. Interpretative scheme of mineral distribution and paleoenvironments in the Kırka borate deposit, Anatolia, till the moment of the deposition of the upper ulexite bed (E) bearing Mg-borates (complete zoning of the deposit is not shown). In this scheme it is interpeted that: (1) synsedimentary, interstitial crystallization occurs in the external zones containing the Na-Ca and Ca borates (margins of the lake and playa-lake settings), and (2) deposition of borax under subaqueous to exposed conditions occurs in Kırka lake (modified from Helvacı and Ortí, 2004, fig. 16).

borax laminae; this growth was also replacive: ulexite pseudomorphs after borax crystals can be observed petrographically.

Mineral zoning. As seen above, the vertical succession of the borate unit is practically symmetrical and constituted by a macrocycle involving these zones: colemanite – ulexite – borax – ulexite - colemanite. The same observation is valid for the lateral facies belt (concentric pattern), which is integrated by: a central body of Na-borate (borax), an intermediate zone of Na/Ca-borate (ulexite) and a marginal zone of Ca-borate (colemanite) (Fig. 4.9).

No petrographic evidence was found in interval (F) for a possible inyoite-to-colemanite transformation, as previously proposed in the literature (İnan *et al.* 1973). Furthermore, the post-depositional burial of the Kırka deposit is considered to be insufficient for such a generalized transformation related to thermal diagenesis. Beside this, the Mg-borates occurrences in interval (E) probably represent the ultimate evaporitic precipitates from the fractionation of the initial solution (instead of any possible reaction product between pre-existing borates and groundwater).

Thus, mineral zoning in the Kırka deposit can be held as primary, not only for borax and ulexite, but also for the colemanite and the Mg borates overlying the central body. This zoning represents the complete evolution of a Na-rich boratiferous saline lake. In it, the existence of a lateral gradient of salinity would have conditioned the concentric pattern (Helvacı and Ortí, 2004) (Fig. 4.10).

4.3.2. Marginal part of the basin (Göcenoluk section)

Recent petrologic studies of samples coming from two deep boreholes (1100 m depth) drilled in a marginal part of the basin, near the Gócenoluk village, 5 km west of Kırka, have recorded a thick borate succession. The borate succession in the 2008-6 borehole is mainly formed by an upper probertite unit (~300m thick) which overlies a lower borax unit (~100m thick). Abundant small tunellite crystals are scattered throughout the sequence. Ulexite is a very minor phase.

The upper probertite unit consists of nodular probertite interbeded with lavas, tuffs and thin dolomite layers. Only two colemanite intervals, less than 3 m thick, have been identified. Backscattered electron images and X-ray mapping of both probertite and colemanite exhibit an internal zonation pattern as a result of high and variable strontium contents (Fig. 2.2D).

The basal borax unit consists of massive beds formed by anhedral centimetric crystals also interbeded with tuffs and dolomites. In both units, borates show evidence of interstitial growth breaking and deforming peloidal dolomite and stromatolitic layers.

Unlike other contemporaneous borate deposits in the Anatolian region, neither metal sulfides nor arseno-sulfides are present in Kırka. Intense water-rock interaction with volcano-sedimentary layers induces the dissolution of feldspars and plagioclases which are usually replaced by probertite. Abundant authigenic zeolites (mainly analcime) and boron-silicates (searlesite) are formed as a consequence of the silica leached from the weathering of silicates.

According to petrographic observations and the internal strontium zonation pattern in both probertite and colemanite crystals, we consider them as primary precipitates which grew interstitially in volcaniclastic sediments and soft dolomitic muds deposited on the bottom of the lake. The absence of well laminated borax in this marginal position suggests that was also formed below the water-sediment interface.

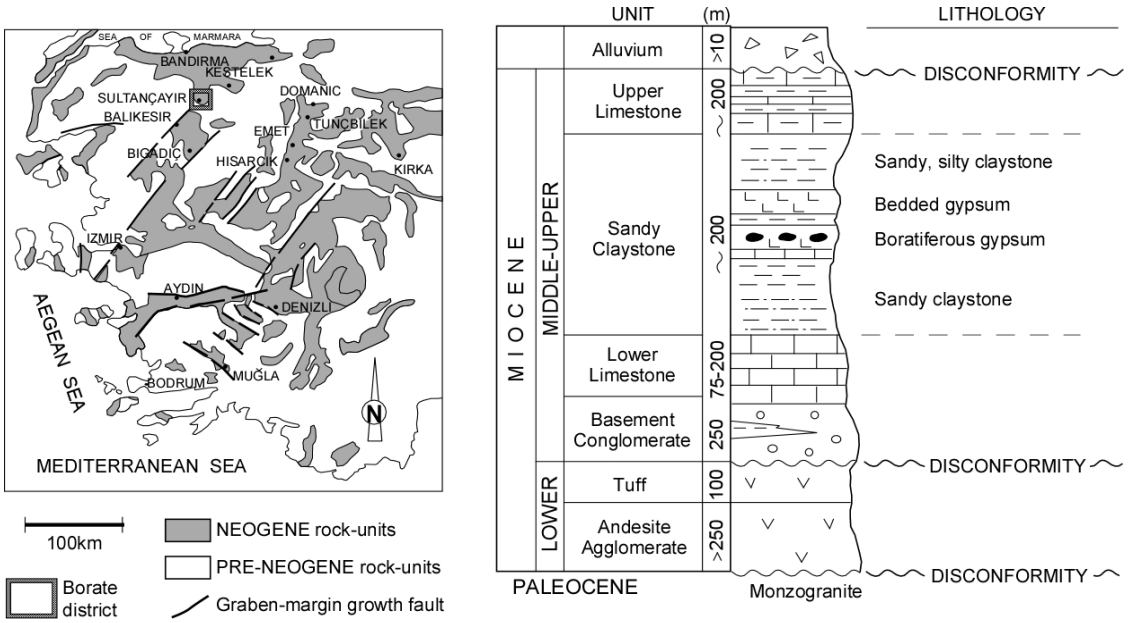

Figure 4.11. Stratigraphic succession of the Neogene Sultançayır Basin of Anatolia (modified from Ortí et al., 1998; Fig. 1).

4.4. Sultançayır Basin

The Miocene volcano-sedimentary succession in this basin contains a thick (up to 200 m) sandy claystone formation (Fig. 4.11). In the central part of the basin, this clastic formation contains an evaporitic unit, the Sultançayır Gypsum, of a Middle-Upper Miocene age, which bears a borate deposit (Fig. 4.12). After its formation, this unit was never buried deeper than 300-400 m.

Evaporitic succession. In outcrop, the Sultançayır Gypsum is made up of secondary gypsum and is characterized by the following facies belts: laminated gypsum and intraformational gypsrudites (debris-flow breccias) in the depocenter; pseudomorphic gypsum (after banded selenites) located on shoals in intermediate positions; and nodular gypsum (formerly sabkha anhydrite) in a wide marginal zone.

The gypsum succession in the depocenter, up to 50 m thick, is formed by at least three complete cycles of lutites-gypsum (the oldest forming the Bedded Lower Gypsum and the two younger forming the Bedded Upper Gypsum). These cycles display shallowing-upward trends. The same trend is displayed by the whole gypsum succession (Fig. 4.13): the depositional environment, from which this succession was formed, evolved from deeper (laminated gypsum, debris-flow gypsum) to shallower water (selenitic gypsum on shoals; interstitially-grown nodular gypsum in subaerial conditions). The debris-flow deposits most probably occurred by instability of the depositional surface linked to seismicity in the basin (Ortí *et al.*, 1998) (Fig. 4.14).

Borate occurrences. In the depocenter succession calcium borates, mainly priceite (pandermite) and howlite, and some colemanite and bakerite to a much lesser extent, are found interbedded within gypsum. In the lowermost cycle, at the beginning of the evaporitic episode (Lower Bedded Gypsum), these minerals have been interpreted as the result of mixing the basinal solutions with borate-rich flows ascending through synsedimentary faults.

The lithofacies of priceite, the major ore mineral in this deposit are varied: finely-laminated, stratiform masses, discontinuous bands, irregular masses and nodules. Some of these lithofacies indicate that priceite grew not only interstitially within the gypsum host, but also as a primary, free precipitate on the lake floor. In particular, the finely-laminated character of some of the priceite levels in alternation with the laminated gypsum clearly indicates that the two minerals were primary phases.

Howlite is present as compact, interstitially-grown, individual nodules (<1 cm up to 1 dm in diameter), in which the crystalline fabric is fine-grained prismatic. Howlite nodules displace gypsum, and replace priceite in the priceite beds.

The occurrence of fragments of both priceite and howlite embedded in the debris-flow gypsum deposits (Lower Bedded Gypsum) can be interpreted that these two major borates were primary precipitates (priceite) or synsedimentary products (priceite, howlite).

Scarce occurrences of colemanite as small nodules or irregularly-shaped features were formed interstitially within the gypsum host. Bakerite as (microscopic) spherulites is also present.

Interaction between borates and the Ca-sulfate diagenetic cycle. The Ca-sulfates underwent a complete diagenetic cycle: the depositional (primary) gypsum changed to

anhydrite during moderate burial, and this diagenetic anhydrite was later re-hydrated into secondary gypsum during final exhumation of the deposit. Given that presently all the gypsum is secondary in this unit (burial anhydritization was total) the presence of a high geothermal gradient in the region during the Miocene can be deduced.

This diagenetic cycle partly affected the borate minerals: (a) the gypsum-to-anhydrite conversion during burial resulted in partial replacement of priceite and accompanying borates (howlite, bakerite) as well as other early diagenetic minerals (celestine) by anhydrite; and (b) final exhumation caused a partial transformation of priceite and howlite into secondary calcite (Fig. 2.7B).

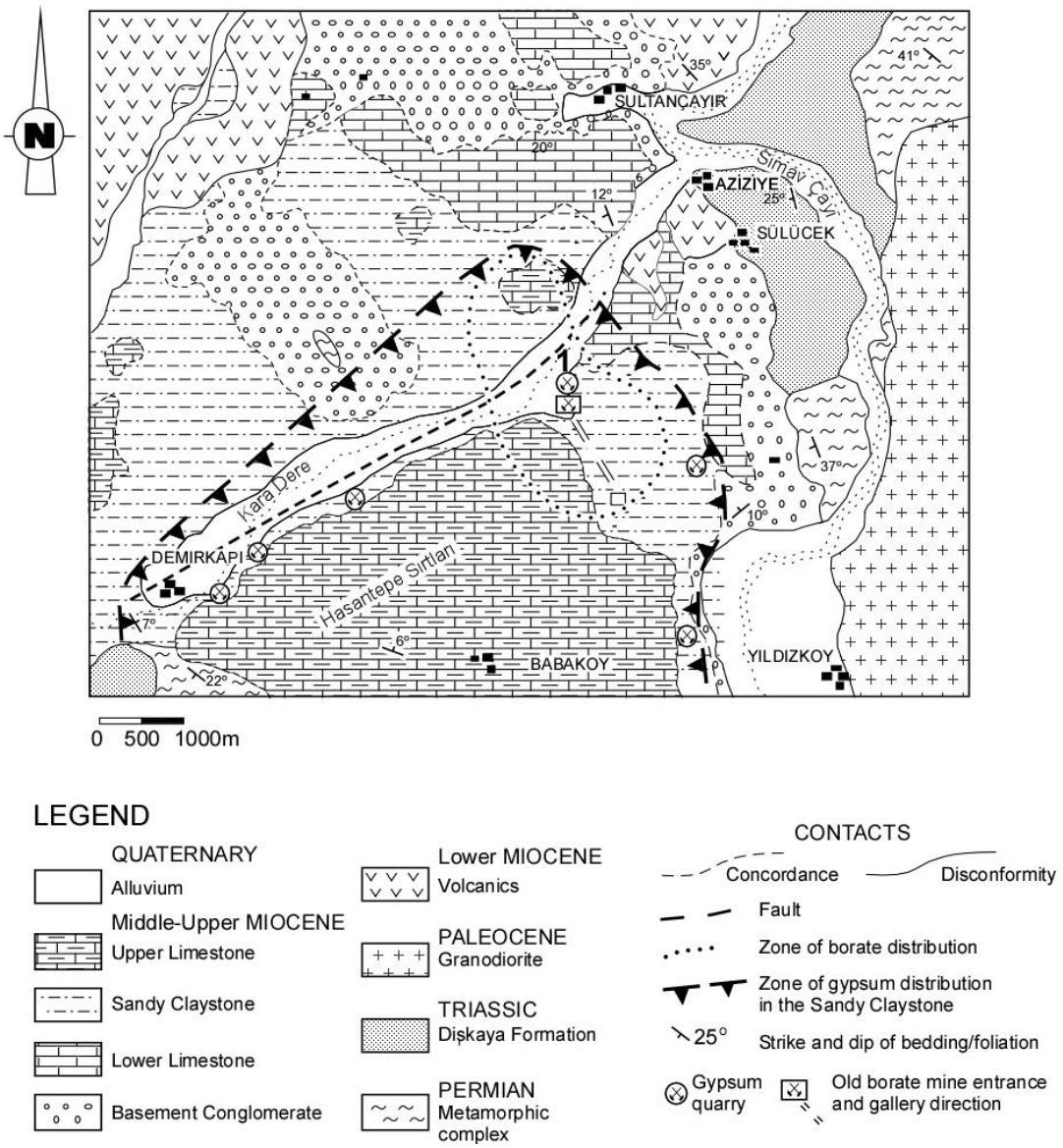

Figure 4.12. Geological map of the Neogene Sultançayır Basin, Anatolia (modified from Ortí et al., 1998; Fig. 2).

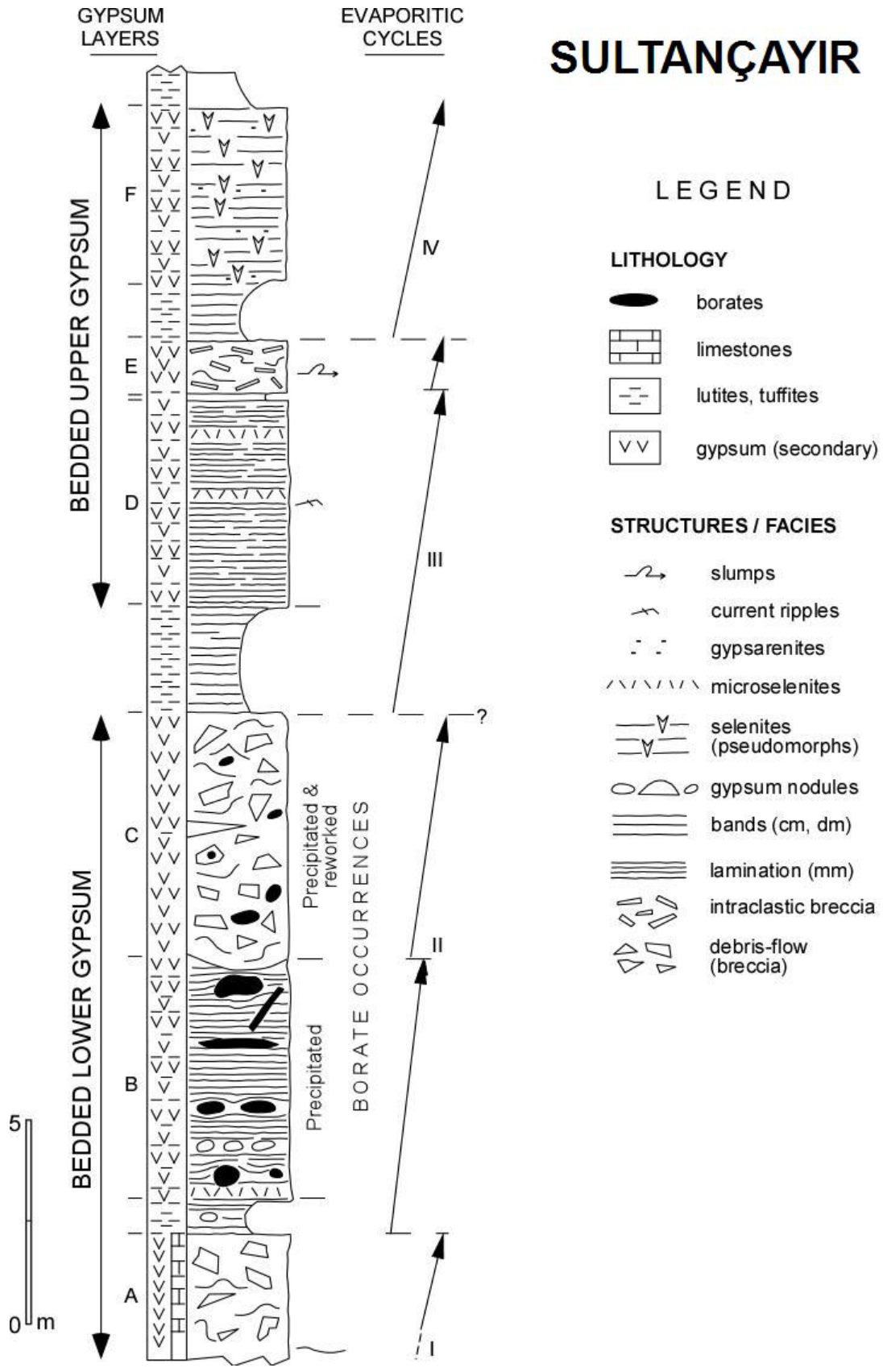

Figure 4.13. Stratigraphic succession in the central part of the Neogene Sultançayır Basin, Anatolia (modified from Ortí et al., 1998, Fig. 4).

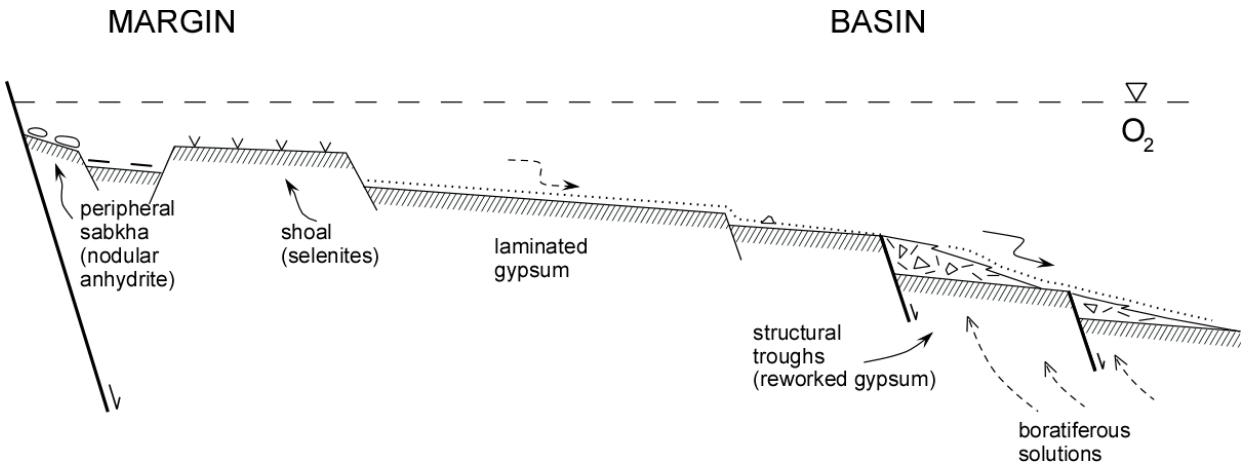

Figure 4.14. Schematic representation of subenvironments during the borate formation (Bedded Lower Gypsum) in the saline lake of the Sultançayır Basin, Anatolia (modified from Ortí et al., 1998; Fig. 5)

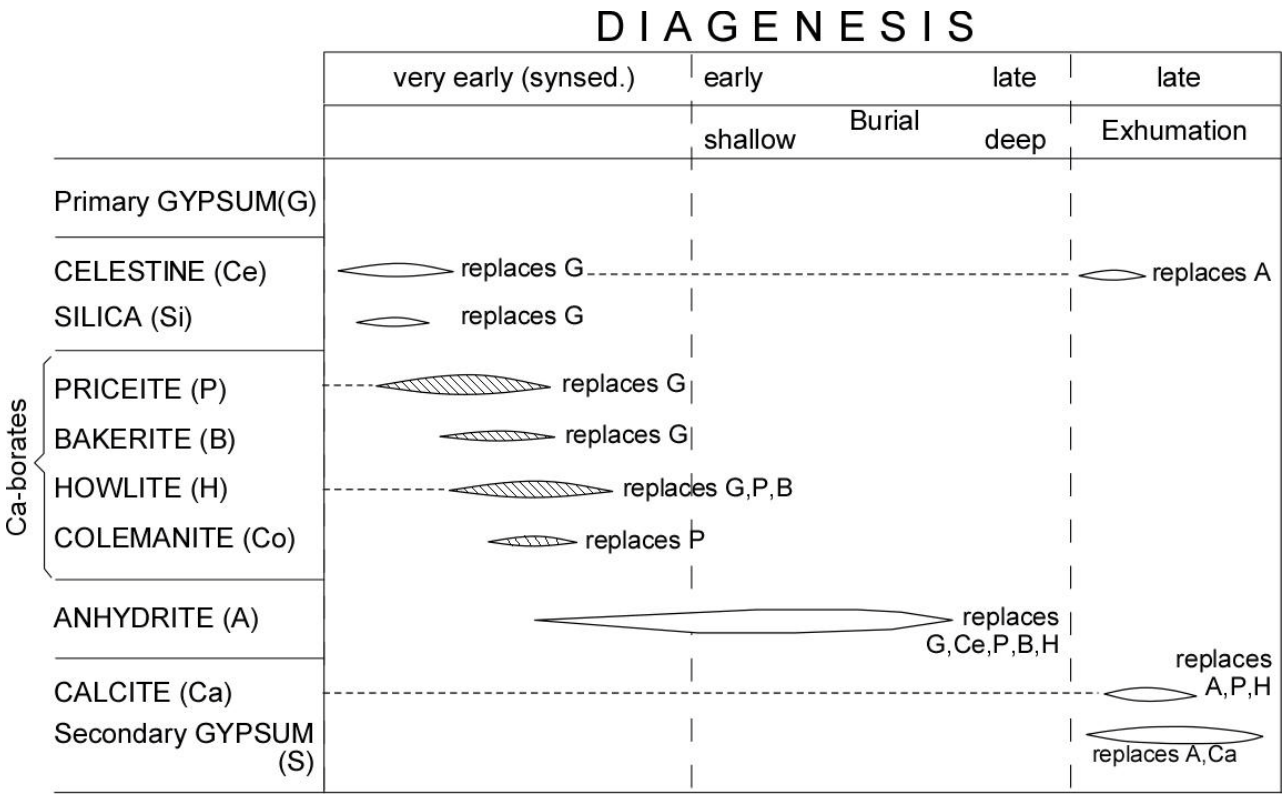

Figure 4.15. Diagram of the genetic processes affecting the main minerals (sulfates, borates, carbonates) in the Neogene Sultançayır Basin, Anatolia. Both the sedimentation and the synsedimentary reworking of gypsum and major borates (priceite, howlite) preceeding the diagenetic phases are not indicated in this diagram. Pandermite is used for priceite (modified from Ortí et al., 1998; Fig.8).

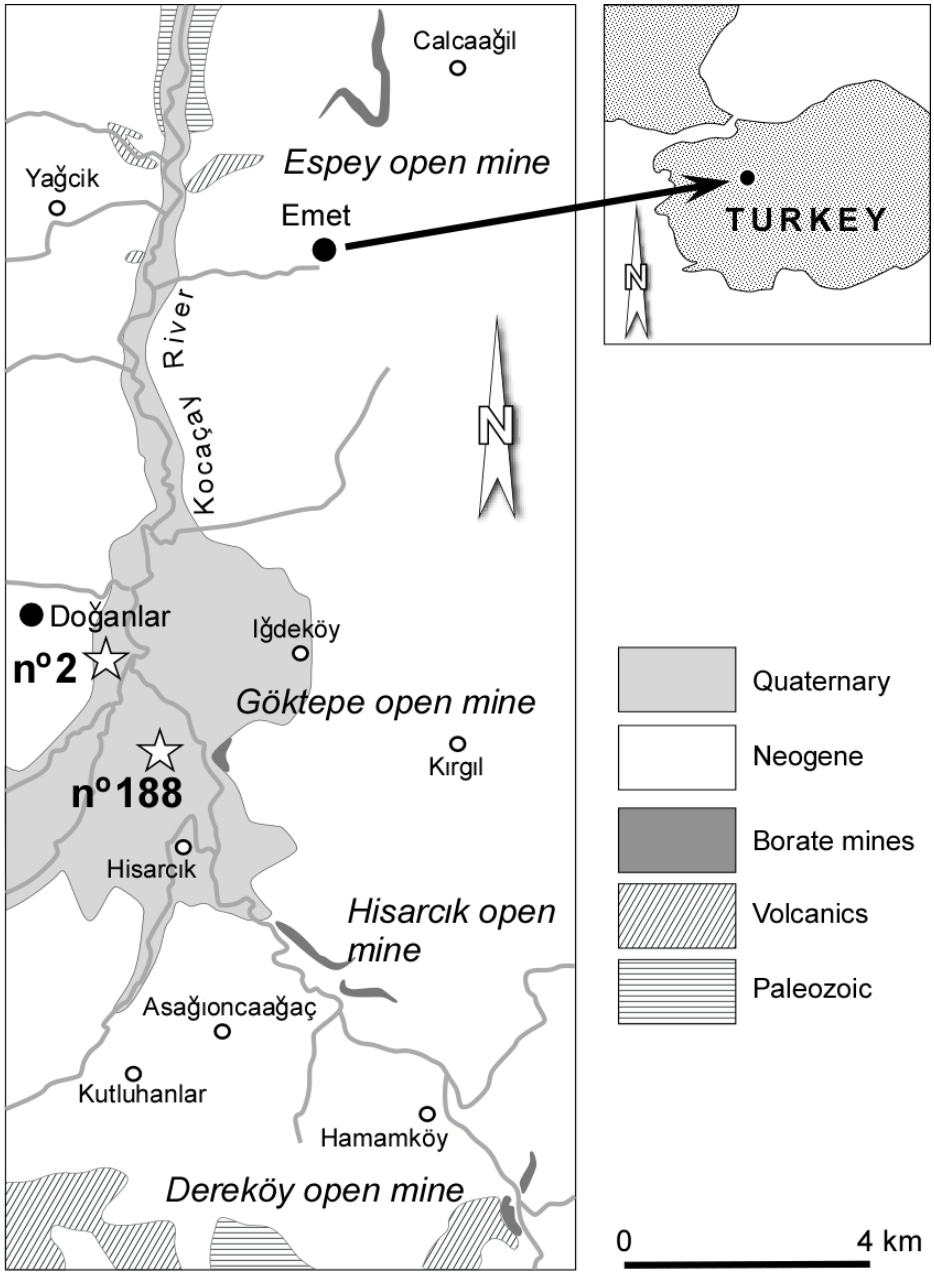

Fig. 4.16. Geological simplified map of the Emet borate district, west Anatolia with main open mine and borehole locations (modified from Helvacı, 1984)

4.5. Emet Basin

In the Emet Basin (Fig. 4.16), a Miocene lacustrine succession exceeding 1000 m in thickness overlies unconformably a basement formed by Paleozoic rocks and an Upper Cretaceous cover. In ascending order, the Miocene succession is formed by: a basal unit of conglomerates; a clastic unit bearing coal seems; a borate-bearing unit (Hisarcık Fm); and an upper limestone unit with chert, marls and clays. Quaternary sediments discordantly overly the Miocene materials (Fig. 4.17). Intense volcanic activity began in the Early Miocene in the basin and continued until at least the Late Miocene (Helvacı, 1984; Çolak *et al.*, 2000). Hydrothermal springs, which currently are depositing calcareous travertines and native sulfur, are active in this basin to the west of the Kocaçay River. The dissolution of Neogene

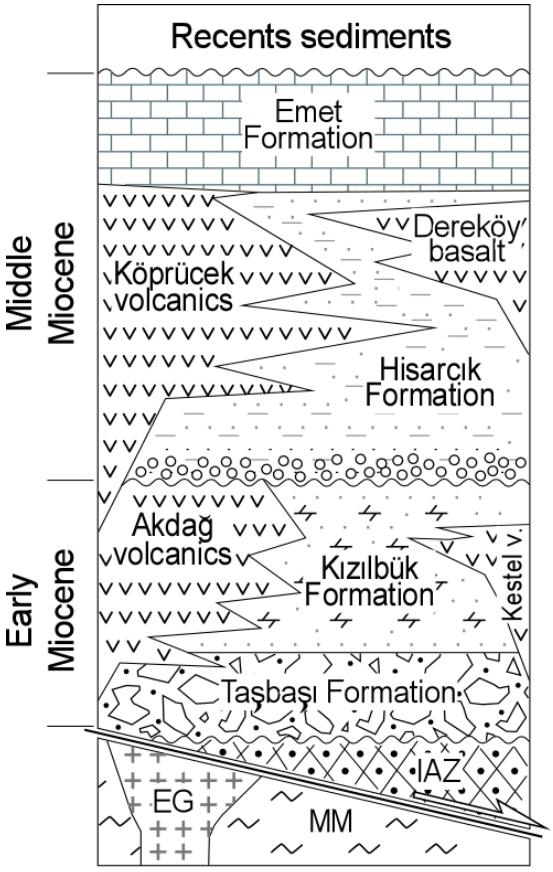

Figure 4.17. Stratigraphic succession of the Neogene Emet Basin, Anatolia (after García-Veigas et al., 2010a; modified from Helvacı, 1984).

sediments is causing high concentrations of B, As and SO_4, and high salinity in the present-day Emet thermal waters (Gemici *et al.*, 2004; Doğan and Doğan, 2007).

4.5.1. Marginal part of the basin

The various outcrops and exploitations located to the east of the Kocaçay River (Espey, Göktepe, Hisarcık, Dereköy) are included in a borate succession of up to 150 m in thickness. This succession (Fig. 4.18) is formed by colemanite layers (5-10 m thick) in alternation with clay and tuff beds, and also by minor amounts of ulexite, hydroboracite, meyerhofferite, realgar and native sulfur (Helvacı, 1984; Helvacı *et al.*, 1993). Colemanite in these layers displays an impressive nodular-to-meganodular, displacive lithofacies, which grew from interstitial brines under synsedimentary conditions in a playa-lake system (Helvacı and Ortí, 1998; Helvacı and Alonso, 2000). Some native sulfur and realgar impregnate or replace the colemanite. Evidence of possible precursor borate phases in these large colemanite nodules is rare: remains of possible ulexite micronodules were observed under the microscope only locally.

4.5.2. Central part of the basin (Doğanlar section)

Two boreholes with continuous rock sampling were drilled near the Doğanlar village by Eti Bor Company (Turkish Government) for exploratory purposes during year 2003 (Fig. 4.19). More than 500 m of a borate-sulfate-chloride succession were intersected by these boreholes. The lithologic cores of this succession show a complex mineral association (García-Veigas *et al.*, 2011). In it, dolomite, probertite, glauberite and halite constitute the major primary phases; other sulfates are anhydrite, gypsum, thenardite, celestine, and kalistrontite; other borates are colemanite, ulexite, hydroboracite, tunellite, kaliborite and aristarainite; sulfides are arsenopyrite, realgar, and orpiment; other carbonate is calcite. Two new minerals (pending of approval by the IMA) have been identified: emetite, $Ca_7Na_3K(SO_4)_9$ (García-Veigas, *et al.*, 2010a) and fontarnauite, $Na_2Sr(SO_4)(B_4O_6(OH)_2)\cdot 3H_2O$ (García-Veigas *et al.,* 2010b) (Fig. 2.12).

Eight units were differentiated in the borehole succession: the basal (C-1) and the top (C-8) units are mainly formed by colemanite; between them, three units of probertite (P-2, P-5, P-7) are found; within these probertite units two glauberite units (G-4, G-5) are interbedded; a halite unit (H-3) occupies the central part. Overall, this succession is dominated by Ca-borates at the base and the top, by Na-Ca borates and sulfates in the intermediate zone, and by Na-chloride in the center (Fig. 4.19).

The main probertite lithofacies are nodular and laminated, while the glauberite and halite lithofacies are basically banded and laminated. Each one of the units identified is characterized by the association of few major minerals (colemanite; probertite-glauberite; probertite-glauberite-halite) and by minor replacive minerals (various sulfates and borates). Bacterially-induced dolomite appears in the lower part of the succession.

This evaporite succession records a significant change of the parent-waters in the lake from initial Ca-rich solutions precipitanting the basal colemanite, to Ca-Na-rich brines from which the probertite and glauberite units formed, and to Na-rich brines from which halite and thenardite precipitated (H-3 unit). According to fluid inclusion compositions, the halite precipitating brine was of the Na-K-Cl-SO_4 type. Although no K-bearing minerals (kaliborite) precipitated as isolated beds in this central part of the basin, their formation during early diagenesis suggests a progressive enrichment of K in the more concentrated Na-brines. After halite precipitation, brines returned to the Na-Ca composition characterized by the precipitation of probertite (P-5 and P-7 units) and glauberite (G-4 and G-6 units), and finished with the colemanite and anhydrite crystallization from terminal Ca-rich type of brines.

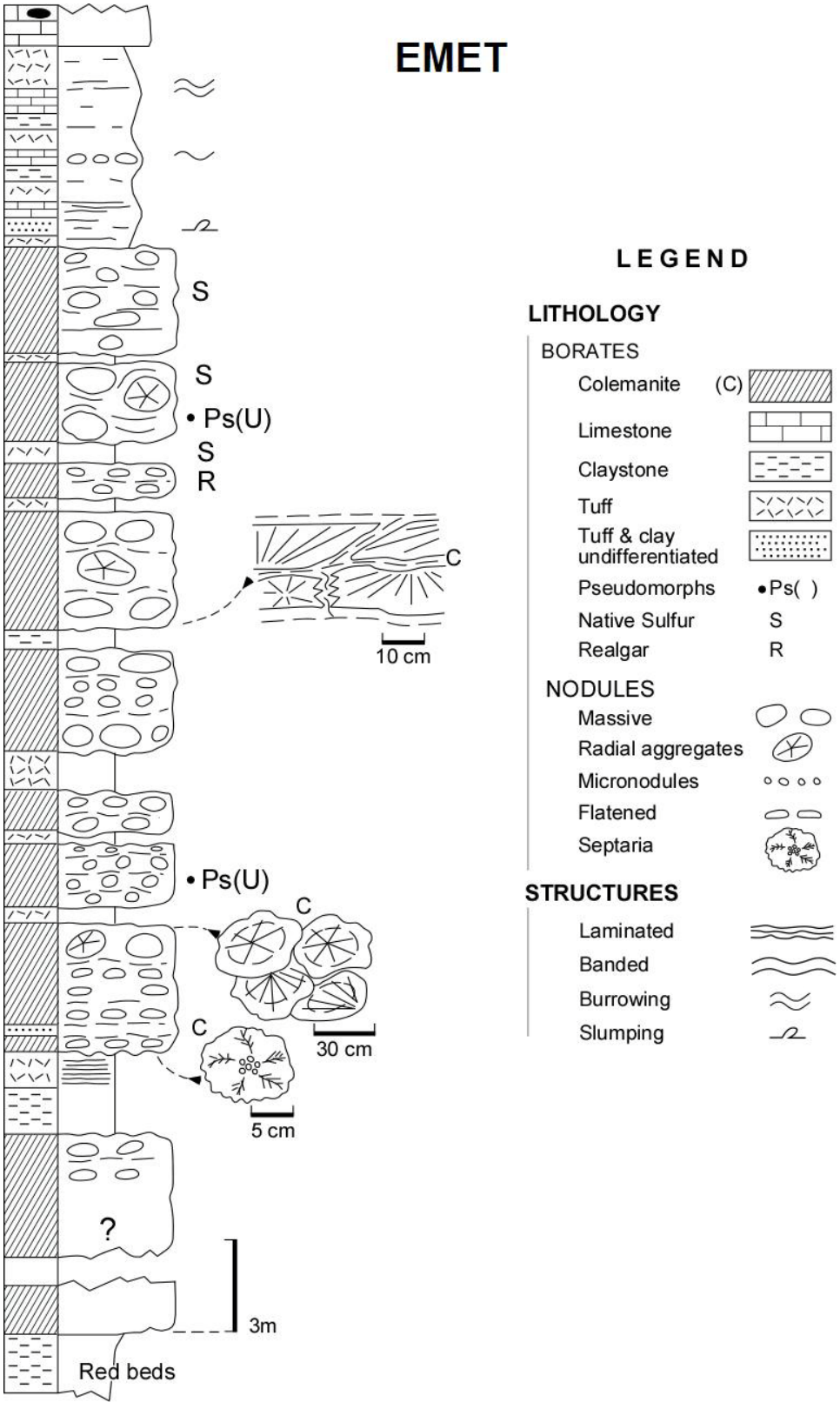

Figure 4.18. Partial stratigraphic succession in the marginal zone of the Neogene Emet Basin. Ps(U) refers to the petrographic presence of some pseudomorphs of ulexite micronodules within the colemanite (modified from Helvacı and Ortí, 1998; Fig. 7A).

Depositional model. The evaporitic model is envisaged as a saline lake surrounded by an extensive, slightly sloped, marginal saline tuff-flat. In this tuff-flat the nodular colemanite succession of the outcrops/exploitations was formed. In the central lake, the water column evolved from shallow and moderately deeper (saline lake) to very shallow (salt-pond).

During the *saline lake stage*, a marked salinity gradient towards the lake center is evidenced by the Ca-borate (colemanite) precipitation in the outer-most belt and by Ca-Na-borates and sulfates (probertite and glauberite) precipitation in both nearshore (interstitially) and in the center of the lake (subaqueously). Both the bottom water and the underground brines in the surrounding saline mud-flat remained under anoxic conditions that favored the microbial sulfate reduction (BSR) of glauberite. As a result of this, sulfide (from the reduced sulfate) and bicarbonate were produced. Sulfide reacted with Fe and As present in the volcaniclastic matrix yielding the precipitation of colloidal arsenopyrite. At the same time, dolomite was formed by the action of microorganisms. The BSR modified the isotopic composition of the remaining dissolved sulfate enriching the precipitated glauberite in heavy isotopes.

During the *salt pond stage*, the lake remained very shallow and the groundwater level dropped in the surrounding saline tuff-flat. The fall of the water table generated oxidizing conditions in the groundwater of this tuff-flat meanwhile reducing conditions remained in the restricted flooded sector. Increasing salinity related to this restriction resulted in the precipitation of probertite, glauberite and halite in the pond, in which biogenic dolomite and arsenopyrite still formed. The change to oxidizing conditions in the underground brine below the surface of the saline tuff-flat, prevented the bacterial reduction of the dissolved sulfate. Thus, interstitial glauberite precipitated with the original isotopic signal. These oxidizing conditions in the units overlying the halite unit avoided the generation of bio-induced dolomite and colloidal arsenopyrite, and favored the biogenic precipitation of As-sulfide (realgar).

Two complex reactions within the lacustrine sediments were: (1) the synsedimentary replacement of the uppermost probertite unit by ulexite related to the contribution of diluted water at the end of the evaporitic event, and (2) the replacement of previous evaporitic minerals by K-bearing (kaliborite and fontarnauite) and Mg-bearing (hydroboracite) minerals during advanced stages of early diagenesis by means of reaction with interstitial brines.

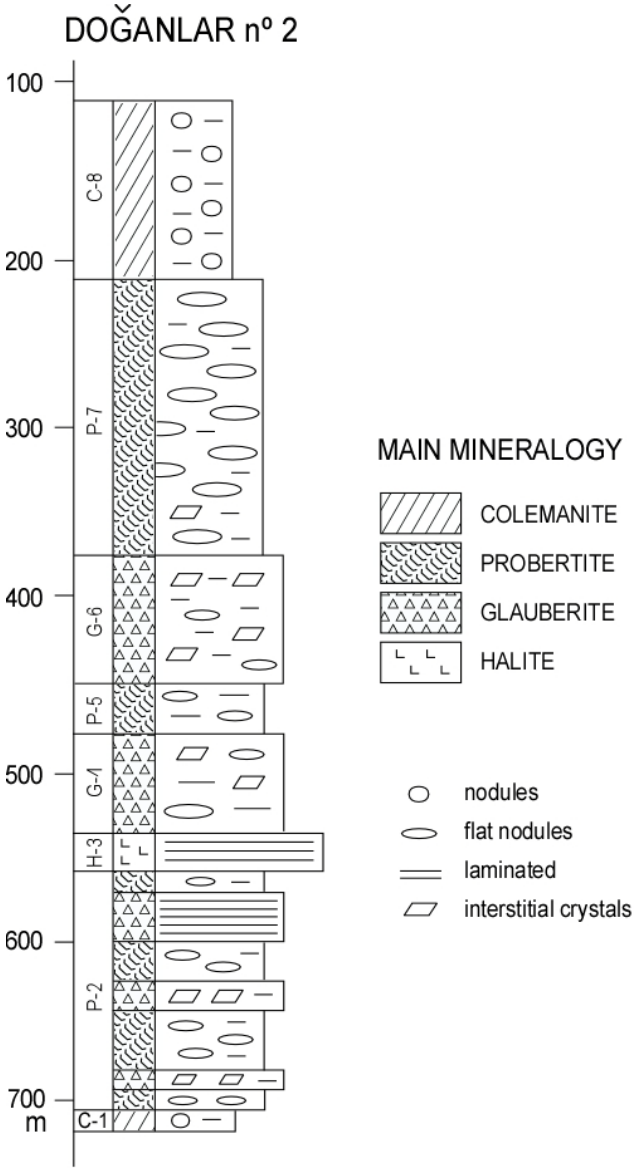

Figure. 4.19. Mineralogical units in the Doğanlar-2 borehole, central part of the Neogene Emet Basin, Anatolia (modified from García-Veigas et al*, 2010a).*

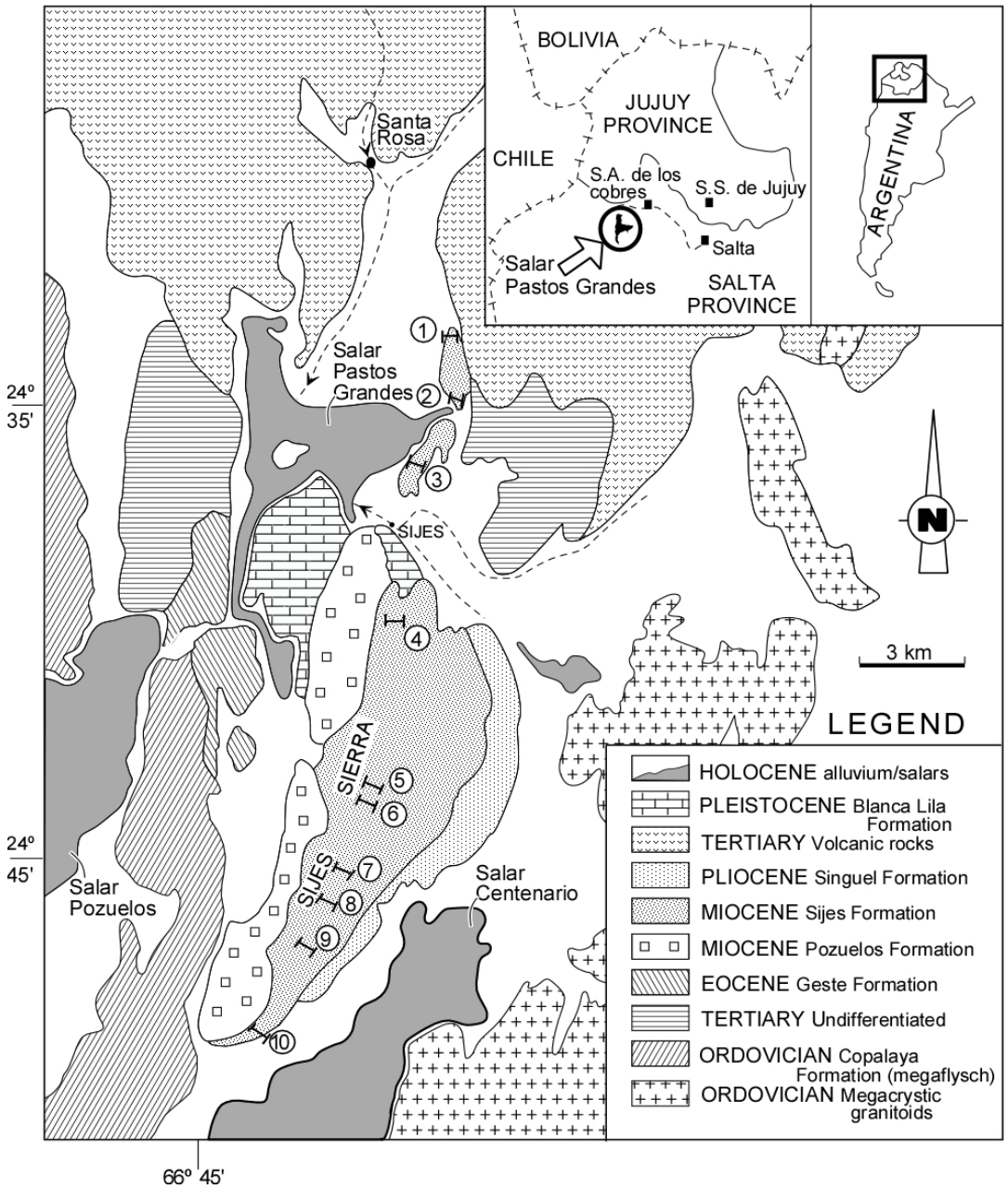

Figure 4.20. Geological map of the Neogene Pastos Grandes Basin in the Sijes Sierra, La Puna region, NW Argentina (modified from Ortí and Alonso, 2000, Fig. 1).

4.6. Sijes Formation (Miocene, La Puna, NW Argentina)

The Pastos Grandes Neogene Basin displays a sedimentary infilling of up to 5000 m in thickness, which was deposited on a variety of non-marine environments (fluvial, alluvial, saline lake) (Fig. 4.20). One of the Miocene formations in the basin is the Sijes Formation, which contains borate deposits of economic interest. This formation, up to 2000 m thick, is constituted by four members, from base to top: Monte Amarillo Mb (330 m thick), Monte Verde Mb (380 m thick), Conglomerate Mb (0 to 200 m thick), and Esperanza Mb (580 m thick). Overlying the Sijes Fm and the Piocene Singuel Fm, the Pleistocene Blanca Lila Fm is made up of claystones and evaporites (Fig. 4.21) (Alonso, 1986; Vandervoort, 1997).

The Monte Amarillo Mb contains an inyoite unit (36 m thick) at the base and an upper hydroboracite unit (137 m thick); the Monte Verde Mb intercalates an inyoite-colemanite unit (113 m thick); and the Esperanza Mb has a colemanite unit (37 m thick) (Fig. 4.22). The most important borate deposits are in the Monte Amarillo Mb. The boron source of these deposits seems to be related to the volcanic and hydrothermal activity in the Central Andes during the Miocene. Also, the presence of As-sulfides (realgar, orpiment) in the Sijes Fm suggests a hydrothermal origin for As.

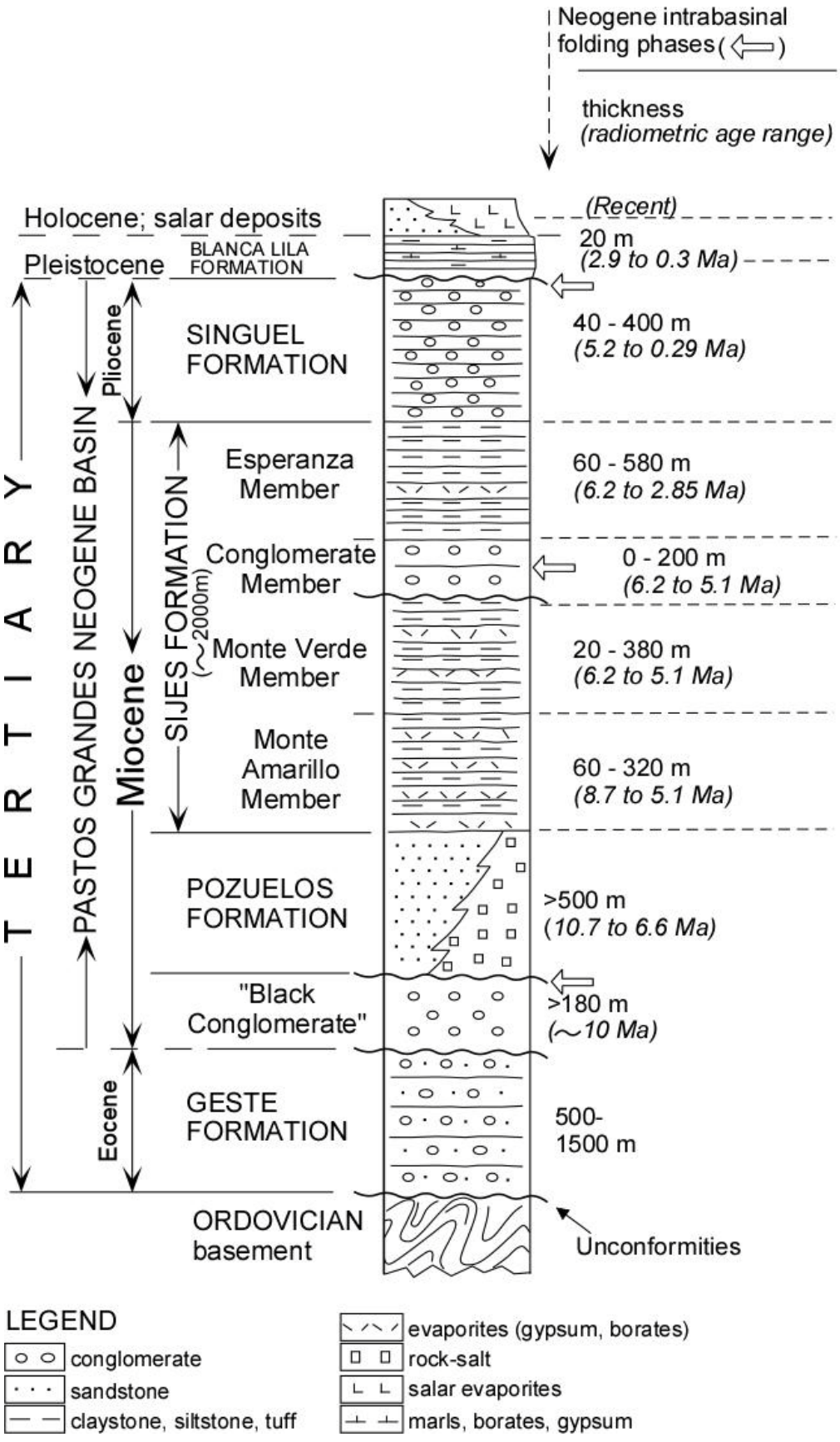

Figure 4.21. General stratigraphic succession in the Neogene Pastos Grandes Basin, La Puna region, NW Argentina (modified from Ortí and Alonso, 2000; Fig. 2).

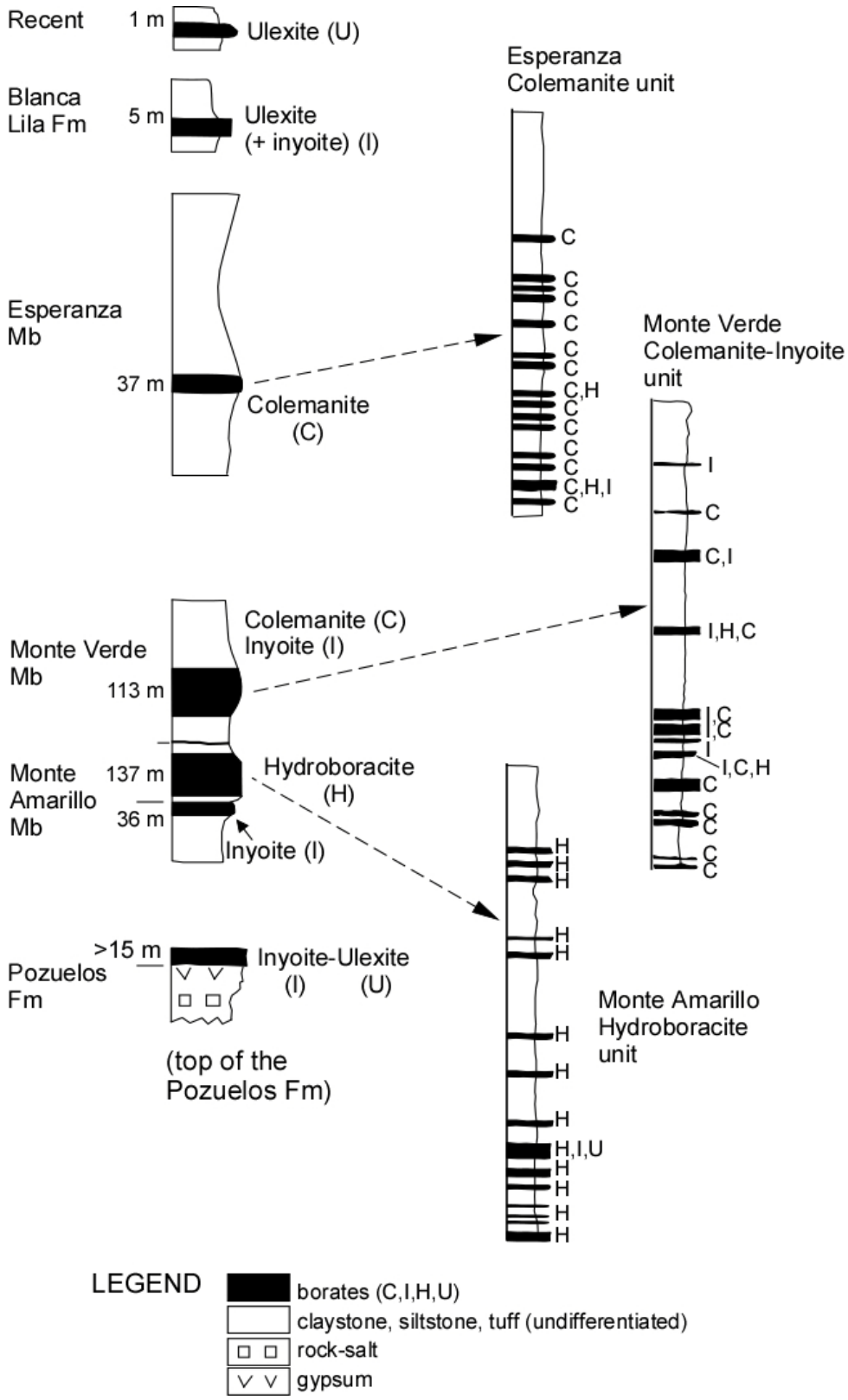

Figure 4.22. Borate units in the various members of the Sijes Fm, in the Blanca Lila Fm, and in the Holocene Pastos Grandes salar (modified from Ortí and Alonso, 2000, Fig. 2).

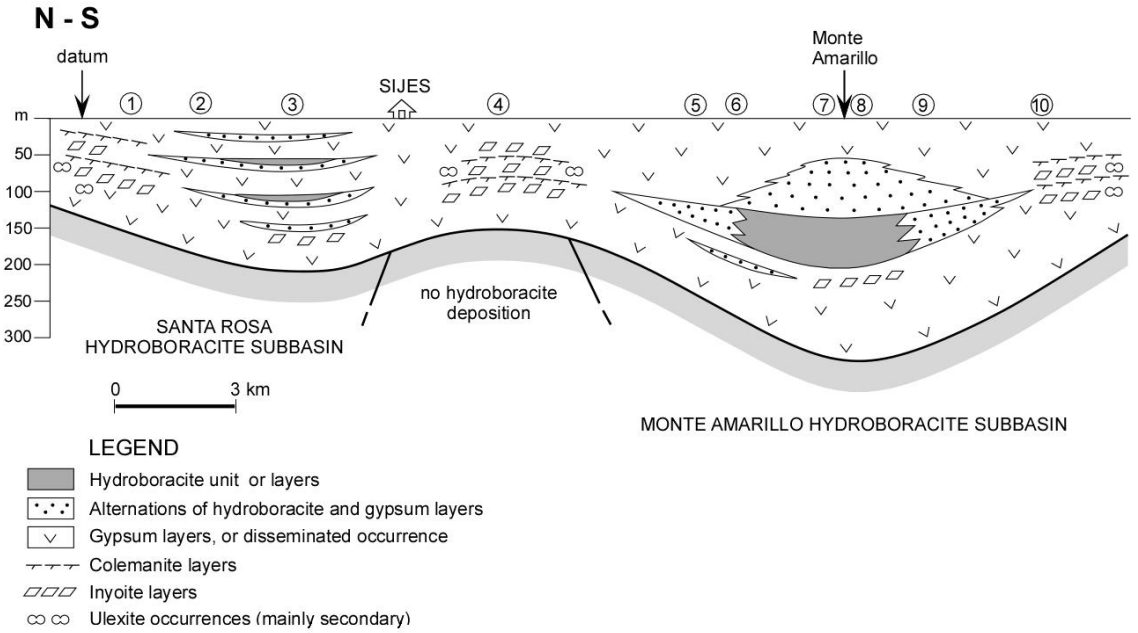

Figure 4.23. Scheme of the borate and sulfate facies distribution in the Santa Rosa and the Monte Amarillo hydroboracite subbasins, Sijes Fm, Neogene, La Puna region, NW Argentina. Datum: top of the Monte Amarillo Mb. The location of the Monte Amarillo section (7) is indicated (modified from Ortí and Alonso, 2000; Fig. 12).

Evaporitic succession in the Monte Amarillo Member. The Monte Amarillo Mb of the Sijes Fm contains the largest known hydroboracite reserves in the world. In this member, the sulfate minerals are secondary gypsum and minor anhydrite, and the borate minerals are hydroboracite with subordinate inyoite and colemanite, and minor ulexite. A maximum burial depth of about 1500 m is estimated for this member.

In this member it is possible to distinguish two coeval, shallow, lacustrine subbasins, the Monte Amarillo and the Santa Rosa subbasins (Fig. 4.23) (Ortí and Alonso, 2000). In them, both vertical and lateral zoning is observed: gypsum is preferentially accumulated in the lower and upper parts of the vertical succession and in the marginal parts of the borate units; hydroboracite is preferentially accumulated in the middle of the successions and in the core of the borate unit; the intermediate zones are characterized by mixed gypsum-hydroboracite layers.

The depositional succession of the Monte Amarillo subbasin, up to 317 m thick (section 7, Fig. 4.23), is formed by the following units in ascending order: siliciclastic unit, gypsum unit, gypsum-inyoite unit, hydroboracite unit (without gypsum), gypsum-hydroboracite unit, hydroboracite unit, and gypsum unit. This succession shows a single, gypsum-hydroboracite-gypsum macrocycle, which is slightly asymmetrical (Fig. 4.24).

The depositional succession of the Santa Rosa subbasin is integrated by two gypsum-hydroboracite macrocycles, with individual thickness between 40 and 70 m. Colemanite as micronodules and radial aggregates is associated with the banded-massive facies of gypsum (Fig. 4.25).

Primary, subaqueous hydroboracite. In the two subbasins, hydroboracite is mainly a primary mineral, which display a number of lithofacies: laminated, banded, massive, globular, intraclastic/brecciated, nodular, enterolithic, in lenticular masses, and in alternations with gypsum. Hydroboracite crystalline fabrics are: fibrous, prismatic, microgranular, radical, blocky-mosaic (anhderal) and drusy. Moreover, hydroboracite cements are also recorded. Alternations of laminated hydroboracite and laminated gypsum also accounts for a primary, subaqueous origin for the two minerals

Mineral zoning. Zoning in the two subbasins is chemical (depositional). Lateral zoning corresponding to precipitation belts grades from the margin to the center: Ca-sulfate – Ca-borate – Ca-Mg borate. Vertical zoning allows us to envisage a lacustrine evolution from an initial dry mud flat with a Ca-sulfate solution, to an advanced stage in which the saline lake was oversaturated with respect to hydroboracite (without gypsum), and to a final stage in which the lake brine progressively returned to its initial Ca-sulfate composition. Sodium appears to have been a minor component of the initial solution. In this evolution, colemanite postdated the precipitation of gypsum, whereas inyoite could accompany the precipitation of both gypsum and hydroboracite. The accumulation of gypsum-free hydroboracite could be related to a sulfate decrease in the precipitating lake brines. The environment remained shallow along the evolution of the saline lake.

These conditions of close precipitation of Ca-sulfates and Ca-borates were possible given that the stability ranges of gypsum, colemanite,

inyoite and ulexite overlap to a considerable degree. Replacements between the various borate minerals during burial diagenesis were not detected.

Calcium-sulfate diagenetic cycle. The generallized presence of secondary gypsum in the Monte Amarillo Mb. indicates that the primary gypsum underwent a complete diagenetic cycle. Along this cycle, the primary gypsum: (1) was first transformed into anhydrite by burial (from early diagenesis to moderate burial diagenesis); (2) it changed to secondary gypsum during final exhumation by the groundwater action.

Interaction between borates and sulfates: gypsum-hydroboracite pseudomorphs. Within the hydroboracite laminae, pseudomorphs after precursor gypsum can be observed petrographically. The study of these pseudomorphs indicates that: (1) mutual replacements between gypsum and hydroboracite occurred under synsedimentary conditions (Fig. 2.9E,F). These replacements resulted in pseudomorphs of both, gysum after hydroboracite and hydroboracite after gypsum; (2) these interactions were partly 'fossilized' and preserved by the gypsum to anhydrite conversion during burial. In this process, anhydrite replaced the preexistent pseudomorphs to some extent; and (3) final exhumation resulted in secondary gypsum pseudomorphs after several types of precursor pseudomorphs. Thus, it can be deduced that diagenetic processes in borates can be studied in connection with the diagenetic cycle of Ca-sulfates.

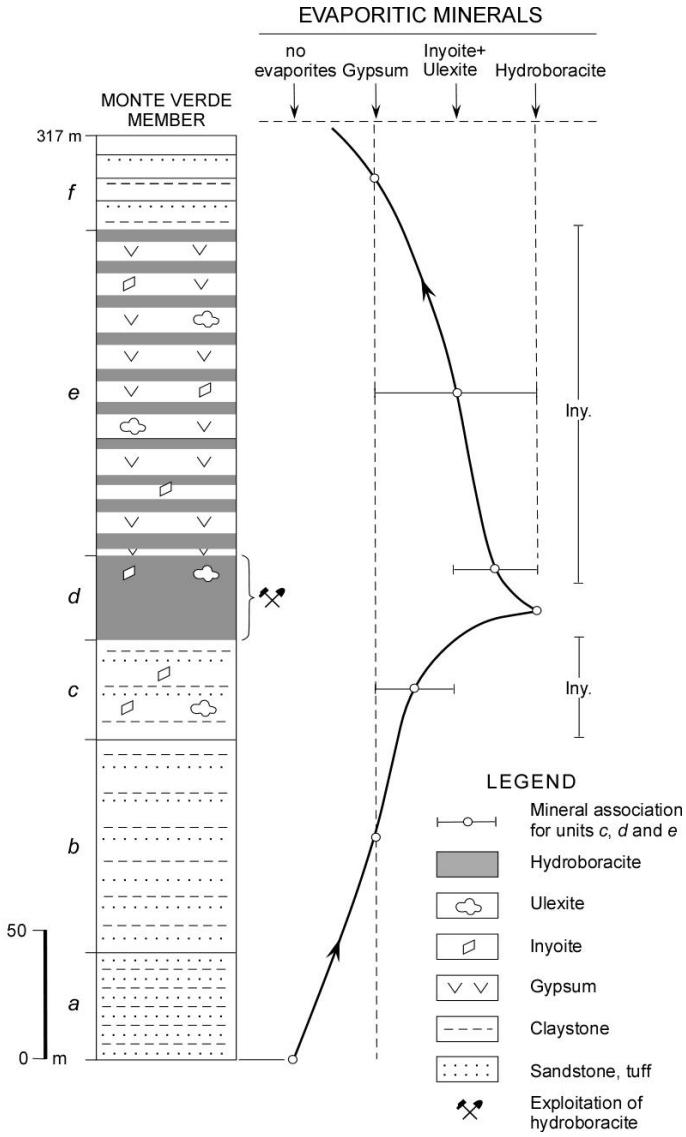

Figure 4.24. Simplified succession of the Monte Amarillo Mb. in the Monte Amarillo subbasin (Sijes Fm, La Puna region, NW Argentina) (modified from Ortí and Alonso, 2000, Fig. 10).

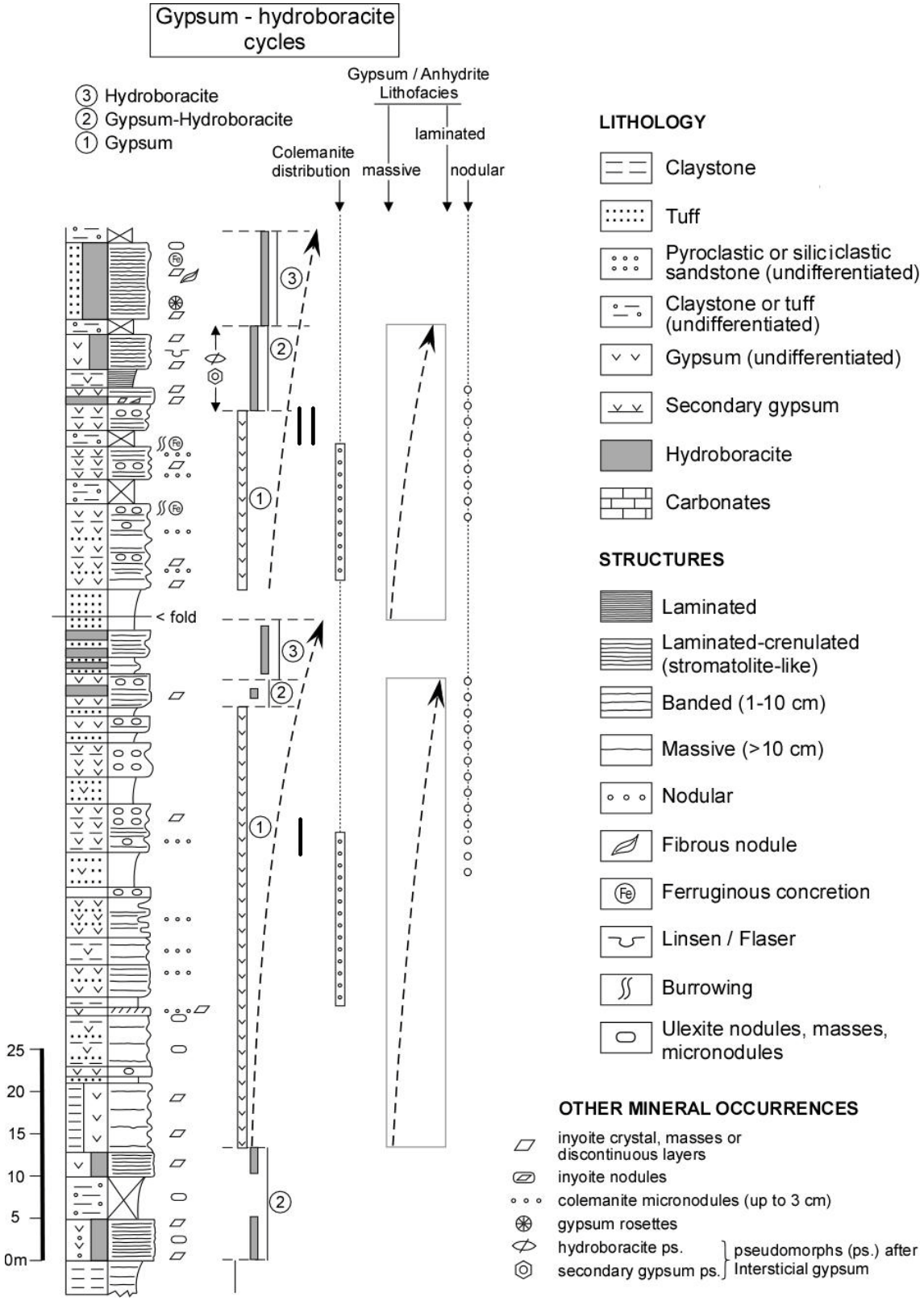

Fiure. 4.25. Partial stratigraphic succession of the Monte Amarillo Mb in the Santa Rosa subbasin, showing two complete depositional cycles (I and II). The base of the succession is the top of the Pozuelos Fm. (La Puna region, NW Argentina) (modified from Ortí and Alonso, 2000, Fig. 11).

REFERENCES

Alonso, R.N., 1986. Ocurrencia, posición estratigráfica y génesis de los depósitos de boratos de la Puna Argentina. PhD Thesis, Univ. Salta, Argentina, 196 pp (unpublished).

Alonso, R.N., 1990. On the origin of La Puna Borates. Acta Geológica Hispánica 34, 144-166.

Alonso, R.N., 1991. Evaporitas neógenas de los Andes Centrales. In: Pueyo, J.J. (Coor.), Génesis de formaciones evaporíticas: modelos andinos e ibéricos. Universitat de Barcelona, Estudi General 2, 15-86.

Alonso, R., Gutiérrez, R., 1984. Zonación de ulexita en los salares de la Puna Argentina. Revista Asociación Geológica Argentina 39, 52-57.

Alonso, R.N., Helvacı, C., Sureda, R.J., Viramonte, J.G., 1988. A new Tertiary borax deposit in the Andes. Mineralium Deposita 23, 299-305.

Anovitz, L.M., Grew, E.S., 1996. Mineralogy, petrology and geochemistry of boron: an introduction. Reviews in Mineralogy 33, 1–40.

Ataman, G., Baysal, O., 1978. Clay mineralogy of Turkish borate deposits. Chemical Geology, 22, 233-234.

Barker, Ch.E., Barker, J.M., 1985. A re-evaluation of the origin and diagenesis of borate deposits, Death Valley Region, California. In: Barker, J.M., Lefond, S.L. (Eds.), Borates: Economic Geology and Production. American Institute of Mining, Metallurgical and Petroleum Engineers. New York, 101-135.

Barker, J.M., Lefond, S.L., 1985. Borates: Economic Geology and Production. American Institute of Minning, Metallurgical and Petroleum Engineers. New York, 274 pp.

Bowser, C.J., Dickson, F.W., 1966. Chemical zonation of the borates of Kramer, California. In: Rau, J.L. (Ed.), Second Simposium on Salt, 1. Northern Ohio Geol. Soc., Cleveland, 122-132.

Chong, G., Pueyo, J.J., Demergasso, C., 2000. Los yacimientos de boratos de Chile. Revista Geológica de Chile 27, 99-119.

Christ, C.L., Clark, J.R., 1977. A crystal-chemical classification of borate structures with emphasis on hydrated borates. Physics and chemistry of minerals 2, 59-87.

Colter, A.J., Nicholson, K., Fairley, J.P. 2004. Source characterization of the Borax lake geothermal system, Alvord Basin, Oregon. Geological Society of American, Abstracts with Programs 36-5, 359.

Coolbaugh, M.F., Kraft, Ch., Sladek, Ch., Zehner, R.E., Shevenell, L., 2006a. Quaternary borate deposits as a geothermal exploration tool in the Great Basin. Geothermal Research Council Transactions 30, 393-398.

Coolbaugh M.F., Sladek, Ch., Kratt, Ch., Shevenell, L., Faulds, J.E., 2006b. Surface indicators of geothermal activity at Salt Wells, Nevada, USA, including warm ground, borate deposits, and siliceous alteration. Geothermal Research Council Transactions 30, 399-405.

Crowley, J.K., 1996. Mg- and K-bearing borates and associated evaporites at Eagle Borax Spring, Death Valley, California: A spectroscopic exploration. Economic Geology, 91, 622-635.

Çolak, M., 1995. The Emet and Kırka borate mines (Turkey). Institut de Minéralogie et de Pétrographie de l'Université de Fribourg (Suisse). Diss. 1099.

Doğan, M., Doğan, A.U., 2007. Arsenic mineralization, source, distribution, and abundance in the Kütahya region of the western Anatolia, Turkey. Environmental Geochemistry and Health 29, 119–129.

García-Veigas, J., Ortí, F., Rosell, L., Gündoğan, I., Helvacı, C., 2010a. Occurrence of a new sulphate mineral $Ca_7Na_3K(SO_4)_9$ in the Emet borate deposits, western Anatolia (Turkey). Geological Quarterly 54, 431-438.

García-Veigas, J., Rosell, L., Alcobé, X., Subias, I., Ortí, F., Gündoğan,I., Helvacı, C., 2010b. Fontarnauite, a new sulphate-borate mineral from the Emet borate district (Turkey). Macla 13, 97-98.

García-Veigas, J., Rosell, L., Ortí, F., Gündoğan,I., Helvacı, C., 2011. Mineralogy, diagenesis and hydrochemical evolution in a probertite-glauberite-halite saline lake (Miocene, Emet Basin, Turkey). Chemical Geology 280, 352-364.

Garret, D.E., 1998. Borates, Handbook of deposits, processing, propertie, and use. Academic Press. 483pp.

González-Barry, C.E., and Alonso, R.N., 1987. El depósito Neoterciario de boratos Esperanza, Sijes, Salta. IX Congreso Geológico Argentino, 2: 63-66.

Gemici, Ü., Tarcan, G., Çolak, M., Helvacı, C., 2004. Hydrochemical and hydrogeological investigation of thermal waters in the Emet area (Kütahya, Turkey). Applied Geochemistry 19, 105–117.

Hardie, L.A., 1968. The origin of the Recent non-marine evaporite deposit of Saline Valley, Inyo County, California. Geochimica et Cosmochimica Acta 32, 1279-1301.

Hay, R.L., Guldman, S.G., 1987. Diagenetic alteration of silicic ash in Searles Lake. Clay and Clay Minerals 35, 449-457.

Helvacı, C., 1977. Geology, mineralogy and geochemistry of the borate deposits and associated rocks at the Emet Valley, Turkey. Ph. D. Thesis, Univ. Nottingham, United Kingdom, 338 pp. (unpublished).

Helvacı, C., 1978. A review of the mineralogy of the Turkish borate deposits. Mercian Geology 6, 257-270.

Helvacı, C., 1984. Occurrence of rare borate minerals: veatchite-A, tunellite, teruggite and cahnite in the Emet borate deposit, Turkey. Mineral. Deposita 19, 217-226.

Helvacı, C., 1994. Mineral assemblages and formations of the Kestelek and Sultançayır borate deposits. In: Nishiyama, T., Kumon, F. and Watable, Y. (Eds), 29th Inter. Geol. Cong., Proceedings, Part A, 245-264.

Helvacı, C., 1995. Stratigraphy, mineralogy and genesis of the Bigadiç borate deposits, western Turkey. Economic Geoogy 90, 1237-1260.

Helvacı, C., Alonso, R.N., 1994. An occurrence of primary inyoite at Lagunita Playa, Northern Argentina. Proc. 29th Inter. Geol. Congr., Part A, 299-308.

Helvacı, C., Alonso, R.N., 2000. Borate Deposits of Turkey and Argentina; A Summary and Geological Comparison. Turkish Journal of Earth Sciences 9, 1-27.

Helvacı, C., Ercan, T., 1993. Recent borate salts and associated volcanism in the Karapınar Basin (Konya), Turkey. Abstract Book of the 46 Geological Congress of Turkey, 102-103.

Helvacı, C., Firman, R.J., 1976. Geological setting and mineralogy of the Emet borate deposits, Turkey. Trans. Inst. Min. Metall., Sect B, 85, 142-152.

Helvacı, C., Ortí, F., 1998. Sedimentology and diagenesis of Miocene colemanite-ulexite deposits (western Anatolia, Turkey). Journal Sedimentary Research 68 , 1021-1033

Helvacı, C., Ortí, F., 2004. Zoning in the Kırka borate deposit, western Turkey: primary evaporitic fractionation or diagenetic modifications?. Canadian Mineralogists 42, 1179-1204.

Helvacı, C., Stametakis, M.G., Zagouroglou, F., Kanaris, J., 1993. Borate minerals and related authigenic silicates in northeastern Mediterranean Late Miocene continental basins. Exploration and Mining Geology Journal 2, 171-178.

Igarzábal, A.P. 1991. Evaporitas cuaternarias de la Puna argentina. In: Pueyo, J.J. (Coord.), Génesis de Formaciones Evaporíticas, Modelos Andinos e Ibéricos, Universitat de Barcelona, Estudi General 2: 333-374.

İnan, K., Dunham, A.C., Esson, J., 1973. Mineralogy, chemistry and origin of Kırka borate deposit, Eskisehir Province, Turkey. Trans. Inst. Min. Metall., Sect. B, 82, 114-123.

Jaffe, H.W., 1996. The crystal chemistry of the borate minerals. In: Jaffe, H.V. (Ed.): Crystal Chemistry and Refractivity. Dover Publications, 352 pp.

Kistler, R.B., Helvacı, C., 1994. Boron and Borates. In: Carr, D.D. (Ed.), Industrial Minerals and Rocks, 6th Edition. Soc. Min. Metallurgy and Exploration, Inc., 171-186.

Koski, A.K., Wood, S.A., 2004. The geochemistry of geothermal waters in the Alvord Basin, southeastern Oregon. In: Wanty, R.B. and Seal, R.R. (Eds.), Water-Rock Interaction Proceedings of the Eleventh International Symposium on Water-Rock Interaction WRI-11-1. A.A.Balkema, Leiden, the Netherlands, 149-152.

Kraft, Ch., Coolbaugh, M., Calvin, W., 2006. Remote detection of Quaternary borate deposits with ASTER satellite imagery as a geothermal exploration tool. Geothermal Research Transactions 30, 435-440.

Littlefield, E., Calvin, W., 2010. Geothermal exploration using AVIRIS remote sensing data over Fish Lake Valley, NV. Geothermal Research Council Transactions 34, 599-603.

Lowenstein, T.K., Risacher, F., 2009. Closed basin brine evolution and the influence of Ca-Cl inflow waters: Dead Valley and Bristol Dry Lake California, Qaidam Basin, China, and Salar de Atacama, Chile. Aquatic Geochemistry 15, 71-94.

Mc Allister, J.F., 1970. Geology of the Furnace Creek borate area, Death Valley, Inyo Country, California. Calif. Div. Min. Geol. Map, sheet 14, 1:24.000, 9 pp.

Melgarejo, J.C., Martin, R.F., 2011. Atlas of Non-Silicate Minerals in Thin Section. Canadian Mineralogists, Special Publications 7, 522 pp.

Mordogan, H., Helvacı, C., 1994. Occurrence and distribution of lithium in the clays of borate deposits and some recent lake waters, Turkey. Geological Congress of Turkey. 1994. Abstracts. Chamber of Geological Engineers of Turkey, p. 149.

Muessig, S., 1958. First known occurrence of inyoite in a playa, at Laguna Salinas. Perú: The American Mineralogist 43, 1144-1147.

Ortí, F., Alonso, R.N., 2000. Gypsum-hydroboracite association in the Sijes Formation (Miocene, NW Argentina): implications for the genesis of Mg-bearing borates. Journal Sedimentary Research 70, 664-681.

Ortí, F., Helvacı, C., Rosell, L., Gündoğan, I., 1998. Sulphate-borate relations in an evaporitic lacustrine environment: the Sultaçayır Gypsum (Miocene, western Anatolia). Sedimentology, 45, 697-710.

Palmer, M.R., Helvacı, C., 1995. The boron geochemistry of the Kırka borate deposit, western Turkey. Geochimica Cosmochimica Acta 59, 3599-3605.

Palmer, M.R., Helvacı, C., 1997. The boron isotope geochemistry of the Neogene borate deposits of western Turkey. Geochimica Cosmochimica Acta 61, 3161-3169.

Schindler, M., Hawthorne, F.C., 2001. A bond-balance approach to the structure, chemistry and paragenesis of hydrosyhydrated oxysalt minerals. I. Theory. Canadian Mineralogists 39, 1225-1242.

Smith, G.I., 1985. Borate deposits in the United States: dissimilar in form, similar in geologic setting. In: Barker, J.M., Lefond, S.L. (Eds.), Borates: Economic Geology and Production. Society of Mining Engineers, New York, 37-51.

Smith, G.I., 2009. Late Cenozoic Geology and lacustrine history of Searles Valley, Inyo and San Bernadino Counties, California. U.S. Geological Survey Professional Paper 1727, 115 pp.

Smith, G.I., Medrano, M.D., 1996. Continental borate deposits of Cenozoic age. In: Grew, E.S., Anovitz, L.M. (Eds.), Boron: Mineralogy, Petrology and Geochemistry. Amer. Miner. Soc. Reviews in Mineralogy 33, 263-298.

Stout, L.M., Blake, R.E., Greenwood, J.P., Martini, A.M., Rose, C., 2009. Microbrial diversity of boron-rich volcanic hot springs of St. Lucia, Lesser Antilles. Microbiology Ecology, 70, 402-412.

Sun Dapeng, 1990. Origin of borate deposits in Xiao Qaidam Lake, Qaidam Basin, China. China Earth Science 1 , 253-266.

Sun Dapeng, Li Bingxiao, 1993. Origin of borates in the saline lakes of China. Seventh Symposium on Salt, vol 1. Elsevier, 177-193.

Sureda, R., 1991. Mineralogia de las rocas evaporíticas. In: Pueyo, J. J., (Coor.), Génesis de formaciones evaporiticas. Modelos andinos e ibéricos. Universitat de Barcelona, Estudi General 2, 15-86.

Tanner, L.H., 2002. Borate formation in a perennial lacustrine setting: Miocene–Pliocene Furnace Creek Formation, Death Valley, California, USA. Sedimentary Geology 148, 259-273.

Vandervoort, D.S., 1997. Non-marine evaporite basin studies. Southern Puna Plateau, Central Andes. Ph.D. Thesis, Cornell University, 177pp (unpublished).

Vinante, D., Alonso, R.N., 2006. Evapofacies del Salar Hombre Muerto, Puna argentina: distribucion y génesis. Revista Asociación Geológica Argentina 61, 286-297.

Zheng Mianping, 1989. Saline Lakes on the Qinghai-Xizang (Tibet) Plateau. Beijing Scientific and Technical Publishing, 431 pp.

Zheng Mianping., Qi, W., Yuan. H., 2005. Characteristics of salt lake boron deposits and magnesium borate deposits of the Quinghai-Tibet Plateau, China. In Mao., J. and Bierlein, F.O., (Eds): Mineral deposit research: Meeting the Global Challenge. Springer Berlin Heildelberg. 1123-112.

APPENDIX : Optical characteristics of some borate minerals (modified from Melgarejo and Martin, 2011)

Borax, $Na_2(B_4O_5(OH)_4)\cdot 8H_2O$
System and space group: monoclinic, *C2/c*
Unit-cell parameters: *a* 11.885, *b* 10.654, *c* 12.206 Å; ß 106.62º
Diffraction lines: 4.82(100), 5.68(90), 2.56(65) Å
Optical constants: α 1.447, β 1.469, γ 1.472; 2*V* 39º
Habit: euhedral crystals, commonly very large, with a short prismatic habit along [001]; also tabular habit on {100}
Relief: marked (-)
Color: colorless
Pleochroism: absent
Cleavage: {100} perfect, {110} good, {010} poor
Interference colors: up to second-order greenish blue
Extinction: oblique in elongate sections
Twinning: {100} rare
Other characteristics: sections perpendicular to the optic axis display a brown or blue anomalous interference color, with no extinction
Interference figure: biaxial negative, *r* > *v* strong

Colemanite, $Ca(B_3O_4(OH)_3)\cdot H_2O$
System and space group: monoclinic, $P2_1/a$
Unit-cell parameters: *a* 8.743, *b* 11.264, *c* 6.102 Å; ß 110.12º
Diffraction lines: 3.13(100), 5.64(50), 3.85(50) Å
Optical constants: α 1.586, β 1.592, γ 1.614; 2*V* 56º
Habit: the euhedral crystals are prismatic along [001]; normally in columnar aggregates arranged in radial forms or in nodules; may be a pseudomorph
Relief: from low to moderate (+)
Color: colorless
Pleochroism: absent
Cleavage: {010} perfect and {001} good, forming 90º angles
Interference colors: may reach the upper part of second order
Extinction: oblique on elongate sections
Elongation: (+)
Interference figure: biaxial positive, *r* > *v*

Howlite, $Ca_2B_5SiO_9(OH)_5$
System and space group: monoclinic, $P2_1/c$
Unit-cell parameters: *a* 12.93, *b* 9.34, *c* 8.60 Å; ß 104º50'
Diffraction lines: 4.14(100), 6.24(90), 3.10(75) Å
Optical constants: α 1.586, β 1.598, γ 1.605; 2*V* large
Habit: tabular habit {100}; in general, radial aggregates of acicular crystals
Relief: moderate (+)
Color: colorless
Pleochroism: none
Cleavage: not evident
Interference colors: up to the beginning of the second order
Extinction: oblique on elongate sections
Interference figure: biaxial negative

Hydroboracite, $CaMg(B_6O_8(OH)_6)\cdot 3H_2O$
System and space group: monoclinic, *P2/c*
Unit-cell parameters: *a* 11.755, *b* 6.685, *c* 8.225 Å; ß 102.72º
Diffraction lines: 5.77(100), 6.68(85), 3.32(50) Å
Optical constants: α 1.522, β 1.534, γ 1.569; 2*V* 63º
Habit: the crystals have a tabular habit on {010}
Relief: low (-) or (+)
Color: colorless
Pleochroism: none
Cleavage: {010} perfect
Interference colors: up to the end of the third order
Extinction: oblique on elongate sections
Elongation: (-)
Interference figure: biaxial positive, *r* < *v*

Inderborite, $CaMg\ (B_3O_3(OH)_5)_2\cdot 6H_2O$
System and space group: monoclinic, *C2/c*
Unit-cell parameters: *a* 12.137, *b* 7.433, *c* 19.234 Å; ß 90.29º
Diffraction lines: 3.35(100), 3.26(80), 3.07(80), 7.14(10) Å
Optical constants: α 1.483, β 1.512, γ 1.530; 2*V* 77º
Habit: euhedral crystals, commonly large
Relief: low, negative
Color: colorless
Pleochroism: none
Cleavage: good on {100}, conchoidal fracture

Interference colors: up to yellow of the third order
Extinction: inclined, almost straight
Interference figure: biaxial negative

Inderite, Mg $(B_3O_3(OH)_5)\cdot 5H_2O$
System and space group: monoclinic, $P2_1/c$
Unit-cell parameters: *a* 11.934, *b* 13.094, *c* 6.886 Å; ß 104.12º
Diffraction lines: 5.66(100), 3.26(100), 5.01(90), 3.34(80) Å
Optical constants: α 1.488, β 1.491, γ 1.505; 2*V* 37º
Habit: the crystals are generally granular; also prismatic, acicular and in radial groups
Relief: marked (-)
Color: colorless
Pleochroism: none
Cleavage: {110} good
Interference colors: up to the end of first order
Extinction: oblique
Interference figure: biaxial positive

Inyoite, $Ca(B_3O_3(OH)_5)\cdot 4H_2O$
System and space group: monoclinic, $P2_1/a$
Unit-cell parameters: *a* 10.621, *b* 12.066, *c* 8.408 Å; ß 114.02º
Diffraction lines: 3.03(100), 7.59(70), 2.29(25) Å
Optical constants: α 1.490, β 1.505, γ 1.516; 2*V* 86º
Habit: short euhedral to anhedral prismatic or tabular crystals, forming coarse spherulitic arrays or massive aggregates
Relief: low (-)
Color: colorless
Pleochroism: absent
Cleavage: good on {001} and {010}, irregular fracture
Interference colors: up to second-order blue
Extinction: oblique
Interference figure: biaxial negative, *r* < *v* weak

Kernite, $Na_2(B_4O_6(OH)_2)\cdot 3H_2O$
System and space group: monoclinic, $P2_1/c$
Unit-cell parameters: *a* 7.016, *b* 9.152, *c* 15.678 Å; ß 108.88º
Diffraction lines: 7.40(100), 6.64(85), 3.25(35) Å
Optical constants: α 1.454, β 1.472, γ 1.488; 2*V* 80º
Habit: the crystals have a tabular or prismatic habit, commonly in radial or columnar aggregates; also allotriomorphic granular or cryptocrystalline
Relief: medium (-)
Color: colorless
Cleavage: perfect {001}, {100}
Interference colors: up to the beginning of the third order
Extinction: oblique in elongate sections
Interference figure: biaxial negative

Kurnakovite, $Mg(B_3O_3(OH)_5)\cdot 5H_2O$
System and space group: triclinic, $P\bar{1}$ (dimorphic relations with inderite)
Unit-cell parameters: *a* 8.344, *b* 10.59, *c* 6.443 Å; α 99.0, ß 108.9, γ 87.2º
Diffraction lines: 7.22(100), 4.90(90), 5.01(80), 4.21(80) Å
Optical constants: α 1.489, β 1.510, γ 1.525; 2*V* 80º
Habit: large crystals, commonly in granular aggregates
Relief: low to medium, negative
Color: colorless
Pleochroism: absent
Cleavage: perfect on {010}
Interference colors: low second-order colors
Extinction: oblique
Interference figure: biaxial negative, *r* > *v*

Meyerhofferite, $Ca(B_3O_3(OH)_5)\cdot H_2O$
System and space group: triclinic, $P\bar{1}$
Unit-cell parameters: *a* 6.617, *b* 8.323, *c* 6.494 Å; α 90.55, ß 101.88, γ 86.62º
Diffraction lines: 8.31(100), 6.47(100), 4.97(25) Å
Optical constants: α 1.500, β 1.535, γ 1.560; 2*V* 78º
Habit: the crystals have a tabular habit on {100}, in some cases are prismatic or acicular*Relief*: low (-) or (+)
Color: colorless
Pleochroism: none
Cleavage: {010} perfect
Interference colors: high orders
Interference figure: biaxial negative, *r* > *v* weak

Priceite, $Ca_2(B_5O_7(OH)_5)\cdot H_2O$
System and space group: monoclinic, $P2_1/c$

Unit-cell parameters: *a* 11.623, *b* 6.976, *c* 12.350 Å; ß 110.70º
Diffraction lines: 10.8(100), 3.48(80), 5.97(70), 2.18 (70) Å
Optical constants: α 1.573, β 1.594, γ 1.597; 2*V* 32-42º
Habit: anhedral platy crystals (rhombic plates) in nodular chalky masses; concretionary, earthy, dull, cryptocrystalline aggregates
Relief: low
Color: colorless, chalky white
Pleochroism: none
Cleavage: perfect on {001} and {110}
Interference colors: up to the second-order blue
Extinction: oblique
Interference figure: biaxial negative, *r* > v strong

Probertite, $NaCa(B_5O_7(OH)_4)\cdot 3H_2O$
System and space group: monoclinic, $P2_1/a$
Unit-cell parameters: *a* 13.43, *b* 12.57, *c* 6.589 Å; ß 100.25º
Diffraction lines: 9.12(100), 2.81(35), 6.62(20), 3.52 (20), 2.94(20) Å
Optical constants: α 1.515, β 1.525, γ 1.544; 2*V* 73º
Habit: acicular or platy crystals in rosettes or radial groups; also as massive aggregates
Relief: low
Color: colorless
Pleochroism: absent
Cleavage: perfect on {110}
Interference colors: up to the second-order yellow
Extinction: oblique
Interference figure: biaxial positive, *r* > v

Teruggite, $Ca_4Mg(AsB_6O_{11}(OH)_6)_2\cdot 12H_2O$
System and space group: monoclinic, $P2_1/a$
Unit-cell parameters: *a* 15.675, *b* 19.920, *c* 6.255 Å; ß 99.33º
Diffraction lines: 12.1(100), 2.79(30), 9.98(20), 8.37(20) Å
Optical constants: α 1.526, β 1.528, γ 1.551; 2*V* 33º
Habit: microscopic acicular crystals aggregated in rounded nodules; also tabular crystals
Relief: low, negative
Color: colorless
Pleochroism: absent
Cleavage: good on {001}, fair on {110}
Interference colors: high second-order colors
Extinction: oblique
Interference figure: biaxial positive, *r* > *v*

Tincalconite, $Na_2(B_4O_5(OH)_4)\cdot 3H_2O$
System and space group: trigonal, *R*32
Unit-cell parameters: *a* 11.140, *c* 21.207 Å
Diffraction lines: 2.92(100), 4.38(90), 8.75(55) Å
Optical constants: ω 1.461, ε 1.474
Habit: rhombohedral crystals, generally cryptocrystalline and possibly pseudomorphic
Relief: marked (-)
Color: colorless
Pleochroism: none
Cleavage: generally not noticeable
Interference colors: up to the end of the first order
Extinction: straight
Interference figure: uniaxial positive

Tunellite, $Sr(B_6O_9(OH)_2)\cdot 3H_2O$
System and space group: monoclinic, $P2_1/a$
Unit-cell parameters: *a* 14.390, *b* 8.213, *c* 9.934 Å; ß 114.03º
Diffraction lines: 6.57(100), 6.97(30), 5.14(30), 6.21(20) Å
Optical constants: α 1.519, β 1.534, γ 1.569; 2*V* 42º
Habit: coarse prismatic and tabular crystals, and nodules of radiating prisms
Relief: very low, either positive or negative
Color: colorless
Pleochroism: absent
Cleavage: perfect on {100}, distinct on {001}
Interference colors: high third-order colors
Extinction: oblique
Twining: possible on {100}
Interference figure: biaxial positive, *r* > *v*

Ulexite, $NaCa(B_5O_6(OH)_6)\cdot 5H_2O$
System and space group: triclinic, $P\bar{1}$
Unit-cell parameters: *a* 8.816, *b* 12.870, *c* 6.678 Å; α 90.36, ß 109.05, γ 104.98º

Diffraction lines: 12.2(100), 7.75(80), 6.00(30) Å
Optical constants: α 1.493, β 1.505, γ 1.529; 2*V* 70-73º
Habit: generally forms subhedral, fibrous crystals grouped in parallel arrays; may transmit images (‘mineral television’, optic fibers), but also in fibroradial aggregates
Relief: low (-)
Color: colorless
Pleochroism: none
Cleavage: {010} perfect, {100} good, {110} poor
Interference colors: up to the end of the second order
Extinction: oblique in elongate sections
Twinning: polysynthetic, common
Interference figure: biaxial positive